UBIQUITOUS OPTICAL WIRELESS COMMUNICATION USING OPTICAL MICRO-CELL SYSTEM

（光マイクロセルシステムによるユビキタス光無線通信）

Charoen Tangtrongbenchasil

A dissertation submitted to
Kochi University of Technology
in partial fulfillment of the requirements
for the degree of Doctor of Philosophy

Graduate School of Engineering
Kochi University of Technology
Kochi, Japan

March 2008

UBIQUITOUS OPTICAL WIRELESS COMMUNICATION USING OPTICAL MICRO-CELL SYSTEM

（光マイクロセルシステムによるユビキタス光無線通信）

Charoen Tangtrongbenchasil

A dissertation submitted to
Kochi University of Technology
in partial fulfillment of the requirements
for the degree of Doctor of Philosophy

Special Course for International Students
Department of Engineering
Graduate School of Engineering
Kochi University of Technology
Kochi, Japan

March 2008

Abstract

Ubiquitous Optical Wireless Communications Using Optical Micro-Cell System

February 2008

by

Charoen Tangtrongbenchasil

M.Sc., Sirindhorn International Institute of Technology

Thammasat University, 2002

Communications have been studied for several decades. Major requirements of present communication researches are high data rate, reliability, flexibility, and mobility. Present utilized communications are radio frequency (RF) communications requiring communication coverage area or overlap transmission of transmitting electromagnetic field both of transmitter and receivers are the most flexible mobile communication systems. However, RF communications have several problems such as low data rate due to radio regulation, low reliability, weak security, electromagnetic interference (EMI) to other appliances, *etc*. Ubiquitous optical free space point-to-point (p-to-p) communications can overcome low data rate, weak security, and EMI problems. Moreover, p-to-p communication can improve the communication reliability. In contrast, optical free space p-to-p communications suffer link alignment problem due to strict p-to-p alignment. To increase link robustness, optical free space communications must be able to operate even when obstacles are placed between transmitters and receivers, so optical micro cell (OMC) with autonomous beam control can overcome link robustness.

This study focuses on realization of optical access link communications both of downlink and uplink communication. At the optoelectronic intelligent OMC hub node, the integrated technology of VCSEL array, vision chip, and electronic switch matrix were implemented as a function of multi mobile users' accessibility. The 4-channel APD and the single VCSEL chip with autonomous beam searching and alignment were implemented at the mobile user terminals to utilize the optical link communication. An approximately 114 Mbps data communication rate was demonstrated. To achieve Gbps data rate, all optoelectronic and signal processing circuits should be implemented in an analog-digital hybrid very large scale integrated (VLSI) circuit.

Table of Contents

Page

List of Figures

Figure Page

Figure Page

List of Tables

Glossary of Symbols

Meaning	Symbol	Unit
Minimum required incident power	$P_{\min}$	W
Average required photon per pulse for a certain BER	$\overline{N}$	-
Planck's constant	$\overline{h}$	J·s
Speed of light	c	m / s
Bit rate	B	bps
Operating wavelength	λ	m
Incident optical power	P_{Rx}	W
Transmitting power from optical Tx	P_{Tx}	W
Operating height	h	m
Optical Rx lens diameter	h	m
Beam divergence	θ	radian or degree
Distance between VCSEL surface and thin lens surface	d_{VL}	m
VCSEL number	n	-
Focal length of thin lens	f_{VCSEL}	m
Operating distance	D_{LS}	m
Beam position of VCSEL i at service area	$V_{s.a.p,i}$	m
Beam angle of VCSEL i at service area	$\theta_{s.a.}$	radian or degree
Uplink beam position in front of the thin lens surface	V_{uplink}	m
Uplink beam angle in front of the thin lens surface	θ_{uplink}	radian or degree
VCSEL pitch	P_{VCSEL}	m
Distance between the vision chip surface and the thin lens surface	d_{VISION}	m
Focal length of vision chip lens	f_{VISION}	m
Beam position at the vision chip surface	V_{VISION}	m
Beam angle at the vision chip surface	θ_{VISION}	radian or degree

Meaning	Symbol	Unit
Signal current	i_s	A
Primary photocurrent of DC value	$i_p(t)$	A
Average of the statistically varying APD gain	M	-
Quantum noise current	i_Q	A
Bulk dark current	i_{DB}	A
Surface leakage current	i_{DS}	A
Thermal (Johnson) noise current	i_T	A
Electron charge	q	C
Bandwidth	B	Hz
Noise figure associated with the random nature of the avalanche process,	$F(M)$	-
Primary detector bulk dark current	I_D	A
Surface leakage current	I_L	A
Boltzmann's constant	k_B	J/K
Absolute temperature	T	K
Load resistance	R_L	Ω
Thershold level to separate bit "0" and "1"	v_{th}	V
Logic "0" signal level	b_{off}	V
Logic "1" signal level	b_{on}	V
Square root of logic "0" variance	σ_{off}	V
Square root of logic "1" variance	σ_{on}	V
Gain bandwidth product	GBP	Hz

Glossary of Abbreviations

Tx	Transmitter
Rx	Receiver
P-to-p	Point-to-point
ARPANET	Advanced research projects agency network
RFC	Request for comment
IPv4	Internet protocol v4
TCP	Transmission control protocol
UDP	User datagram protocol
SMTP	Simple mail transfer protocol
HTTP	Hypertext transfer protocol
RF	Radio frequency
WiFi	Wireless fidelity
IR	Infrared
IrDA	Infrared data association
GPS	Global positioning system
EMI	Electromagnetic interference
FSO	Free space optics
LED	Light emitting diode
RONJA	Reasonable optical near joint access
BER	Bit error rate
PIN-BJT	Positive-intrinsic-negative bipolar junction transistor
FOV	Field of view
CCR	Corner cube retroreflector
BW	Bandwidth
LOS	Line of sight
LED	Light emitting diode
ETSI	The Europen telecommunications standards institute
EOM	Electro-optic phase modulator
OOK	On-off-keying

OOK	On-off keying
WDM	Wavelength division multiplexing
VCSEL	Vertical-cavity surface-emitting laser
S.C.	Signal conditioner
MAC	Media access control
OHC	Overhead camera
PLL	Phase-locked loop
APD	Avalanche photodetector
SNR	Signal-to-noise ratio

Chapter 1

Introduction

Communication is a process allowing humans to exchange information by one of several methods[1]. Communication requires a kind of symbols, a kind of languages, or a kind of patterns to exchange the information. For example, speaking and singing are used for auditory means whereas body language, sign language, touch, or eye contact are used for nonverbal means or physical means. Fig. 1.1 shows communication scheme consisting of purpose, format, content, source, channel, and destination[1]. When human need to exchange some information, usually they must have some *purposes* for a specific communication *e.g.* entertainment, education, *etc.* Human consequently choose their desired *content* (information *e.g.* what, when, where, why, *etc.*) to transfer to another side by a specific *format* (voice, message, *etc.*). Besides, communication must have *source* who transfers the information and *destination(s)* whom to receive(s) the information. In addition, a *path* or *channel e.g.* telephone, fax, *etc.* between source and destination must be selected.

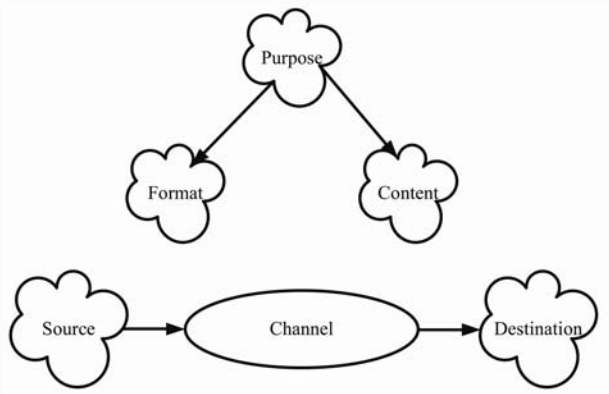

Fig. 1.1. Communication scheme.

The following is an example of communications; a company manager would like to assign a job to an engineer to improve production performance via an email. The purpose of this situation is to improve the production performance. The content is how to improve the production performance. The format is by writing the email. Source and destination are the

company manager and the engineer, respectively. The channel is internet or intranet transfering that email.

In term of engineering, the information is always represented in term of signal[2,3]. Transmission of the signals over a long distance for a purpose of the communication is called telecommunication[2-5]. In earlier, telecommunications involved the usage of smoke signals, drums, or semaphore to represent information *e.g.* enemies come, request for help, *etc*. At present, telecommunications involve the sending/receiving the information in form of electromagnetic waves by electronic transmitters (Tx) /electronic receivers (Rx)[2-7]. The devices based on telecommuncation purposes such as televisions or radios for broadcast communications and telephones for full duplex point-to-point (p-to-p) communications are common in many parts of the world. These devices including computer networks, public telephone networks, radio networks, and television networks are also able to connect to many networks. Computer communication across the internet is one of most popular and flexible telecommunications[7,8].

The legacy history of telecommunications began with usage of smoke signals and drums in Africa, the Americas, and parts of Asia[9,10]. However, the beginning of modern telecommunications was referred to the invention of electrical telegraph[11]. In 1839, Sir Charles Wheatstone and Sir William Fothergill Cooke constructed the first commercial electrical telegraph that employed the deflection of needles representing messages with over 21 kilometresoperating distance[11]. In 1876, Alexander Graham Bell invented the conventional telephone[12]. In 1849, Antonio Meucci invented a device allowing the electrical transmission of voice over a line[13-14]. In 1893, the Franklin Institute, Nikola Tesla described and demonstrated the principles of wireless telegraphy[15]. In 1901, Guglielmo Marconi established wireless communication between Britain and the United States earning him the Nobel Prize in physics in 1909[15,16]. In 1925, John Logie Baird, Scottish inventor, demonstrated the transmission of moving silhouette pictures, which were accounted the first true television pictures[17,18]. For flexible connection between different local networks, advanced research projects agency network (ARPANET) developed the request for comment (RFC) process, which is very important for the earlier internet, and published RFC 1 in 1969[19]. In 1981, RFC 791 and RFC 793 introduced the internet protocol v4 (IPv4) and the transmission control protocol (TCP), respectively. In 1980, a more relaxed transport protocol that did not guarantee the orderly delivery of packets, which was called the user datagram protocol (UDP), was publish as RFC

768[20]. In 1982, an e-mail protocol, simple mail transfer protocol (SMTP), was introduced in RFC 821[20]. In 1996, hypertext transfer protocol 1.0 (HTTP/1.0) a protocol that makes the hyperlinked internet possible was introduced in RFC 1945[20].

Table 1.1 Timeline of communications and telecommunications[1,2,4,6,19].

Mediums	Year	Development
Text editing and storage	3000 BC	Papyrus
	59 BC	First newspaper, Acta Diurna ordered by Julius Caesar
	100 AD	Paper
	1000 AD	Pens, first Chinese printing presses (Pi Sheng)
	1400 AD	First European printing presses (Gutenberg)
	1500 AD	Pencils
	1800 AD	Typewriter
	1960 AD	Computers and text editors
Distance communication	2400 BC	Couriers, first postal systems
	490 BC	Heliograph
	1600 AD	Maritime flags
	1790 AD	Semaphore
	1900 AD	Signal lamps
Audio	3000 BC	Communication drums, horn
	1838 AD	Telegraph
	1848 AD	Telephone
	1896 AD	Radio
Image and Audio	1897 AD	Computer
	1927 AD	Television
	1969 AD	Computer networking
	1983 AD	Internet

Table 1.1 shows timeline of communications and communications which are classified following type of mediums; text editing and storage, distance communication, audio, and image and audio. From the developments of telecommunications, it shows that earlier purpose

of communications is to transmit some information making both of source and destination(s) understand to each other. The later development purposes were changed to be well organized platform for entertainment, increasing flexibility, mobilities, *etc.* Wireless communications thus are one of the candidates for present and future developments in telecommunication engineering due to flexibility, potential of mobility and potential of ultra high speed. At present, the wireless communcations are much more popular than the past due to price, flexibiltiy, *etc.* The wireless communications are commonly used in the telecommunications industry. The telecommunications hardware systems, which use some form of medium (*e.g.* radio frequency (RF), infrared light, laser light, visible light, acoustic energy, *etc.*), transfer information without the implementation of wires. The information is transferred in this manner over both short and long distances.

At present, there are 2 major mediums, which are implemented as carrier mediums for wireless communication, are RF and optics[21,22]. The RF medium involves electromagnetic wave spreading such as microwave for long range line-of-sight *e.g.* general antennas, *etc.* or short range communication *e.g.* bluetooth, wireless fidelity (WiFi), *etc.* The optics medium involves light spreading such as infrared (IR) short range communication, *e.g.* remote controls, infrared data association (IrDA), *etc.* Wireless communication applications may involve p-to-p communications, point-to-multipoint communications, broadcasting, cellular networks, or other wireless networks[21,22]. The term of wireless early comes into public usage to refer to a radio Rx or transceiver establishing its usage in the field of early wireless telegraphy. Now, the wireless is used to describe modern wireless connections such as in cellular networks and wireless broadband internet. Wireless is also used in a general sense to refer to any type of operations that is implemented without the implementationn of wires, such as wireless remote control, wireless energy transfer, ubiquitous sensing *etc*[23].

In the history of wireless technology, Heinrich Rudolf Hertz demonstrated the electromagnetic waves theory in 1888, which was important and the origin of wireless communications, stated that electromagnetic waves can be transmitted and caused to travel through space as straight lines[24,25]. There are many popular appliances based on the radio electromagnetic spectrum *e.g.* radios, televisions, cellular phones, *etc.* Common examples of wireless equipments in use today include:

- Cellular phones and pagers: providing the connectivity for portable and mobile applications, both personal and business.
- Global positioning system (GPS): allowing drivers of any vehicles to check and locate their locations anywhere on earth. Futhermore, drivers can look for maps or routes for going to their destination.
- Cordless computer peripherals: the cordless mouse is a common example; keyboards and printers can also be linked to a computer via short range wireless.
- Satellite television: allowing viewers in almost any location to select from hundreds of channels.

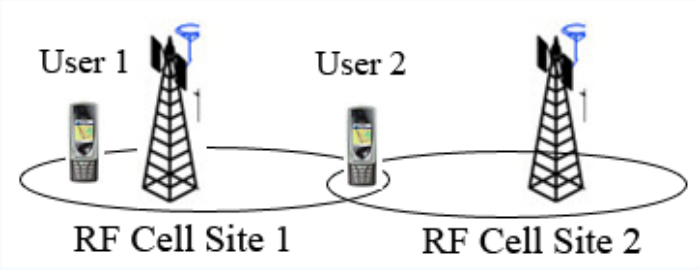

(a)

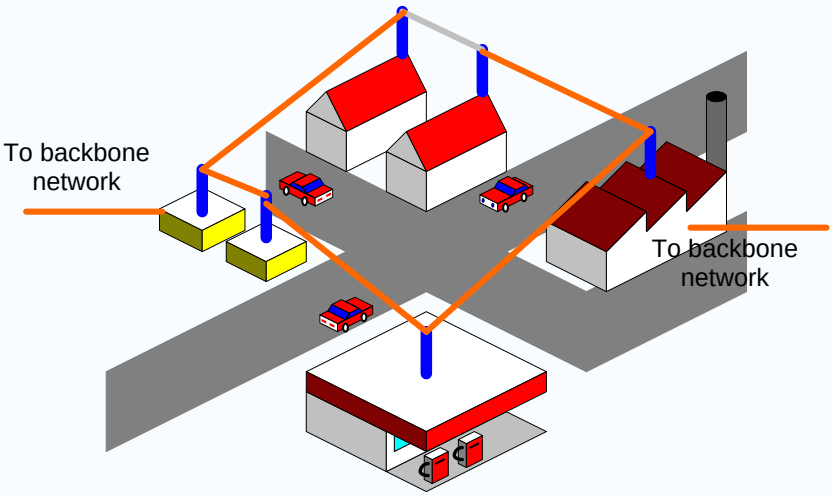

(b)

Fig. 1.2. Examples of wireless cell sites (a) RF cell site and (b) optical cell site.

Wireless networkings are employed to achieve a variety of telecommunications demands. A wireless transmission method is a logical choice to network segment that frequently change locations. The following situations justify the usage of wireless technology:

- To span a distance beyond the capabilities of typical cabling.

- To avoid obstacles such as physical structures, *etc*.
- To provide a backup communication links in case of normal networks failure.
- To link portable or temporary workstations.
- To overcome situations of cabel installed difficulty or financially impractical.
- To remotely connect mobile users or networks.

The early development of wireless communications based on RF medium. RF is a widely spreading electromagentic spectrum with spherical spreading, so mobile users can access to a RF cell site at any position or any angle with respect to the RF cell site as shown in Fig. 1.2 (a). There are several advantages as follows;

- Very high flexibility.
- Multi user acessibility but requiring time sharing, frequency sharing, or coding.
- Not require p-to-p communication.
- Full duplex transmission.
- Dependent from light luminescense.

However, the RF wireless communications still have several problems as follows;

- Requiring radio license operation.
- Not too high data rate due to radio regulation.
- Low secruity due to widely spreading electromagnetic spectrum.
- Protocol intransparency.
- Easy to be interfered due to nearby RF spectrum.
- Bad EMI behaviour.

Above disadvantages can be overcome, if medium is changed to optics. Thus, the later development of wireless communication is optics medium or optical communication that began with laser developments that started to develop light phone or photophone in 1960s by Alexander Graham Bell [26,27]. Optical wireless communication or free space optics (FSO) communcation is one of telecommunication technology that employs the propagation of light in free space to transmit data between two or more[28-31]. FSO is also implemented to communicate between space craft; outside of the atmosphere, signal distortion is negligible

small as operating in optical fiber system[28,30]. There are several advantages of employing optics as medium as follows;[57-63]

- Quick link setup.
- Radio license free operation.
- High transmission security.
- Potential of high bit rates and low bit error rates.
- No Fresnel zone necessary.
- Full duplex transmission.
- Protocol transparency.
- Great EMI behavior.
- In some devices, the beam can be visible, faciliating aiming and detection of failures.

However, there are several limitations of FSO, when FSO operates terrestial ares as follows[30-35];

- Beam dispersion of light source.
- Atmospheric absorption *e.g.* rain, fog, snow, scintillation, smoke, *etc.*
- Background light luminescense.
- Shadowing.
- Pointing stability in wind.

Light emitting diodes (LEDs) is one of FSO devices that applicable for short distance low data rate communication[39-41]. IrDA is another very simple form of FSO communications[36,37]. The possible communication distance of FSO is up to the order of 10 km, but the distance and data rate of connection is highly dependent on atmospheric conditions[29-32]. The light beam distribution angle can be very narrow for long distance access making FSO hard to intercept, but security is improved. FSO provides vastly improved EMI behavior using light instead of RF[29-35]. FSO can also implemented red visible light, as in this installation of a reasonable optical near joint access (RONJA) system[42]. The light does not come from a laser, but instead of a high intensity LED. The intensity vanishes beyond a few steps outside of the narrow beam path. The operating range is 1.4 km at 10 Mbps data rate[42]. These limitations cause propagation loss of of optical signal power through optical Rx, consequently bit error rate (BER) increases[43-52]. To overcome propagation loss of optical signal power in free space,

increasing optical power of source is one of the solutions[43,44,48-51]. To increase optical source power against the propagation loss vs transmission of optical power, human eyes can be harmed[53-56]. To keep an eye safe environment, FSO systems have a limited laser power density by allowing IEC, eye safe standard[55]. Thus, long transmission FSO beam diameter must be expanded.

However, optical wireless communications is not so flexible, due to strictly requiring p-to-p link communications[64-72]. Mostly, optical wireless communication for outdoor usage is fixed p-to-p communications[73-75] such as on the top of building as shown in Fig. 1.2 (b). The outdoor usages of optical wireless communications are implemented either the total operating cost of optical fiber implementation or the difficulty of optical fiber installation are high. In addition, the laser sources, which are used for outdoor usages, are not classified as eye safe class 1 or 1M[53-56]. Outdoor mobile optical free space communications are possible but they have several problems *e.g.* high backgroud noise from sunlight, cell site coverage area is narrow, require high optical power for link communications that can harm human eye, *etc.* By these disadvantages, the mobile optical free space communications are commonly for indoor usage[64-72]. Fig. 1.3 shows an indoor optical free space communication layout consisting of optical cell sites that integrate optical transceivers and mobile users that have compact optical transceiver. For typical operation of indoor optical free space communication, optical cell sites are located at the top of the floor which has average height at 5 meters for residential and commercial zones. So, the high optical uplink and downlink power is not necessary. Less than 1 mW transmission power for uplink and downlink is possible for sub Gbps data rate[49,76-78]. Consequently, the transceiver of optical cell sites and mobile users are compact due to the advance technology in optoelectromechanics. Security is also high due to narrow beam or small service area.

In the past, many optical free space communication link researches were conducted. IrDA is one of the simple and flexible optical communication link but it is able to operate only short range only 1 meter with 115.2 kbps bit rate[36]. The maximum receiver threshold and the minimum transmitter intensity are 4 $\mu W/cm^2$ and 40 mW/Sr, respectively.

A three-segment pyramidal fly-eye detector is one of the better optical communication link that has bit rate of 10 Mbps with 70º field of view (FOV) but structure is complex[79]. The simulaiton model of a single photodetector was positive-intrinsic-negative bipolar junction

transistor (PIN-BJT) featuring 120º FOV, 70 MHz bandwidth (BW), noise current of 2.7 $pA/\sqrt{Hz}$, 5 mm^2 photosensitive area, responsivity of 0.5 A/W, and operating wavelength range of 350 nm – 1100 nm[79]. Using three of these photodetectors can perform 360º FOV with 10 Mbps simulated bit rate and -35.7 dBm sensitivity[79]. The diffuse cofiguration of pyramidal fly-eye detector can vanish the line of sight (LOS) component. For hybrid configuration, the LOS was increased to be 120º[80].

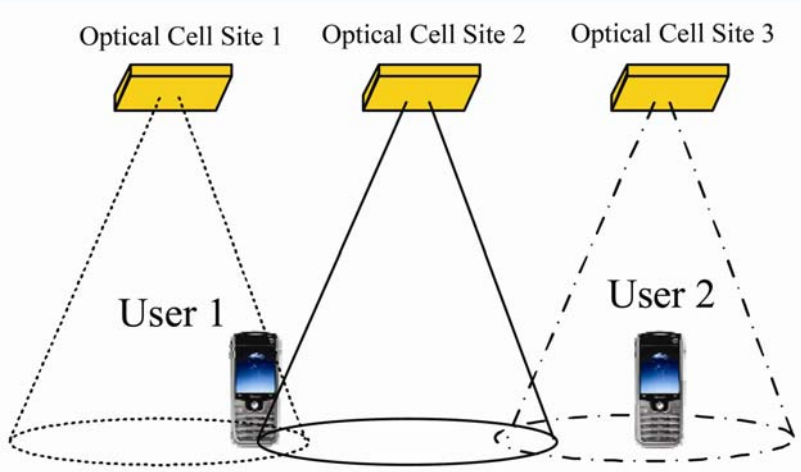

Fig. 1.3. An indoor optical free space communication layout.

The next generation of optical communication link is the usage of white LEDs featuring as a function of lighting equipment and communication devices simultaneously[39-41]. The communication bit rate was achieved as high as 800 Mbps but using white LEDs as the function of lighting equipment, it consumed a lot of emission power and size is huge[39-41]. the potential of his system could as fast as 10 Gbps[40]. Ref. 41 shows the study of shadowing and blocking rate. This system transmitted optical power as 50 W with center luminous intensity of 2700 cd[41], which is bright enough for lighting equipment[41]. The same generation of optical communication link was developed using red LEDs as a function of traffic light which was able to transmit audio at 128 kbps for outdoor usage[80]. Due to the function of traffic light for outdoor usage, the high emission power was extremely required and consequently the physical size was huge[80].

Besides, the corner cube retroreflector (CCR) with modulator was an alternative choice for optical communication link[81-83]. Using CCR based optical communication link, two

modulation techniques were implemented; 1) using electro-optic phase modulator (EOM)[82] or 2) using vibration of CCR as a function of on-off-keying (OOK)[84]. The usual EOM operating voltage is several tens volt but Zhou et. al. reduced the operating voltage of EOM from several tens volt to only approximately 5 volt[83].

1.1 Motivation

At present, wireless communications *e.g.* mobile phone, wireless LAN, *etc.* play the important roles either commercial available or researches. The major mediums are RF and optics mediums as described in previous section. RF medium has several advantages but the performance is limited by radio regulation and the protection of EMI to other appliances. So, optics medium or optical wireless communication is an alternative solution to overcome EMI problem and radio regulation but optical wireless communication is not so flexible due requirement of p-to-p link communication. The optical wireless communication links have been classified depending on the existence of LOS path between Tx, Rx, and the degree of directionality; directed, distributed, or hybrid[86-90]. Directed links improve power efficiency as minized path loss but this kind of systems strictly requires alignment technique for both of Tx and Rx. Directed links make systems less convenience for practical applications.

One of most attractive configurations is the distributed system. Operation under this configuration does not require a direct LOS or strictly alignment between Tx and Rx because the photonic waves are spread as uniform distribution[88-90] making system to be the most robust an flexible configuration. However, distributed system suffers power detection problem due to trade-off of eye-safe power density, coverage distance, and signal bit rate. To compensate both directed and distributed links problems for high speed optical wireless communication, a combination of two solution concepts is proposed; one is optical micro-cell (OMC) hub node using well organized compact opto-electronic matrix array devices[67-72] and another is high sensitive mobile user terminal which features optical Rx such as avalanche photodiode (APD) with autonomous lens posture beam control[67-72] for non-directed links with improved receiving power at the mobile user terminal.

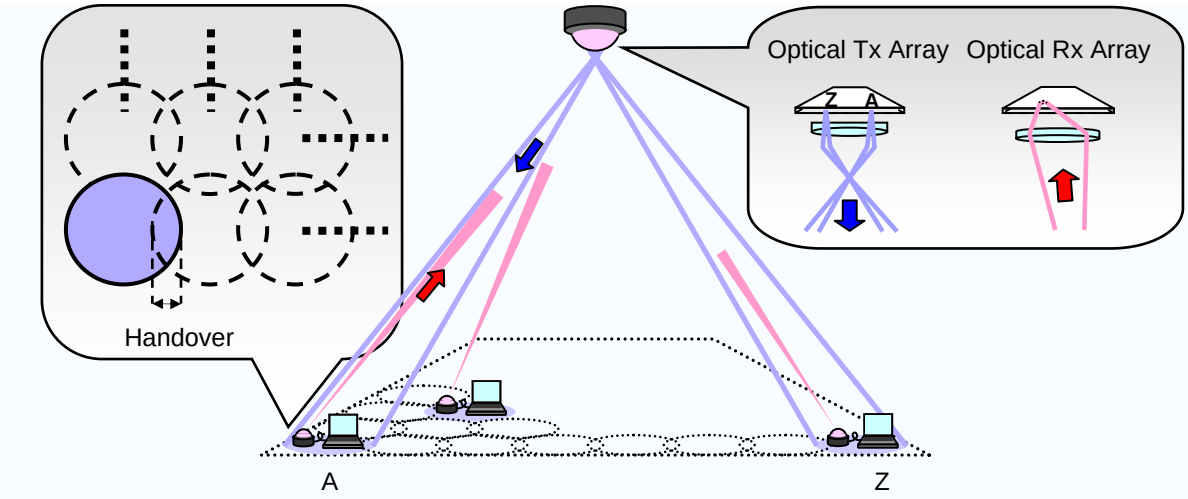

Fig. 1.4. The optical micro cell layout.

Typical system concept of the OMC is shown in Fig. 1.4[67-72]. The concept of OMC has several advantages; potential of ultra high speed communication due to no radio regulation, size is compact due to the advance technology in opto-electronics, p-to-p multi user accessibility due to the implementation of optical Tx/Rx array with cell switching matirxes, high flexibility due to autonomous intelligent beam searching and link control, and low power consumption. The OMC system consists of an optoelectronic array hub node and mobile user terminals. Hub node consists of an optical Tx array with a single lens and an optical Rx array with a single lens. Electronic switching matrixes are required for selecting the proper communication channels of the optical Tx array and the optical Rx array for multi user accessibility. Hub node also requires signal processing modules amplifying and filtering the detected optical signal. The signal processing modules also control the electronic switching matrixes for selecting the proper communication paths. At mobile user terminal, an optical Tx and a 4-channel optical Rx are required as the optical Tx and the optical Rx, respectively. Signal from the 4-channel optical Rx is processed by signal processing module amplifying, filtering, and controlling user terminal posture. The signal from the 4-channel optical Rx is also employed as a communication data.

1.2 Scope of Study

The general indoor optical wireless communications are employed single channel of optical Tx and single channel of optical Rx as a pair of uplink beam and downlink beam. For example,

IrDA systems employ the single channel of optical Tx and the single channel of optical Rx as pair for full-duplex communication but the operating distance is too short and bit rate is also low[36]. Using visible white LED is an alternative solution to overcome the short operating distance and low bit rate but it dissipates a lot of power and risk to human eyes damage[39-41]. Other solutions, *e.g.* pyramidal fly-eye detectors, link communication using CCR, have potential of higher bit rate and longer operating distance but their systems is complex[80,82-85]. Another simple solution for multi user p-to-p optical link communication is OMC, which consists of an intelligent compact opto-electronic hybrid array technology for hub node and an intelligent autonomous beam searching and alignment user terminal, that utilizes optical link communication for multi moblie user terminals.

The commercial available indoor optical wireless communication wavelengths are 850 nm band and 1550 nm band. The eye safer wavelength is 1550 nm but the optical Tx and optical Rx costs are still high, so the design and implementation in this study based on wavelength at 850 nm and visible wavelength due to cost reduction.

1.3 Organization of the Report

This report consists of 4 chapters. The organization of this report is shown in Fig. 1.5. It begins with chapter 1, overview of the wireless communication in both of RF and optical communications and also gives a comparison of the advantages and disadvantages of RF and optical communications. In addition, the overview of OMC system is also discussed in this section. After that motivation and scope of study are given.

In chapter 2, the concept designs and the requirements of optics, electronics and signal processing for OMC system are discussed. They follow with the physical design and mathematical estimation both of the hub node and the mobile user terminal. The total design and the expected performance are stated in last section.

In chapter 3, the experimental setups are first discussed. Consequently, the optical experimental results and electronics and signal processing experimental setups are also discussed, respectively.

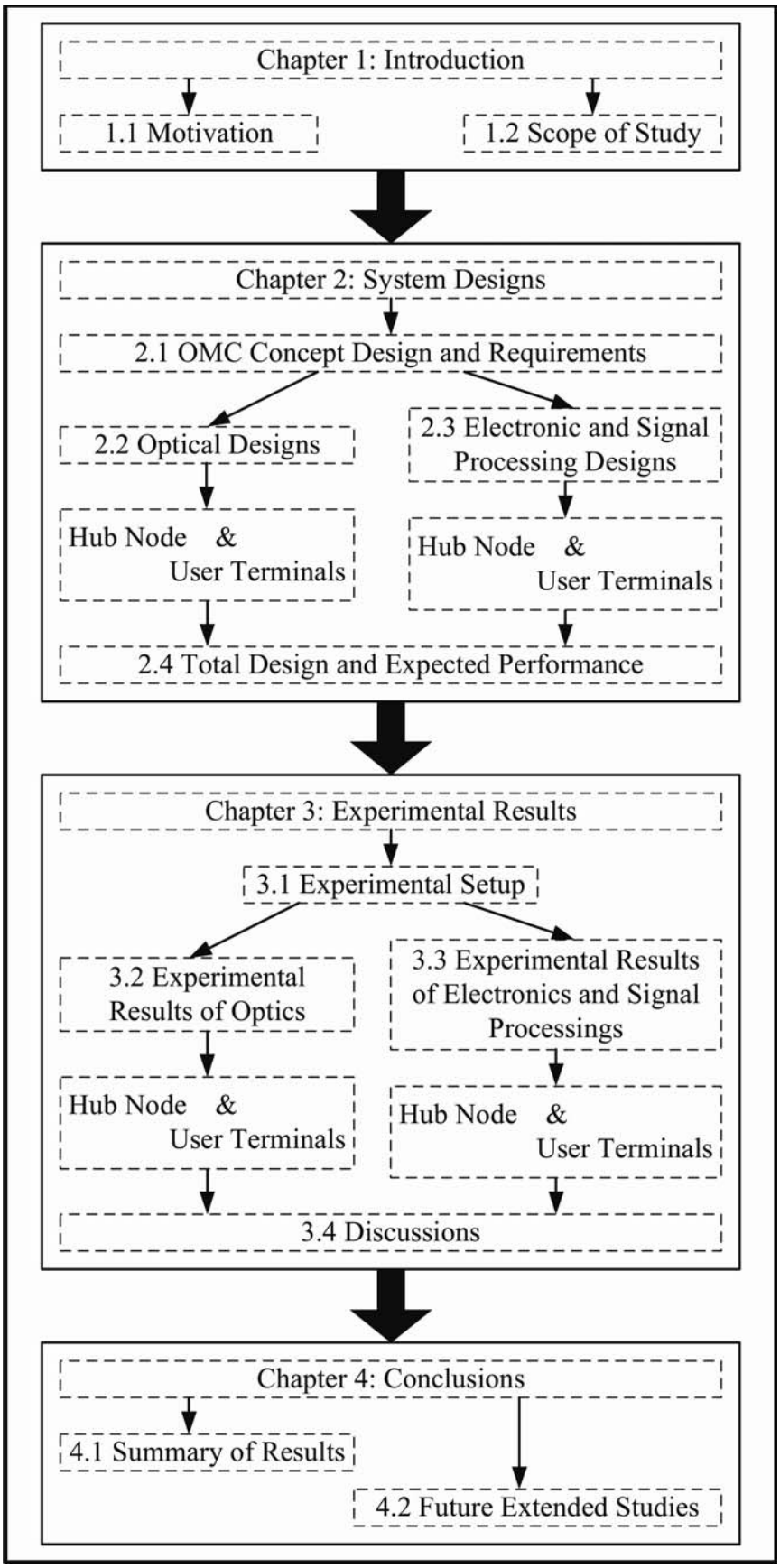

Fig. 1.5. The organization of the report.

Finally, the summary of this study and the future extended studies in ubiquitous optical free space communication are given in the last chapter which is chapter 4.

Chapter 2

System Designs

Optical micro-cell system or OMC system is a simple and optimized configuration for ubiquitous high speed optical free space p-to-p access link communication. As mentioned in previous chapter, it consists of the intelligent opto-electronic array integrated compact hub node and the intelligent autonomous beam searching and alignment mobile user terminals. OMC system can utilize optical link communication for p-to-p multi moblie user terminals.

The content of this chapter including the concept hardware designs and requirements of OMC are given. The detail design in both of optical, electronics, and signal processing design are also proposed in late chapter. Finally, the design concept for primitive setup system is summarized at the end of this chapter.

2.1 Optical Micro-Cell Concept Design and Requirements

The different kinds of link for ubiquitous optical free space communications have been classified, depending on the existence of a LOS path between the Tx and Rx, and the degree of directionality (directed, distributed, or hybrid)[86-89]. Directed links improve power efficiency as minimized path loss but this kind of systems strictly requires alignment technique for both of Tx and Rx. The directed links make systems less convenience for practical utilities. One of most attractive configurations is distributed system. Operation under this configuration does not require a direct LOS or strictly alignment between Tx and Rx because the photonic waves are spread as uniform distribution[68-89] making system to be the most robust and flexible configuration. However, distributed systems suffer power detection problem due to eye-safe power density, coverage distance, signal bit rate, and signal BER. To compensate both directed and distributed links problems for high speed optical free space communications, a combination of two solution concepts is required; one is OMC opto-electronic array integrated compact hub node[67-72] and another is high sensitive mobile user terminals which feature optical Rx array with autonomous lens posture beam control[67-72] for non-directed links with improved receiving power at the mobile user terminal. D. C. O'Brien, et. al. implemented 5-channel optical Rx array highly optimizing for beam detection and

signal communication but fabrication cost is still high and sensitivity is too low[63-65]. The commercial available 4-channel optical Rx array developing for beacon usage was capable for implementation of the similar characteristic to detect beam direction and signal communication and cost consequently can be reduced.

There are several researches that related to the operations and applications of optical Tx/Rx array did in the past. The optical free space link communications with handover process of the optical Tx and Rx array was proposed by F. Parand, et. al. in 1999[93]. However, the BER of this system was not sufficient as 0.1[93]. The operation of the optical detector array with the group of optical Tx that identically equipped with a laser and a transmitting telescope was present by D. Bushuev and S. Arnon in 2002[94]. The data coding of this system is a simple on-off keying (OOK) which operated in the wavelength division multiplexing (WDM) standard[94]. The stationary optical array link communication mathematical model and simulation that simulated 9 cell array in both of optical Tx and Rx link was shown by A. Polishuk and S. Arnon in 2002[95]. In 2003, the optical free space interconnection topologies were presented by A. G. Kirk[96]. This system showed the 2-D optical interconnection of microchannel relay, clustered interconnect, and macrolens systems[96]. In addition, the operation with different micro and macro lens system was proposed[96]. In 2004, the cellular of multi optical Rx channel with a single macro lens system and the in-line VCSEL array with micro-lens array system were presented by S. Jivkova, et. al[97]. This system can operated at 200 Mbps with FOV of less than 45^{o}[104]. However, this system required the operating optical power as high as 5 dBm at bit rate of 200 Mbps with BER = 10^{-9} [97]. The experimental study of 2-D high power vertical-cavity surface-emitting laser (VCSEL) devices for free space optical communications was presented by M. Yoshikawa et. al. in 2005[98]. This experimental study based on 2x2, 3x3, and 4x4 simultaneously driven VCSEL array resulting very clear eye diagram[98]. However, this system operated well at very high optical power of 20 mW and 40 mW of 3x3 and 4x4 multi-mode 850 nm VCSEL 2-D array, respectively[98].

On the other hand, the researches, which based on optical communications, mainly focused on the optical Rx designs[99-114]. The researches in these researches can be mainly classified to be PIN detectors, APD detectors, and CMOS sensors. All of these researches were interested in increasing bandwidth, increasing bit rate, low noise amplification, wide dynamic range, and low driving voltage operation. The optimum performances of the optical Rx designs were published by W. Z. Chen, et. al. in 2004 and 2005[111-112]. These optical Rx based on 0.18 μm

CMOS technology with low operating voltage as 1.8 V[111-112]. The maximum operating bit rate was 10 Gbps[111-112]. However, the best optical sensitivity was only -13 dBm at BER of 10^{-12} with $2^{31}-1$ pseudo-random bits[111-112].

Combining the past researches techniques either optical link communication or optical Tx/Rx development, ubiquitous indoor optical free space p-to-p communications have potential to be realized. The ubiquitous optical free space p-to-p communications require high speed communication (potential of several Gbps), p-to-p multi-user accessibility (position and format), and flexibility. Most of the past researches of optical free space communications based on stationary system or fixed p-to-p communication between the top of buildings[64-70]. These systems are proper for the location that the installation of optical fiber is difficult and installation and maintenance cost are high[64-70]. However, these systems consumed a lot of transmitted optical power that risked to damage human eye[53-56]. In addition, most of these optical devices are classified as eye-safe class 3 or lower[53-56].

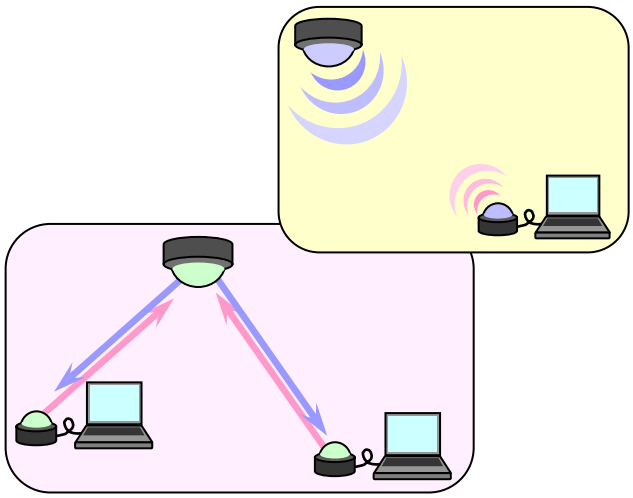

Fig. 2.1. General indoor ubiquitous optical free space communications.

Fig.2.1 shows general indoor ubiquitous optical free space communications. For ubiquitous optical free space communications, there are several approaches that were mentioned in previous chapter *e.g.* IrDA[36], visible white LEDs as lightening equipment[39-41], pyramidal fly-eye detector[70], etc. Those approaches have several disadvantages. IrDA can operate only short range with low bit rate[36]. Visible white LEDs, which implemented as lightening

equipment dissipate a lot of energy due to lightening function, can damage human eye due to high optical power density[39-41]. Pyramidal fly-eye detector can operate wide FOV with high bit rate but structure is complex and huge[70]. By the advance opto-electronic technology, the compact integrated opto-electronic Tx/Rx arrays and electronic switch matrixes, which are the key components of OMC system, are possible to fabricate. Thus, simple and compact OMC system can overcome above disadvantages. Using photonics as a communication medium has the potential of ultra high speed communication but it depends on the operating distance, bit rate, bit error rate, transmitted optical power, and optical Rx structure. P-to-p multi-user accessibility can be implemented by employing optical Tx array, optical Rx array, and electronic switching matrix to select the proper communication path between the intelligent opto-electronic integrated array compact hub node and the intelligent mobile user terminals with autonomous beam searching and alignment that utilized optical link communication. Consequently, the flexible OMC system can be achieved.

The system concept of hub node, which is named as OMC system, is shown in Fig.2.2. It consists of an intelligent opto-electronic integrated array compact hub node and mobile user terminals. Hub node consists of an optical Tx array and an optical Rx array acting as optical transmitter and receiver arrays, respectively. Electronic switching matrixes are additionally required to select the proper communication channels for multi-user accessibility. Hub node also requires signal processing modules amplifying and filtering the detected optical signal. The signal processing modules also control the electronic switching matrixes for selecting the proper communication paths. This OMC system is able to control service area size and interface with p-to-p multi user terminals. On the intelligent hub node side, it originally interfaces with Ethernet system that con nects with optical fiber link which has capacity of several Gbps. Both of uplink and downlink data are fed in and out by processing module that employs as network management. Moreover, processing module is able to amplify, filter, and select the proper uplink and downlink interface to the mobile user terminals. Using the optical Tx array or the optical Rx array with a single lens can control service area size by adjusting the focal length of operating lens or change the distance between the optical Tx/Rx array surface and lens surface.

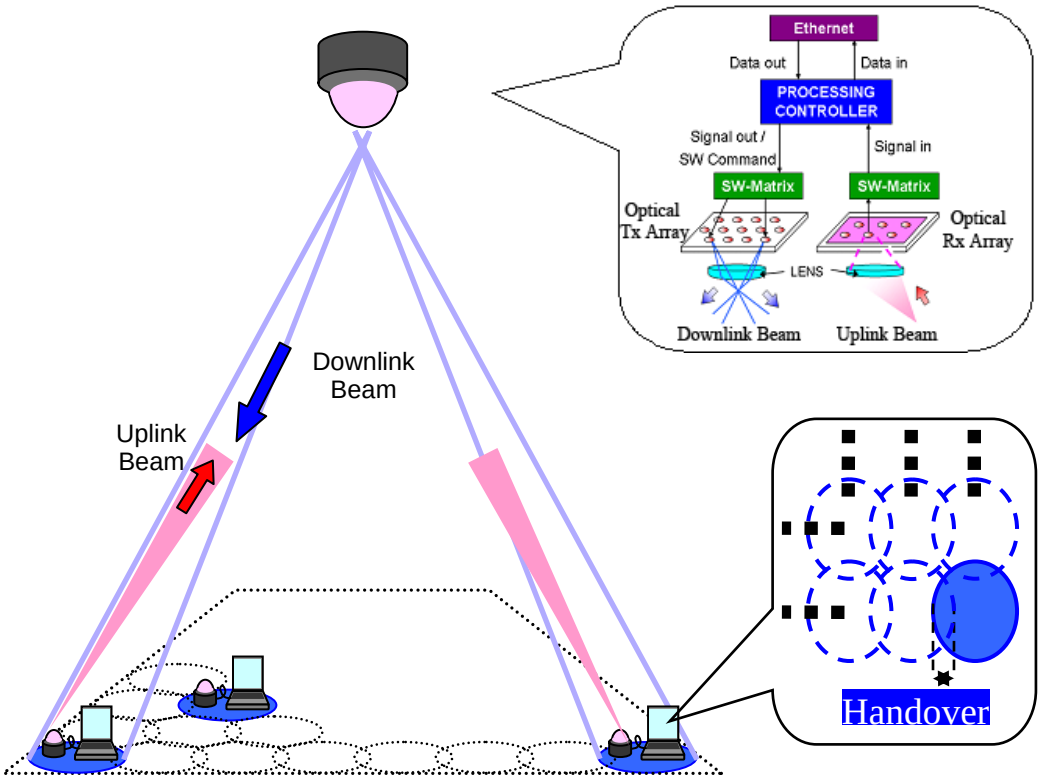

Fig. 2.2. Optical micro cell system concept.

At mobile user terminals, a single optical Tx with a single lens and a 4-channel optical Rx array with a single lens are employed as Tx and Rx, respectively. When the mobile user terminals move into a service area of a hub node, the 4-channel optical Rx array with a single lens of user terminal detected communication light intensity, and then posture was automatically adjusted. Consequently, the received signals were filtered and amplified by signal conditioner module (S.C.) to adjust to be proper voltage level and frequency band for further signal processing (see Fig.2.3). The filtered and amplified signals are also transmitted to the mobile user terminal's controller to decide and then the mobile user terminal's controller sends a control command to adjust lens posture to achieve balanced optical signal condition. When balanced optical signal condition are realized, the mobile user terminal's controller then transmits a command to initiate link with the intelligent hub node by media access control (MAC) address and initialized command to hub node

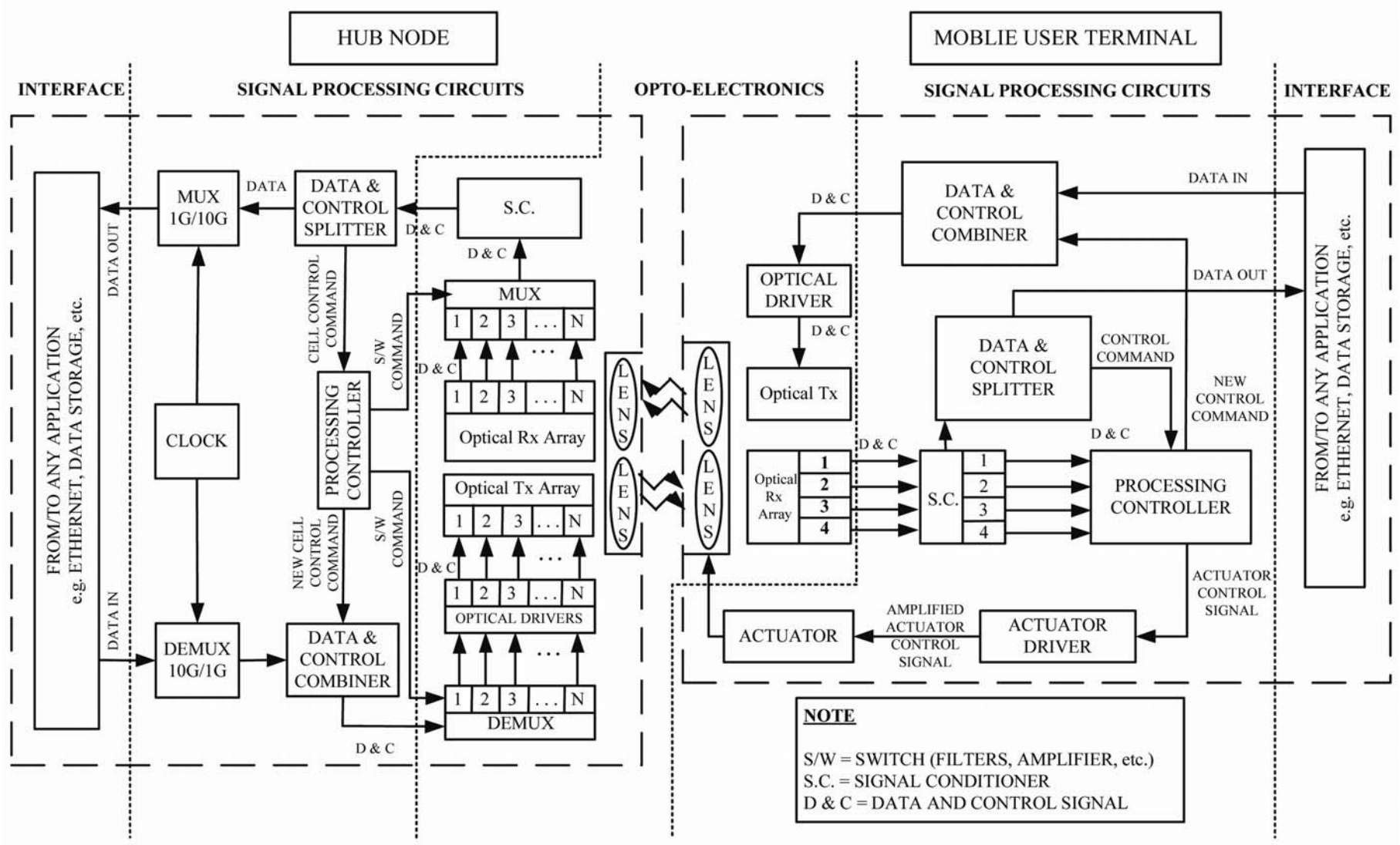

Fig. 2.3. System hardware control block diagram of OMC's hub node and mobile user terminal[72].

via the mobile user terminal optical Tx. When the intelligent hub node receives MAC address and initialized command, the intelligent hub node's controller acknowledges user terminal and waited for next commands for next communications. Fig.2.3 shows the overall optoelectronics, signal processing & control circuit, and interface module block diagram. As can be seen in Fig.2.3, the OMC system can operate not only Ethernet but also overhead camera (OHC) projector and other communication devices, even though the interfaced protocol is changed.

For multi user accessibility, when the other mobile user terminals move into the service area of hub node, electronic switching matrix switches data to different cells or service areas of optical Tx array in the same intelligent hub node. In this situation, control command (*e.g.* cell number and/or handover requirement) is required to insert in transmitted signal both of the intelligent hub node and the mobile user terminal. On the other hand, the control command of a mobile system is not necessary wideband. Sub-Mbps control command is sufficient for real time cell switching and the mobile user terminal autonomous posture controls. In order to combine control command (low speed signal; sub kbps) and data signal (high speed signal; faster than 100 Mbps) in a single frame communication, phase-locked loop (PLL) circuits that acts as a frequency synthesizer to generate a clock signal for the data buffer in Tx and a clock recovery system in Rx to retrieve the clock[91]. The PLL detail operation will be discussed in section 2.3.

2.2 Optical Designs

Present popular commercial available optical communication wavelengths are 850 nm and 1500 nm. Eye safer wavelength is 1550 nm but optical components at 1550 nm wavelength are still expensive. The optical design in this study based on 850 nm. In addition, this study is a primitive study to verify and realize the function of the ubiquitous optical free space communication links, thus the design in this study based on 1 meter operating distance. In fact the operating distances for the practical utilities, e.g. residential and commercial zones, are approximately 4 meter. Thus, this section discusses the design both of primitive design at 1 meter operating distance and practical design at 4 meter operating distance.

The minimum optically detected power is the first important factor for the design. The minimum required incident power ($P_{\min}$) can be calculated by[92]

$$P_{\min} = \bar{N}\frac{\bar{h}cB}{2\lambda}, \qquad (2.1)$$

where $\bar{N}$ is the average required photon per pulse for a certain BER,

$\bar{h}$ is Planck's constant $= 6.626\times10^{-34}$ J·s,

c is speed of light $= 3\times10^{8}$ m/s,

B is bit rate [bps], and

λ is operating wavelength $= 850$ nm.

Based on eq. 2.1 with different bit rate and BER, the minimum required incident power to the receiver is shown in Fig.2.4. For the potential bit rate at 10 Gbps with out background noise, the required incident power is less than -70 dBm while 100 Mbps data rate requires the incident power less than -90 dBm. Both bit rates require small optical power that does not harm human eyes. For the practical utilities, the design of optical receivers add 20 dBm from the calculation of $P_{\min}$, due to background noise[92].

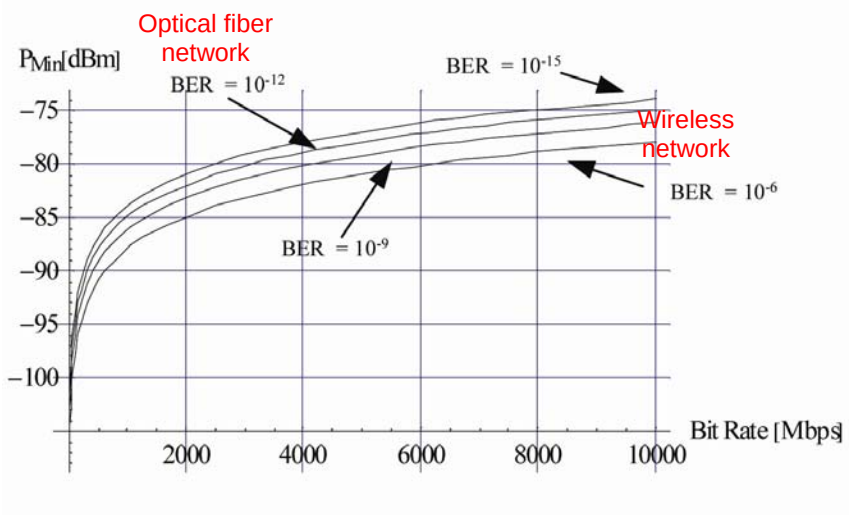

Fig. 2.4 Minimum optical power requirement for various bit rates and various bit error rates.

The design of the optical Rx extremely requires estimating the received optical power. For example, let the optical Tx uniformly transmits 2 mW optical power with beam divergence at 22°, the optical power density is reduced at longer operating length (note as operating height in this study). However, the incident optical power can be improved using lens to focus receiving beam to the optical Rx. The incident optical power (P_{Rx}) can be calculated as[92]

$$P_{Rx} = P_{Tx}\left(\frac{d}{2h\tan(\theta)}\right)^2, \qquad (2.2)$$

where P_{Tx} is the transmitting power from optical Tx [W],

h is operating height [m],

d is optical Rx lens diameter [m], and

θ is beam divergence [radian or degree].

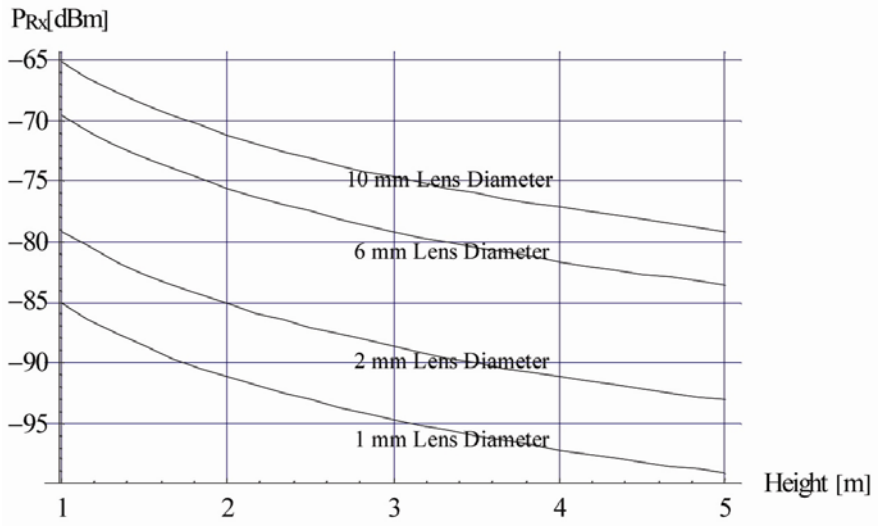

Fig. 2.5 The received optical power at various operating heights and various received lens diameters at 2 mW optical Tx.

Fig.2.5 shows the received power with different operating height and different lens diameter using 2 mW optical Tx. At BER of 10^{-6} with 6 mm diameter lens, the potential maximum bit rate is approximately equal to 5 Gbps (see Fig.2.4 and 2.5). As can be seen in Fig.2.5, the lens diameter can improved the optical sensitivity. If the lens diameter increases with similar focal length, the received optical power consequently increases. It implies that the optical design has the trade-off between communication speed (bit rate) and compactness.

The received optical power does not depending on the optical Rx design but depends on optical Tx design too. Usually, optical sources have beam divergence for a certain angle, so optical power density at higher operating height is reduced. This design of the stationary optical Tx and the optical Rx array with movable lenses is able to reduce background noise

due to optical misalignment as shown in Fig.2.6. The background noise (nearby signal source) is focused out of optical Rx head (see Fig.2.6). Only the background noise that is inserted in the same position of signal source can degrade the optical sensitivity of this system.

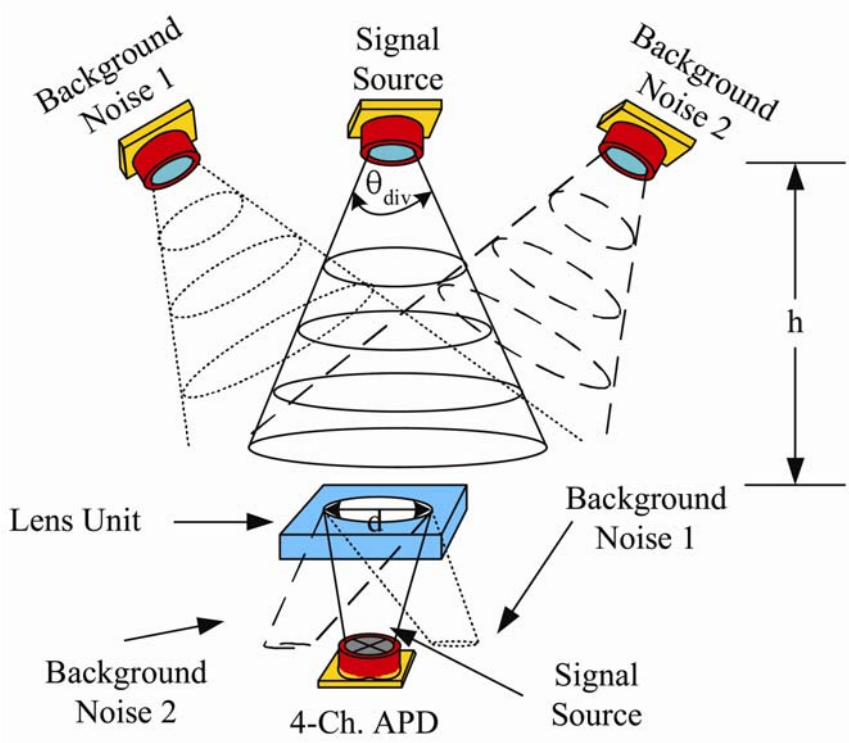

Fig. 2.6 Signal beam and background noise beams misalignment effects.

2.2.1 Hub Node Designs

As mentioned in previous section, the hub node requires the p-to-p multi user accessibility, so the optical Tx array, the optical Rx array, and the electronic switch matrix. In this section, the detail discussion will be given.

In this study, 850 nm oscillation wavelength VCSEL array and 64x64 pixel vision chip are employed as the optical Tx array, and the optical Rx array. For downlink scheme, the VCSEL array with a single thin lens is implemented as the optical Tx array to expand the service area or downlink beam to the mobile user terminals as shown in the upper part of Fig.2.7. The service area cell position is inversely proportional to the VCSEL cell position (see Fig.2.7). By this same configuration, if the vision chip with a single thin lens is implemented as the optical Rx array to focus the uplink beam from mobile user terminals, the mobile user terminal

position can be recognized. Fig.2.7 shows the expansion of OMC beam service area and middle far field IR viewgraph of cell beam positioning of hub node at 35 cm operating distance.

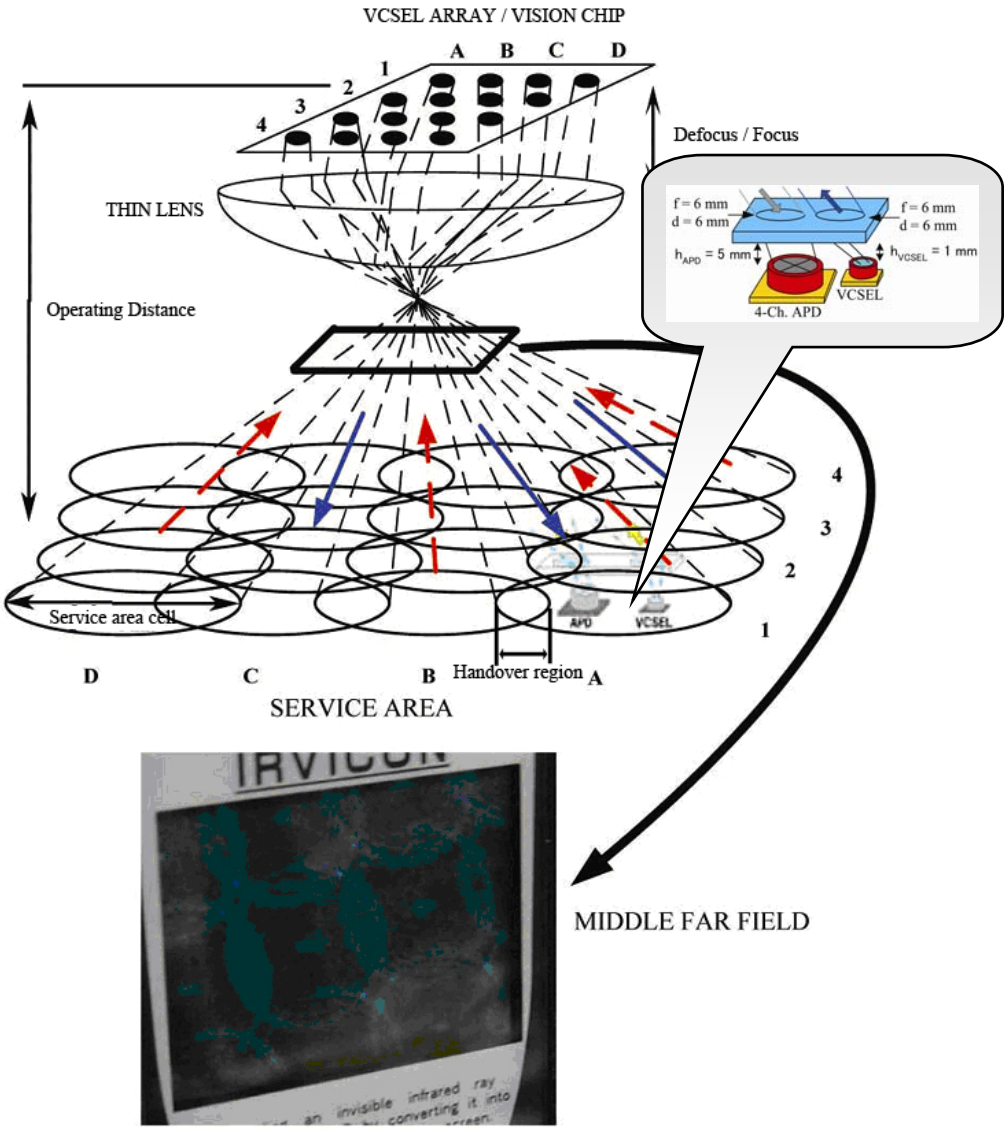

Fig. 2.7 The expansion of OMC beam service area and middle far field IR viewgraph of cell beam positioning of hub node at 35 cm operating distance[72].

As can be seen the concept layout design and the expansion of OMC beam concept in Fig.2.2 and Fig.2.7, respectively, this section discusses the hub node service area design. Due to insufficient 2-D VCSEL array not commercial available, our design is changed to 1x8 in-line VCSEL array that functions as the optical Tx array. Fig.2.8 shows the service area design of

hub node consisting of 1x8 in-line VCSEL array and a thin lens. Beam position of each VCSEL cell that strikes to thin lens must firstly be calculated. The referent position is located at the center of VCSEL array. Each VCSEL cell is separated by 250 μm. In addition, the average beam divergence is 24º. Consequently, the beam position ($V_{pos,i}$, where I = 1, 2, 3, …, 8) of each VCSEL can be calculated using ray transfer matrix (see appendix B) as[115]

$$V_{pos,i} = d_{VL} \tan(\frac{\theta_{div}}{2}) + (n \pm 1.5) \cdot P_{VCSEL} \qquad (2.3)$$

where d_{VL} is the distance between VCSEL surface and thin lens surface,

θ_{div} is VCSEL beam divergence,

n is VCSEL number, and

P_{VCSEL} is VCSEL array pitch.

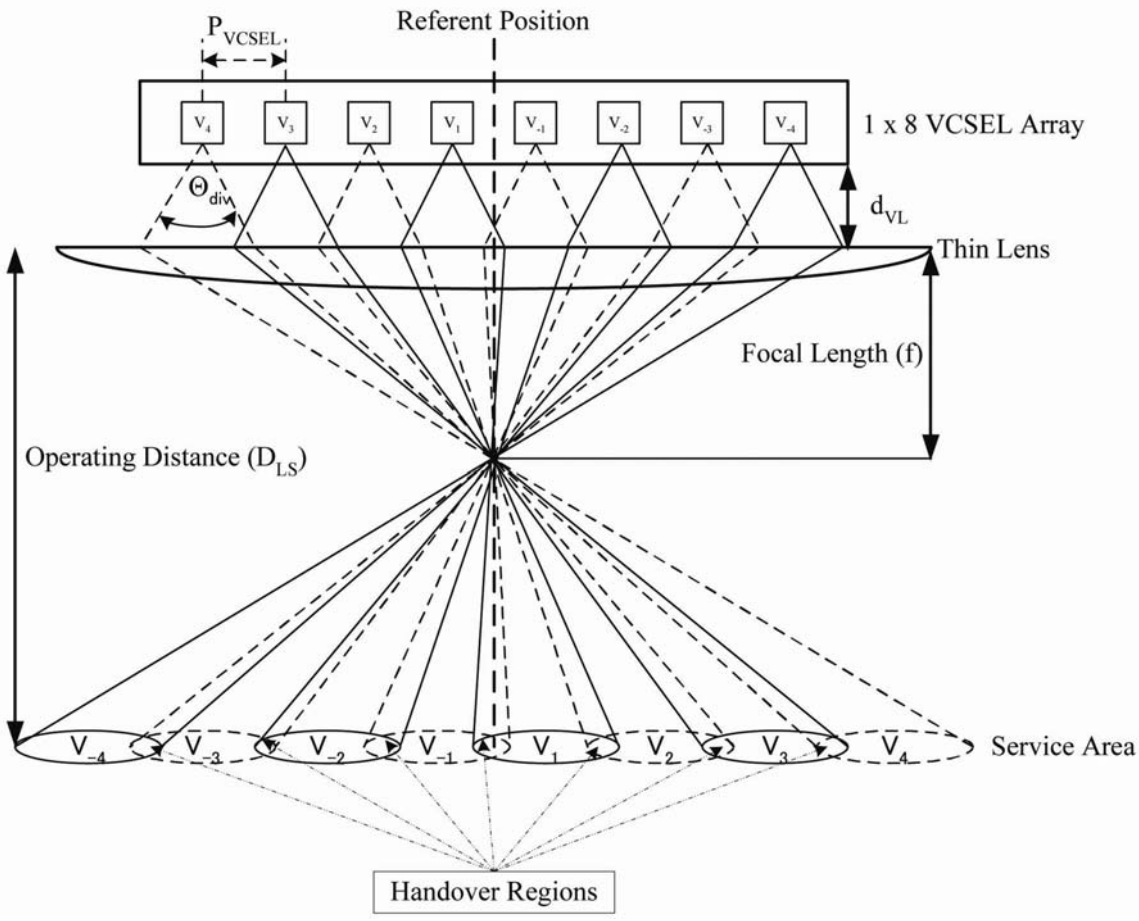

Fig. 2.8 Service area layout design of hub node.

Note that + sign is for left end beam and – sign is for right end beam. From the primitive design, the 6-mm focal length lens and the 30º service area beam divergence are required. Moreover, the operating distance is decided to be 4 meter. Then, apply ray transfer matrix to calculated the distance between VCSEL surface and thin lens surface as

$$\begin{bmatrix} V_{s.a.p,i} \\ \theta_{s.a.} \end{bmatrix} = \begin{bmatrix} 1 & D_{LS} \\ 0 & 1 \end{bmatrix} \cdot \begin{bmatrix} 1 & 0 \\ -\dfrac{1}{f_{VCSEL}} & 1 \end{bmatrix} \cdot \begin{bmatrix} V_{pos,i} \\ 0 \end{bmatrix} \tag{2.4}$$

where f_{VCSEL} is focal length of thin lens,

D_{LS} is the operating distance,

$V_{s.a.p,i}$ is the beam position of VCSEL i at service area, and

$\theta_{s.a.}$ is the beam angle of VCSEL i at service area.

From eq. 2.4, the beam position and beam angle of each VCSEL at each service can be simplified as

$$V_{s.a.p,i} = \left(1 - \frac{D_{LS}}{f_{VCSEL}}\right) V_{pos,i} \text{ and} \tag{2.5}$$

$$\theta_{s.a.} = -\frac{V_{pos,i}}{f_{VCSEL}} \tag{2.6}$$

Substitute eq. 2.5 into 2.6 and solve for the 30º service area beam divergence (half of beam divergence = 15º for 2.6), so d_{VL} = 3.5 mm. Consequently, the exact service area beam divergence is equal to 30.2º.Using the above condition and 2.5, the beam postion of each VCSEL can be calculated and shown in Table 2.1.

As can be seen from Table 2.1, the service area of each VCSEL cell is equal to 1.17 meter with handover region of 0.82 meter. In addition, the single VCSEL service area is only 0.17 meter. Consequently, the total service area of in-line VCSEL array in this design is equal to 2.16 meter.

However, the service area beam design can be improved by 1) changing of distance between VCSEL surface and thin lens surface which is directly proportional to the service area size and service area beam divergence or 2) changing of focal length of thin lens which is inversely proportional to the service area size and service are beam divergence.

Table 2.1 Beam position of each VCSEL at 4-meter operating distance.

VCSEL Number	Left Position (meter)	Rigth Position (meter)
4	-0.09	-1.08
3	0.08	-0.91
2	0.25	-0.74
1	0.41	-0.59
-1	0.59	-0.41
-2	0.74	-0.25
-3	0.91	-0.08
-4	1.08	0.09

On the other hand, the vision chip, which is employed in this study, is supported from NAIST. The construction of the vision chip is based on VDEC rohm 0.35 μm CMOS technology. It has 64x64 operating pixels with pixel size of 100x100 μm^2. For the signal processing block diagram will be discussed in next section. Table 2.2 shows vision chip specification. From this specification, the uplink beam of the mobile user terminals must employs at 650 nm or in red color region.

Table 2.2 Vision chip specification.

Parameter	Specification
Peak Respond Wavelength	650 nm
Speed	10 Mbps
Sensitivity	0.04 A/W
Number of Pixels	64 x 64 Pixels
V_{out}	Open Drain
I_{out}	2- 3 mA

The vision chip with the thin lens featuring the mobile user terminal position recognition can perform multi user accessibility using the same concept as shown in downlink beam design for uplink beam from the mobile user terminals. Modify eq. 2.4 that is the downlink beam design, the uplink beam design can be obtained as

$$\begin{bmatrix} V_{VISION} \\ \theta_{VISION} \end{bmatrix} = \begin{bmatrix} 1 & d_{VISION} \\ 0 & 1 \end{bmatrix} \cdot \begin{bmatrix} 1 & 0 \\ -\dfrac{1}{f_{VISION}} & 1 \end{bmatrix} \cdot \begin{bmatrix} V_{uplink} \\ \theta_{uplink} \end{bmatrix} \tag{2.7}$$

where V_{uplink} is the uplink beam position in front of the thin lens surface,

θ_{uplink} is the uplink beam angle in front of the thin lens surface,

d_{VISION} is distance between the vision chip surface and the thin lens surface.

f_{VISION} is the focal length of vision chip lens

V_{VISION} is the beam position at the vision chip surface, and

θ_{VISION} is the beam angle at the vision chip surface.

From eq. 2.7, the beam position and beam angle at the vision chip surface can be simplified as

$$V_{VISION} = \left(1 - \frac{d_{VISION}}{f_{VISION}}\right) V_{uplink} + d_{VISION}\theta_{uplink} \text{ and} \tag{2.8}$$

$$\theta_{VISION} = -\frac{V_{uplink}}{f_{VISION}} + \theta \tag{2.9}$$

Apply eq. 2.8 and 2.9, the beam position and beam angle ath the visioh chip pixel can be determined. This concept is the reverse process of the downlink beam determination.

2.2.2 User Terminal Designs

As mentioned in previous section, the mobile user terminals require the p-to-p communication. For mobile flexibility, the mobile user terminals must automatically adjust the communication beam to utilize the optical link communication for both of uplink and downlink communications. In addition, the autonomous beam searching and alignment are the necessary

technique that optimizes the optical link during the handover region. By the mentioned requirements, the single optical Tx and the optical Rx array with autonomous posture control are employed as the optical transceiver for the mobile user terminals as shown in Fig.2.9.

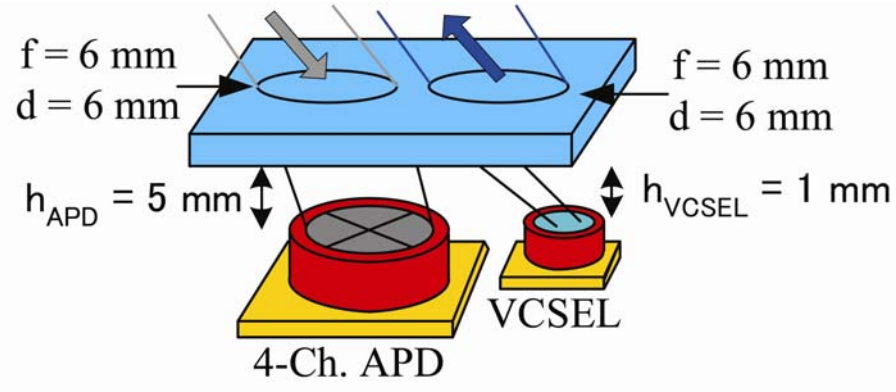

Fig. 2.9 Layout design of the mobile user terminal with autonomous beam searching and alignment technique.

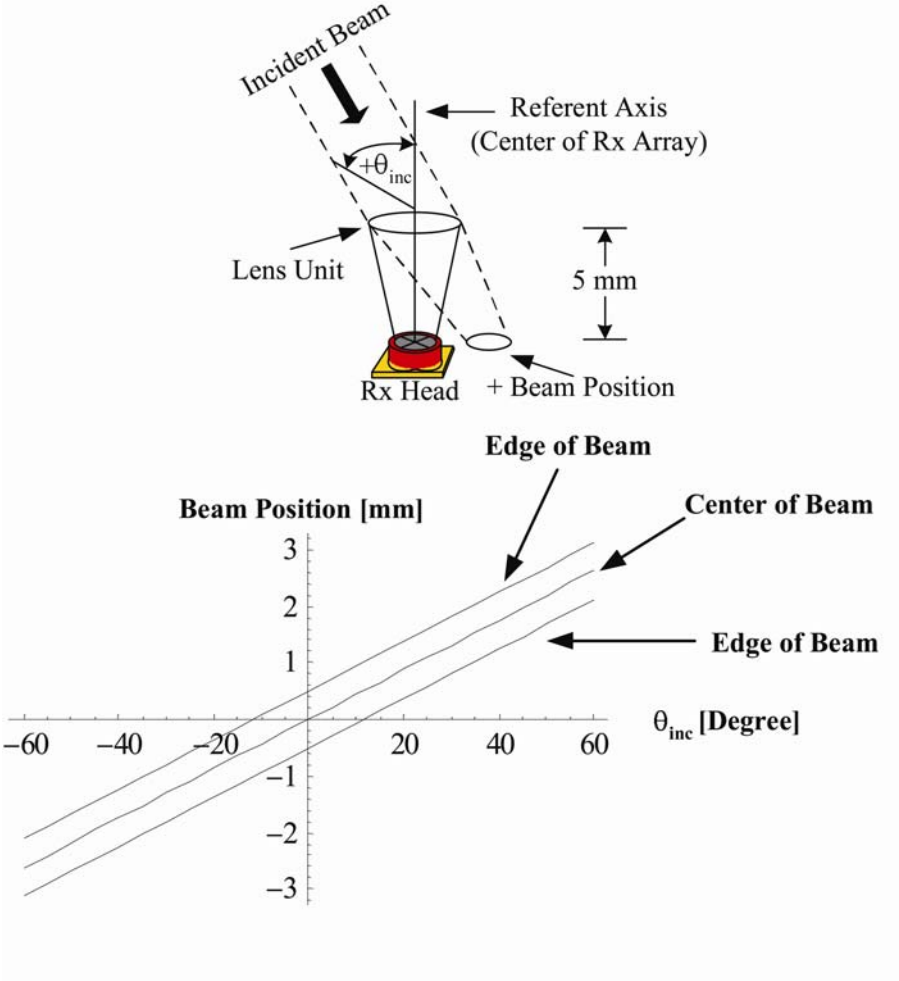

Fig. 2.10 Beam position with various incident beam angles.

The commercial available optical Rx array, which is 4-channel avalanche photodetector (APD), is employed as the optical Rx array at the mobile user terminal for downlink communication. This APD has circular detecting surface which has 1 mm diameter. For uplink communication, a single VCSEL is employed as the optical Tx at the mobile user terminal. To integrate the autonomous beam searching and alignment, two lenses with moving posture, which are implemented for the 4-channel APD and the single VCSEL, are highly required. The 6 mm focal length lens with 6 mm diameter is employed for the Rx side of the mobile user terminal. Because of the detecting surface diameter of the 4-channel APD is equal to 1 mm, so the 5 mm height between this lens and APD surface is chosen. Then, the focusing beam diameter at the APD surface is consequently equal to 1 mm. Fig.2.10 shows the beam position with various incident beam angles. It implies that the focusing downlink beam diameter on the 4-channel APD surface in every incident has identical size which is 1 mm. By adjust the posture within a few mm, the FOV can be increase to be ±60º. By setup easiness for uplink, the similar lens, which is The 6 mm focal length lens with 6 mm diameter, is chosen for the optical Tx of the mobile user terminal. However, the height between this lens and VCSEL surface was changed to be 1 mm, due to beam divergence and the moving posture during autonomous beam searching and alignment operation. When the mobile user terminals change their position the incident beam angle is changed causing the beam misalignment. If the autonomous beam searching and alignment technique is applied, the uplink beam can automatically returned to the hub node to complete the optical link communication for any moving position under the service are of hub node.

There are 4 possibilities that the 4-channel APD with the single stationary lens can detect the downlink beam; 1) balanced condition is the optimized optical link, 2) peak only one channel is when the mobile user terminals slightly move their position, 3) only one channel can detect is when the mobile user terminals move their position beyond, and 4) Undetectable is when the mobile user terminals move their position out of the capability of beam focusing on the 4-channel APD surface. Fig.2.11 shows angle dependence diagram of downlink beam on the 4-channel APD when lens is stationary. In order to optimized the downlink beam in any situation to balanced condition, the autonomous beam searching and alignment must be applied. This techinique will be discussed in next section.

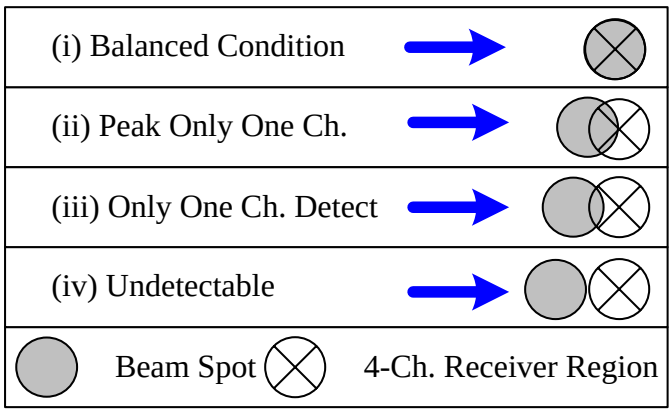

Fig. 2.11 Angle dependence diagram[71].

The sensitivity of a photodetector is described in term of the minimum detectable optical power. The optical power necessary to produce a photocurrent of the same magniture of the total noise current or equivalently a signal-to-noise ratio (SNR) of 1. The mean-square signal current of APD is[92]

$$< i_s^2 >=< i_p^2(t) > M^2 \qquad (2.10)$$

where i_s is the signal current,

$i_p(t)$ is the primary photocurrent of DC value, and

M is the average of the statistically varying APD gain.

There are types of noise in optical communication using APD as the optical Rx which are the quantum noise current, the bulk dark current, the surface leakage current, and the thermal (Johnson) noise current. Table 2.3 shows noise current approximatly in APD receiver.

Note that q is electron charge $=1.6\times10^{-9}$C , B is bandwidth, M is the average of the statistically varying APD gain, $F(M)$ is noise figure associated with the random nature of the avalanche process, I_p is the primary current, I_D is the primary detector bulk dark current, I_L is the surface leakage current, k_B is Boltzmann's constant (1.38×10^{-23}J/K), T is absolute temperature, and R_L is load resistance.

Table 2.3 Noise current approximation in APD receiver[92].

Quantum noise current (i_Q^2)	$2qI_pBM^2F(M)$
Bulk dark current (i_{DB}^2)	$2qI_DBM^2F(M)$
Surface leakage current (i_{DS}^2)	$2qI_LB$
Thermal (Johnson) noise current (i_T^2)	$\frac{4k_BT}{R_L}B$

So the SNR of the APD receiver can be estimated as[92]

$$\frac{S}{N}=\frac{<i_p^2>M^2}{2q(I_p+I_D)M^2F(M)B+2qI_LB+4k_BTB/R_L} \tag{2.11}$$

The optimum gain at the optimum SNR can be calculated by differentiating (2.11) with respect to M to obtain[92]

$$M_{opt}^{x+2}=\frac{2qI_L+4k_BT/R_L}{xq(I_p+I_D)} \tag{2.12}$$

Note that (2.12) can be obtained if and only if the sinusoidally modulated signal with $m = 1$ and $F(M)$ are approximated by M^x.

For the digital communication, the BER must be determined. In case of equally likely hood, the BER can be obtained as[92]

$$\begin{aligned}\text{BER}=P_e(Q)&=\frac{1}{\sqrt{\pi}}\int_{Q/\sqrt{2}}^{\infty}e^{-x^2}dx\\&=\frac{1}{2}\left[1-\text{erf}\left(\frac{Q}{\sqrt{2}}\right)\right]\end{aligned} \tag{2.13}$$

The Q parameter is defined as[92]

$$Q = \frac{v_{th} - b_{off}}{\sigma_{off}} = \frac{b_{on} - v_{th}}{\sigma_{on}} \qquad (2.14)$$

where v_{th} is the thershold level to separate bit "0" and "1",

b_{off} is logic "0" signal level,

b_{on} is logic "1" signal level,

σ_{off} is the square root of logic "0" variance, and

σ_{on} is the square root of logic "1" variance.

2.3 Electronics and Signal Processing Designs

In previous section, the optical design both of uplink and downlink communications were discussed. In this section, the signal processing and opto-electronics primitive designs will be analyzed and discussed. As can be seen the system block diagram of OMC system of the hub node and the mobile user terminals in Fig.2.3, it consists of a pair of the hub node and the mobile user terminal. In fact, the OMC system has potential for multi user accessibility, so the control command that is employed to control the link communication (service area operation, handover process, etc.) must be inserted in a single frame communication for robustness and alignment mechanism. In addition, the signal data rate of optical wireless communication system is able to reach 1 Gbps for each mobile user terminal to overcome recent millimetre wave RF wireless access systems. On the other hand, sub-Mbps control command signal is sufficient for real-time cell switching and the mobile user terminal autonomous posture control. The high speed data acts as sub carrier of the control command. The data signal bit rate of an optical wireless system is very high (approximately 1 Gbps or faster). The beam cell control command signal speed is sufficiently high even bit rate is a few kbps.

The common modules, which are implemented in both of the hub node and the mobile user terminals, are the signal & control combining and recovery schemes. In primitive design, approximately 100 Mbps data signal and 9.6 kbps control signal are combined by a large-scale-integrated circuit (LSI) using a phase-locked loop frequency-shift keying (PLL-FSK) technique as frequency synthesizer (see Fig.2.12). The 100 Mbps non return to zero (NRZ) data signal and the 9.6 kbps control command signal are combined by LSI using the PLL-FSK

technique[98] and transmitted via VCSEL both of the hub node and the mobile user terminal. At Rx of the hub node and the mobile user terminals, clock recovery scheme restore data signal and control command signal as shown in Fig.2.13[98]. Both of signal combination and restoration are performed by 0.1% synthesized frequency modulation. Fig.2.14 shows the clock recovery spectrum of the received signal. The 100.1 MHz clock frequency shows the "1" keying data and the 100 MHz frequency shows the "0" keying data of the control signal. The “1” keying and “0” keying frequencies are compared by PLL clock recovery circuit. The signal containing a high speed data and cell number information from the hub node is received by the mobile user terminals. The mobile user terminals report their position in the coverage area of the current cell and requests handover. The direction of laser beam of the hub node can be switched by electronic switch matrix module. Then, beam direction and posture of each mobile user terminals can refine without link break or re-initialization.

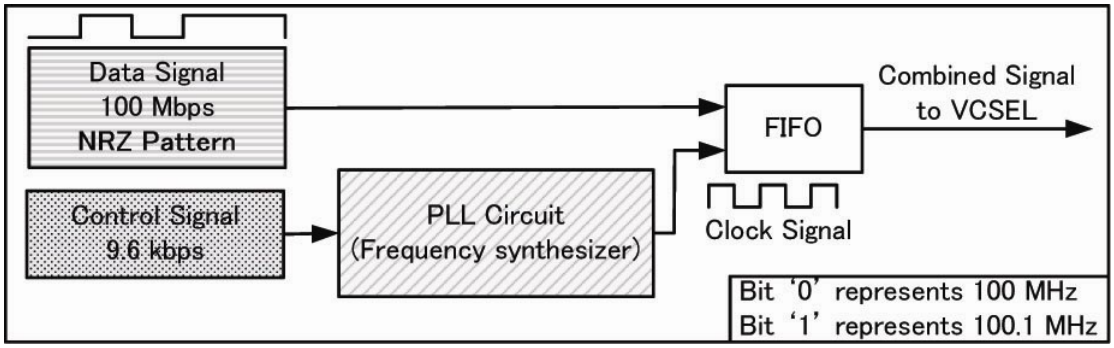

Fig. 2.12 Data and control signal combination scheme[91].

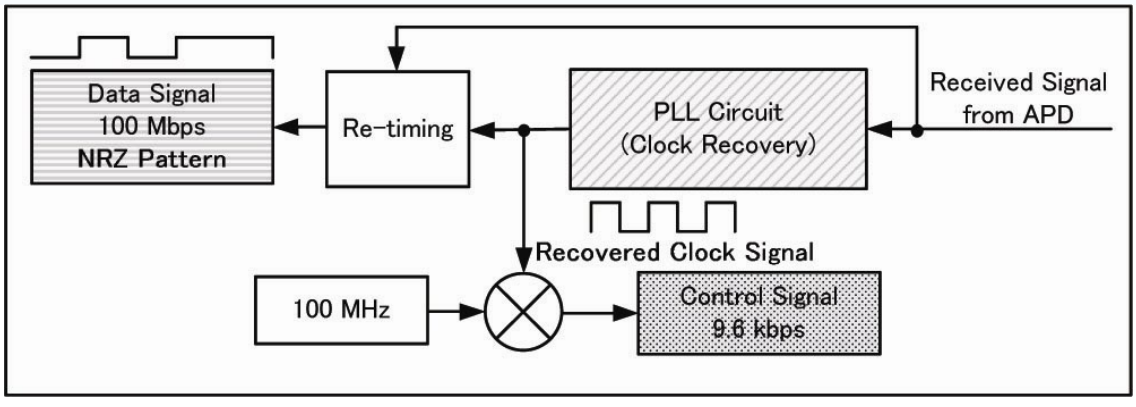

Fig. 2.13 Data and control signal recovery scheme[91].

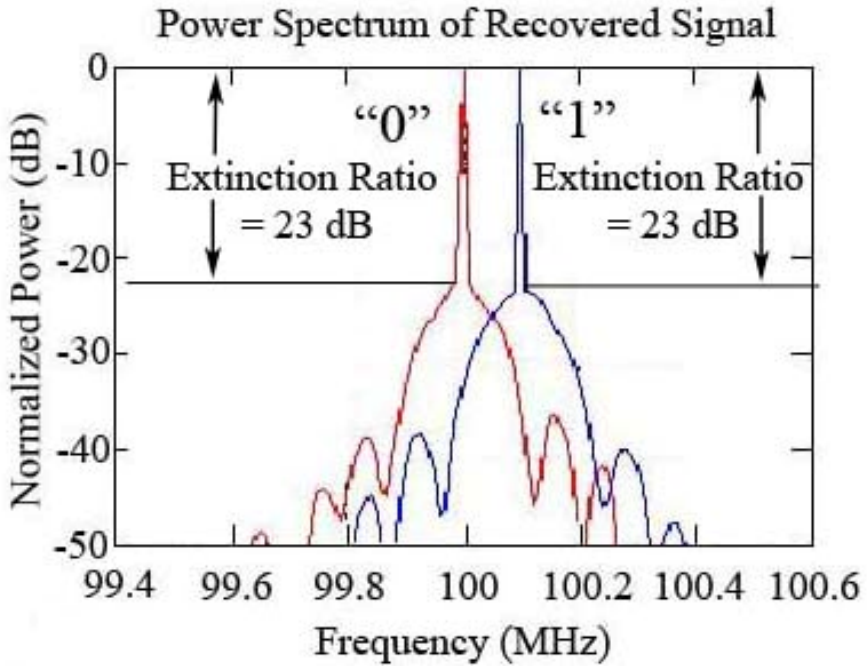

Fig. 2.14 Clock recovered analyzed spectrum of received signal[91].

The electronics and signal processing of the hub node and the mobile user terminals will be discussed in next section. The design of the hub node mainly bases on the practical utilities of the 1x8 VCSEL array and the 64x64 pixel vision chip that are employed as the optical Tx array and the optical Rx array, respectively. The functional usage of 1x8 VCSEL array is designed by the author, so the detail discussion can be discussed. However, the 64x64 pixel vision chip is designed by Nara Institute of Science and Technology (NAIST), so the detail discussion of the 64x64 discussion cannot be fully discussed. The author can discuss only the practical usage and signal processing concept.

On the other hand, the electronics and signal processing designs of the mobile user terminals are totally designed by the author. The detial discussion can be given. In the overview of the mobile user terminals, the single VCSEL chip with the single thin lens and the 4-channel APD with the single thin lens that are implemented in the same moving posture module are employed as the optical Tx and the optical Rx array, respectively. In addition, the intelligent autonomous beam searching and control, which is required feature, will be discussed in this section.

2.3.1 Hub Node Designs

For the electronics design for the hub node, VCSEL array at oscillation wavelength at 850 nm with electronic switch matrix or demultiplexer are required for multi mobile user accessibility. The demultiplxer requires two signals which are the data signal from the data and control combiner of the hub node and the switch command from the processing controller of the hub node as shown in Fig.2.15.

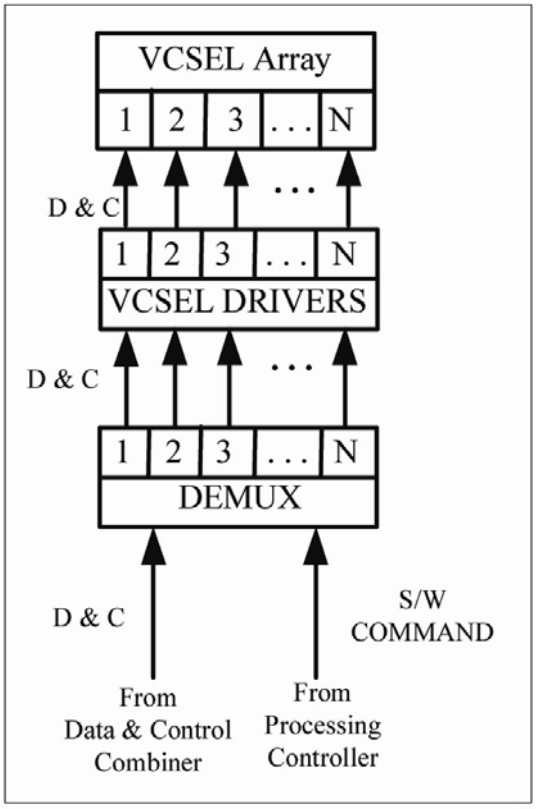

Fig. 2.15 Optical Tx array with switch matrix block diagram.

Due to unavailable of 2-D 8x8 VCSEL array and 2-D electronic switch matrix in our laboratory, the 1x8 in-line VCSEL array and the combination of solid state relays are primitively implemented instead. Fig.2.16 showns the schematic of 1x8 in-line VCSEL array with switch matrix using the combination of solid state relays (The relay coils are excluded). Bias-T with 1.9 bias voltage is employed as VCSEL driving voltage. The simulated signal from the data and control combiner is implemented using pulse pattern generator (PPG). Apply the switch command to the combination of solid state relays, this system can work similar idea as the VCSEL array with electronic switch matrix.

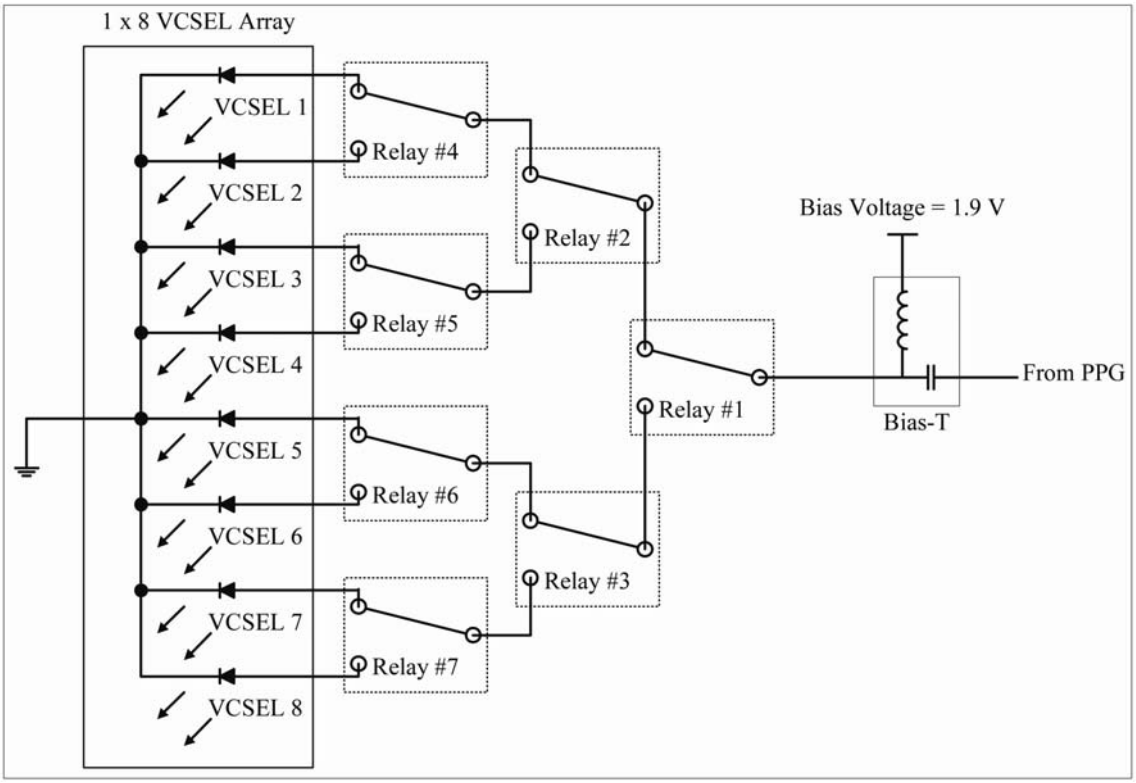

Fig. 2.16 Schematic of 1x8 in-line VCSEL array with switch matrix using the combination of solid state relays.

On the vision chip design, at first our block diagram is designed based on 8x8 2-D optical Rx array. The vision chip is designed as the optical Rx array. Then, the detected signals are feed to the multiplexer or electronic switch matrix by the switch command from the processing controller of the hub node to select the proper communication optical Rx to process in the S.C. The received signal that is processed in S.C. has the output in the digital format. This signal will be process further in the data and control splitter as mentioned at the beginning of this section. Fig.2.17 shows the block diagram design of visio chip. However, our design is not avaible for the commercial vision chip. So, NAIST re-designed to employ 64x64 pixel vision chip with 2-D decoder (x and y decoders) as shown in Fig.2.18. The vision chip pixel is connected to the transimpedance amplifier (TIA) circuit that convert the current signal into the voltage signal. Then, the signal from TIA is fed to the post amp to filter and amplify to obtain the better SNR. On the other hand, the switch command is from field programmable gate array (FPGA) that also controls other parts of the vision chip. From this design, the simultaneously 4 different pixels can be obtained in 3.3 volt level or low voltage differential signal (LVDS)

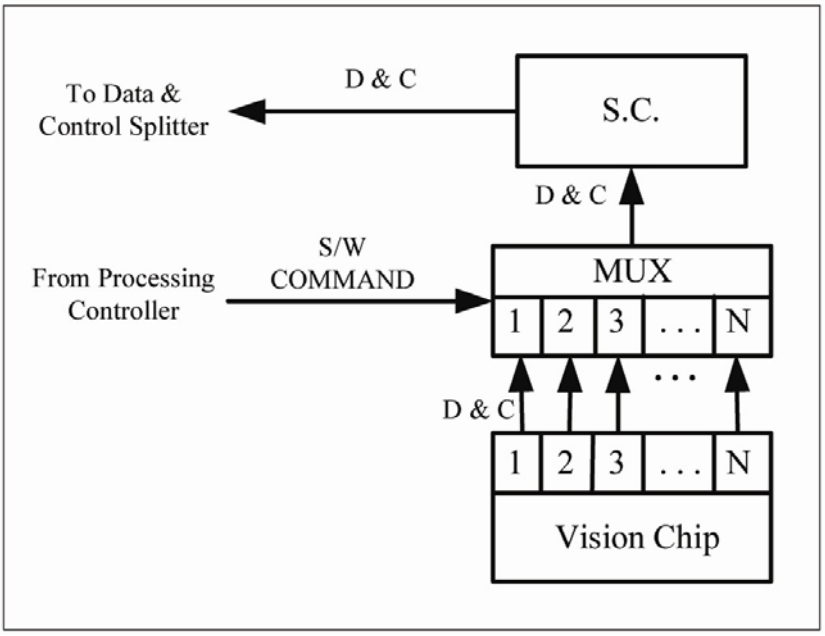

Fig. 2.17 Design block diagram of vision chip.

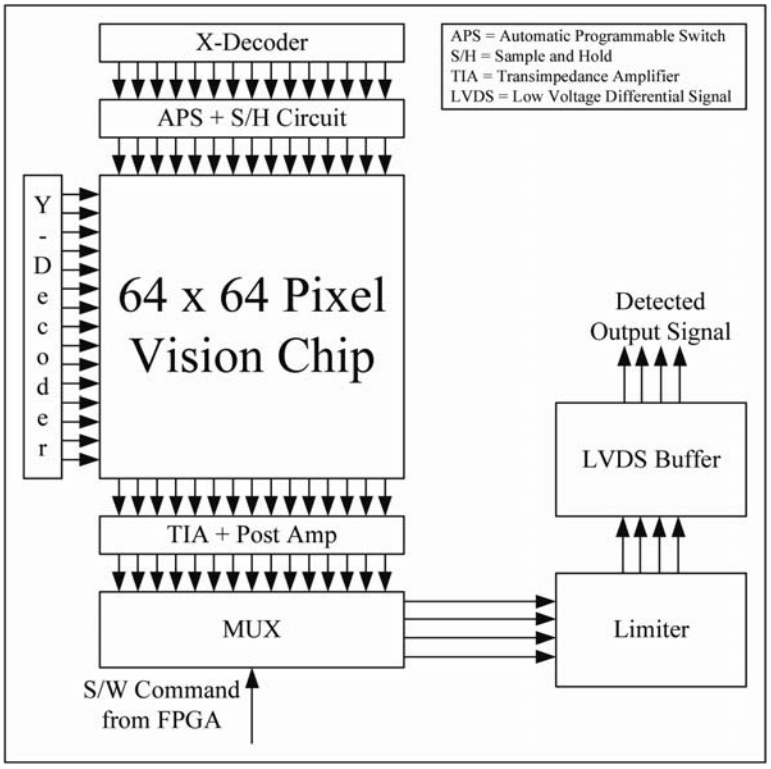

Fig. 2.18 Design block diagram of vision chip from NAIST.

2.3.2 User Terminal Designs

For the electronics design for the mobile user terminal, red laser diode (LD) at oscillation wavelength at 660 nm and the 4-channel APD array are implemented. The transmission path of the mobile user terminal receives the signal from the signal and control combiner of the mobile user terminal and adjusts to the proper electrical signal for VCSEL driving by bias-T with 2.4 bias voltage. The simulated signal from the signal and control combiner module is implemented using PPG instead. Fig.2.19 shows the transmission path of the mobile user terminal.

On the receiver side, the 4-channel APD is connected with TIA and S.C. as shown in Fig.2.20. The 4-channel APD converts the optical signal to the small current signal. TIA converts the detected current signal to voltage signal. Then, the signal from TIA is processed further by S.C. which contains the low pass filter with DC amplifier and band pass filter with AC summing amplifier. The signals from the DC amplifier, which have 4 channels, are sent to the processing controller of the mobile user terminal to process for the autonomous beam searching and alignment function. On the other hand, the signal from the AC summing amplifier is sent to the signal and data splitter of the user terminals.

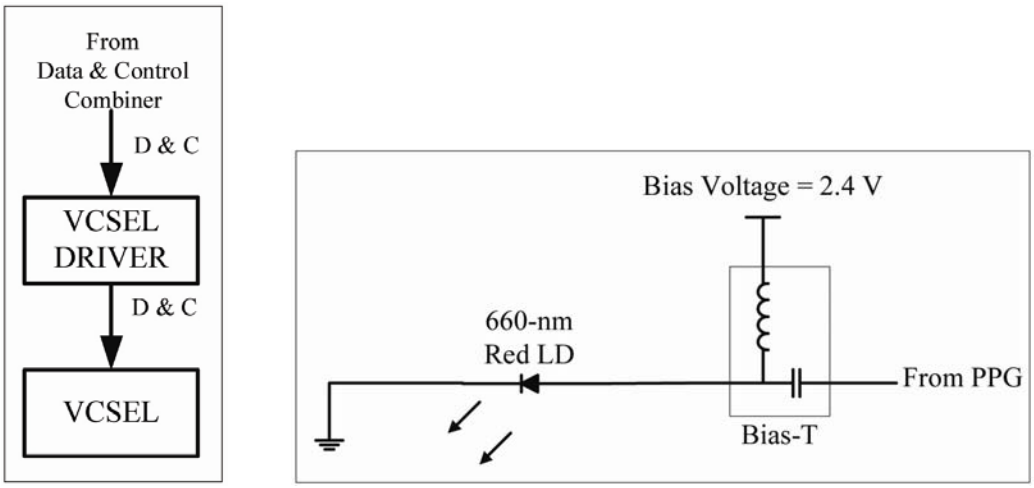

Fig. 2.19 Transmission path of the mobile user terminal (a) block diagram and (b) schematics.

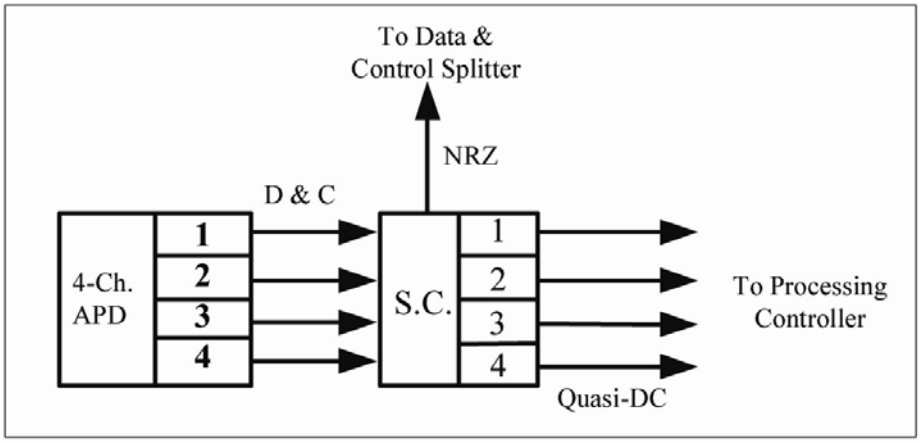

Fig. 2.20 Receiving path of the mobile user terminal.

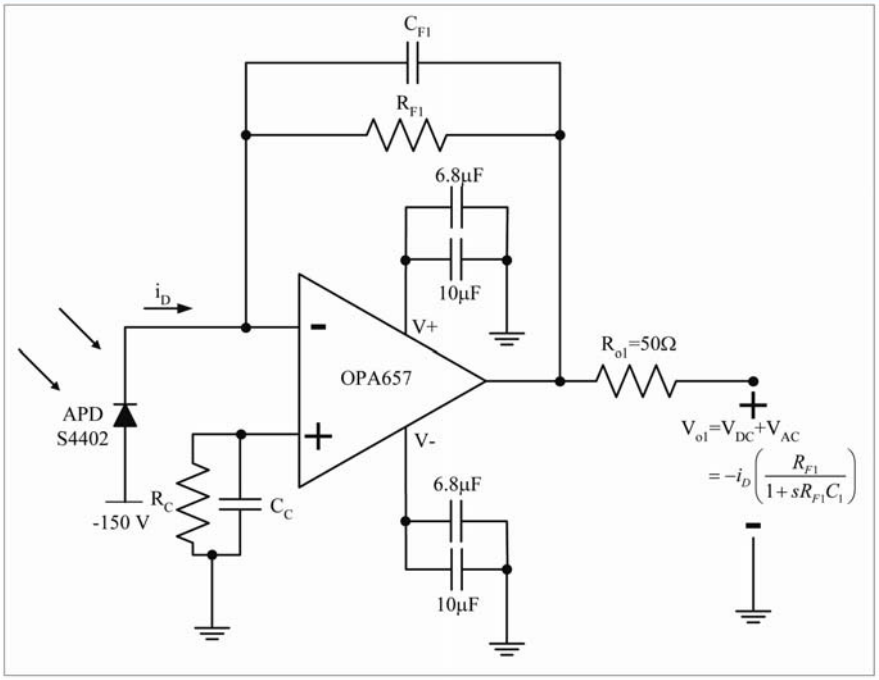

$R_{F1} = C_{F1}$ are feedback resistor and capacitor, respectively.
$R_C = C_C$ are compensated resistor and capacitor, respectively.

Fig. 2.21 Schematic of one channel APD with TIA.

The schematic of one channel APD with TIA is shown in Fig.2.21. The mobile user terminal required 4 identical circuit of the APD with TIA. The S4402 4-channel APD array and OPA657 op-amps, which has 300 MHz 3 dB cut-off frequency and 1.6 GHz gain bandwidth product (GBP), respectively, are implemented. The -150 V is the bias voltage for the S4402.

The output signals contain the average intensity that detects by APD or V_{DC} and the non-return to zero (NRZ) signal which is the communication data. Furthermore, this circuit requires the DC compensation technique to reduce the offset voltage when there is no received data (see appendix C). The circuit BW can be calculated from

$$f_c = \sqrt{\frac{GBP}{2\pi R_{F1} C_D}}, \tag{2.15}$$

where GBP is gain bandwidth product equals to 1.6 GHz (from datasheet of OPA657),

C_D is internal capacitor of APD at bias voltage (-150 volt) equals 10 pF.

Signal that is used in this study is 100 Mbps NRZ signal, so cut-off frequency is set to be approximately 100 MHz. Using 2.15 to determined R_{F1}, $R_{F1} \approx 1.5k\Omega$. The feedback capacitor C_{F1} can be determine by

$$\frac{1}{2\pi R_{F1} C_{F1}} = \sqrt{\frac{GBP}{2\pi R_{F1} C_D}}. \tag{2.16}$$

Then C_{F1} can be obtained as 1pF.

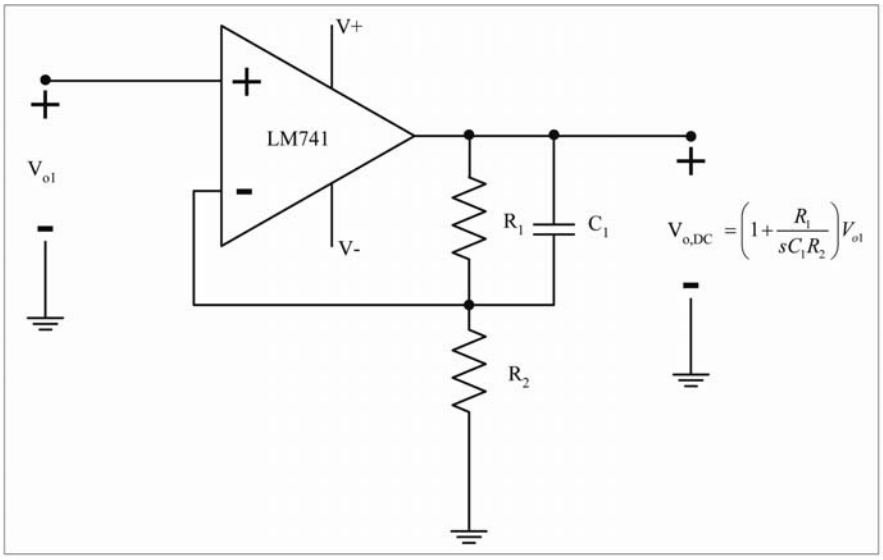

Fig. 2.22 Schematic of low pass filter and DC amplifier.

The signal from TIA is splitter to 2 circuits for the autonomous beam searching and control that processes the average intensity of the 4-channel APD and communcation data that process only the NRZ signal (is called AC signal in this study).

Input of the low pass filter and DC amplifier circuit is V_{01} from TIA circuit. This circuit amplifies the average intensity of detected signal from APD circuit and suppresses the high frequency from NRZ signal. Fig.2.22 shows schematic of low pass filter and DC amplifier using non-inverting configuration. Amplification can be set by the ratio of R_1 and R_2. The minimum gain of this circuit is equal to 1 or unity gain. The output of the low pass filter and DC amplifier circuit can be obtained as

$$V_{O,DC} = \left(1 + \frac{R_1}{sC_1R_2}\right)V_{o1} \tag{2.17}$$

If higher gain or higher output voltage level is required, connecting DC amplifier in cascade fashion results higher gain and higher order of low pass filter.

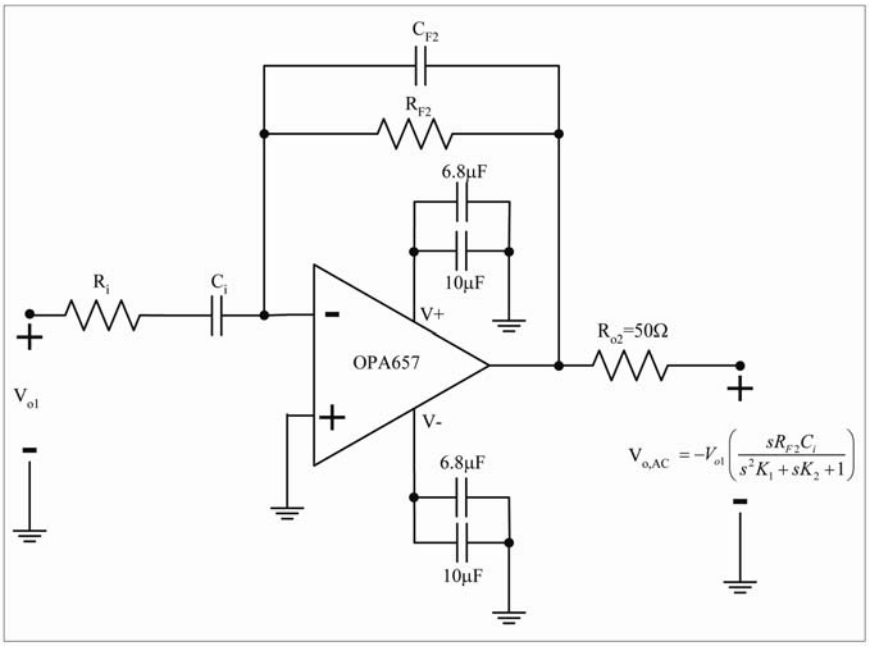

Fig. 2.23 Schematic of band pass filter and AC amplifier.

Input of the band pass filter and AC amplifier circuit is V_{01} from TIA circuit. This circuit does not amplify the average intensity of detected signal from APD circuit but it amplifies the fluctuation of signal (NRZ signal). Fig.2.23 shows schematic of band pass filter and AC amplifier using inverting configuration. The amplification 5 was chosen, due to cut-off frequency characteristic of OPA657. $R_{F2} = 560\Omega$ and $R_{o1} = R_{i1} = 51\Omega$ were chosen for the DC amplification. The 150 Hz low cut-off frequency [high pass filter characteristic] was selected to suppress the DC signal from TIA circuit, so the C_{i1} can be calculated from

$$f_{c,l} = \frac{1}{2\pi(R_{o1} + R_{i1})C_{i1}}. \tag{2.18}$$

when $\left.\begin{matrix} R_{o1} = R_{i1} = 51\Omega \\ f_{c,l} = 150\text{Hz} \end{matrix}\right\}$, C_{i1} is equal to 10 μF, then the actual low cut-off frequency is approximately equal to 156 Hz.

The 100 MHz high cut-off frequency [low pass filter characteristic] was selected to suppress high frequency noise, so the C_{F2} can be calculated from

$$f_{c,h} = \frac{1}{2\pi R_{F2} C_{F2}}. \tag{2.19}$$

When $\left.\begin{matrix} R_{F2} = 560\Omega \\ f_{c,h} = 100\text{MHz} \end{matrix}\right\}$, C_{F2} is equal to 3 pF, then the actual high cut-off frequency is approximately equal to 94.73 MHz.

If higher gain or higher output voltage level is required, connecting AC amplifier in cascade fashion results higher gain and higher order of band pass filter.

To increase the detected signal strength, the summation of signal is required. So the AC summing amplifier, which adds the detected, filtered, and amplifier from 4-channel APD, TIA and band pass filter and AC amplifier, is designed as shown in Fig.2.24. The output signal of this circuit can be estimated by

$$V_{O,SUM} = -\left(\frac{R_{F3}}{R_{i1}} V_1 + \frac{R_{F3}}{R_{i2}} V_2 + \frac{R_{F3}}{R_{i3}} V_3 + \frac{R_{F3}}{R_{i4}} V_4 \right) \tag{2.20}$$

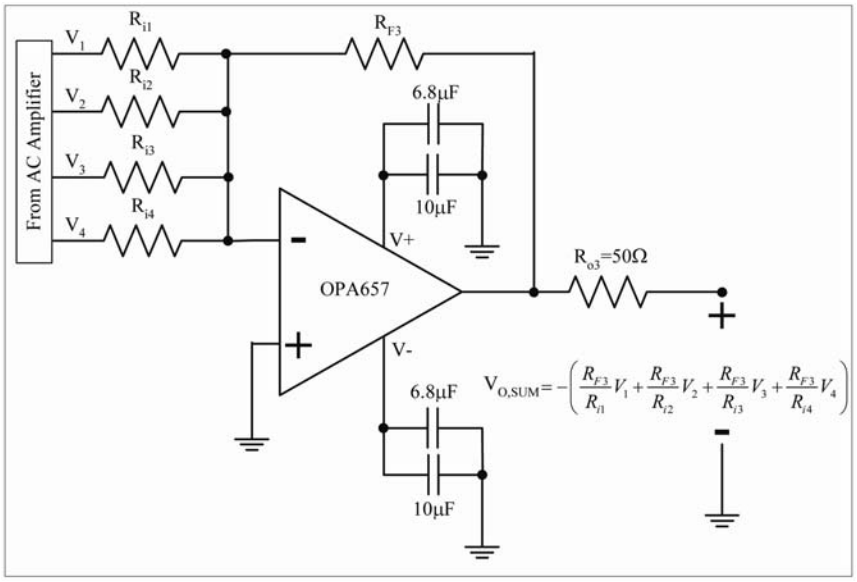

Fig. 2.24 Schematic of AC summing amplifier.

For the same amplification gain, R_{i1}, R_{i2}, R_{i3}, and R_{i4} are set to the identical value.

The schematic of processing controller for the autonomous beam searching and alignment is shown in Fig.2.25. This circuit has 4 analog channels from DC amplifiers as inputs to port A0 – A3 (internal 8-bit A/D converter of PIC controller). Outputs of this controller are to control the direction of motor into forward direction and reverse direction in both of *x*-axis and *y*-axis at port B0 – B3.

Fig.2.26 shows the block diagram of the autonomous beam alignment. PIC 16F715 is implemented as the processing controller for the autonomous beam searching and control. The processing controller processes the A/D to measure the average intensity of the detected signal from 4-channel APD, then, comparison of top with bottom channels and left with right channels are executed. If the top channel intensity is higher than bottom channel, it means the downlink is close to top channel, and then the processing controller gives command to stepping motor driver to move the posture to top channel by one step. Because of the

processing speed of processing controller is fast enough, the multi step movement of the stepping motor is not required. Using this control technique, there is no overshoot or oscillation of posture movement.

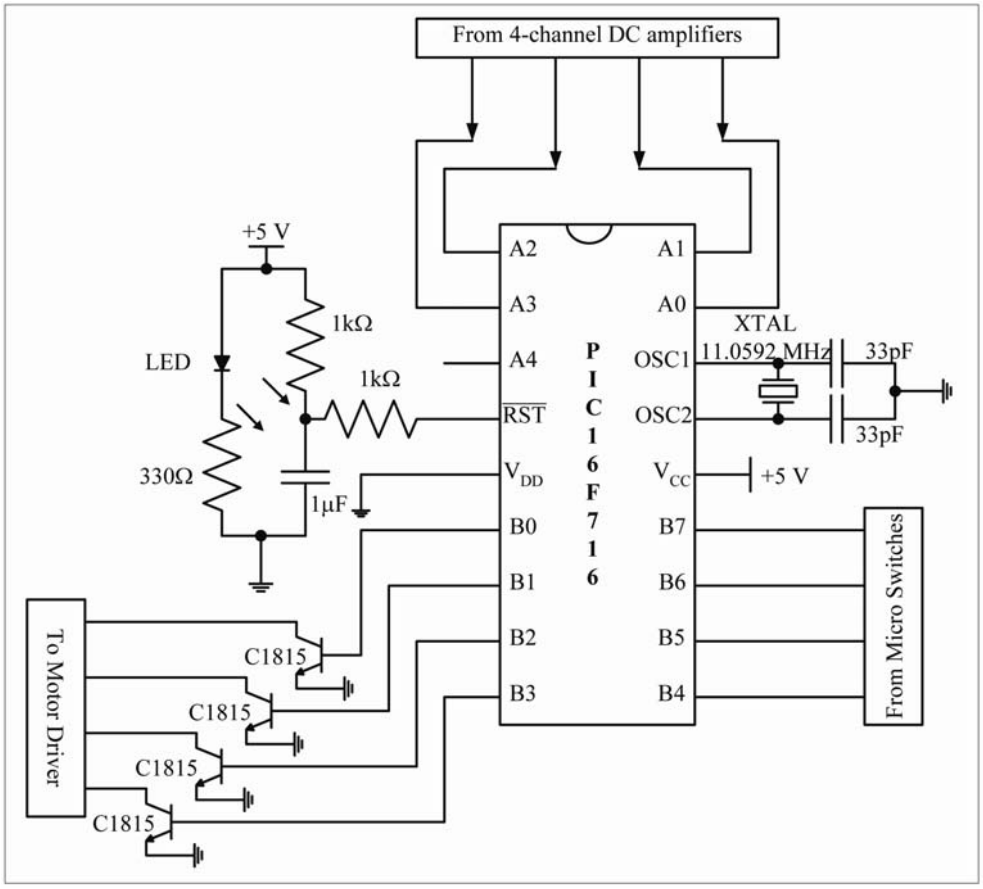

Fig. 2.25 Schematic of processing controller for the autonomous beam searching and alignment.

In practice, when the low average intensity is detected, the A/D cannot work properly, consequently, the malfunction of autonomous beam alignment is occurred. To overcome this problem, the autonomous beam searching technique is required. The additional micro switches detecting the edges of posture, which are top, bottom, left, and right edge, are required. When the average intensity is lower than the threshold, the processing controller stops the autonomous beam alignment and works on the autonomous beam searching. The autonomous beam searching starts by move the posture to the starting searching position, and then step by step move the posture like spiral shape until the average intensity is higher than the threshold

level as shown in Fig.2.27. The processing controller returns to work on the beam alignment process.

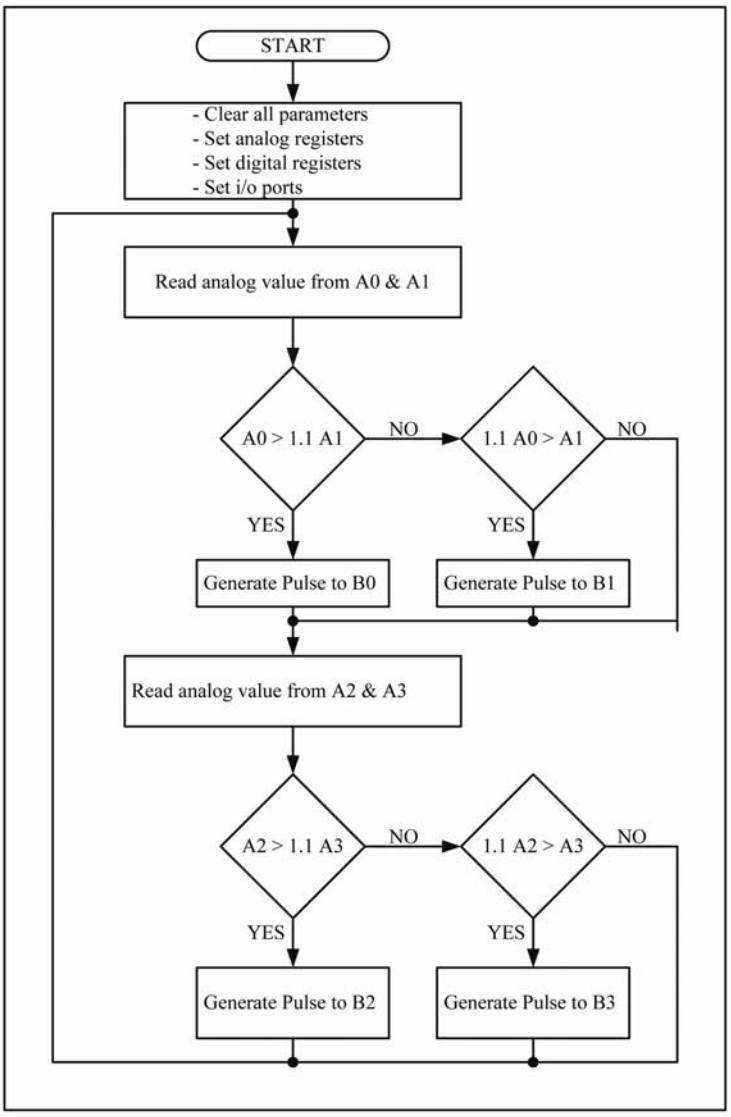

Fig. 2.26 Block diagram of the autonomous beam alignment[72].

2.4 Design Concept for Primitive Setup System

In this chapter, the concept of the total optical link of the indoor ubiquitous free space communication using OMC system was explained and discussed. The hub node has potential for multi user accessibility using the optical Tx/Rx array with the electronic switch matrixes. Moreover, the potential communication bit rate is beyond Gbps level due to photonic medium. On the mobile user terminals, the autonomous beam searching and alignment technique is able

to optimize the optical link communication even the mobile user terminals move their position under the service area of hub node.

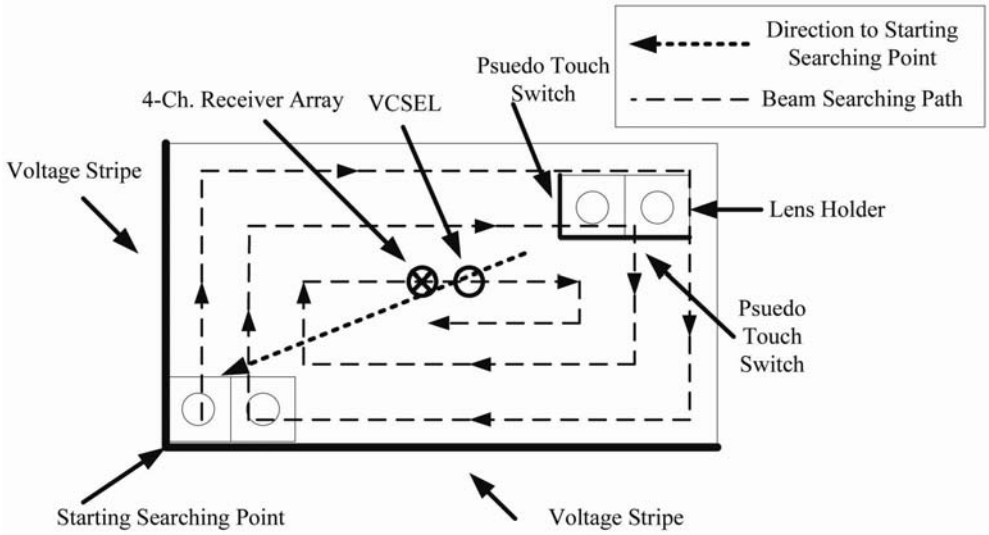

Fig. 2.27 Autonomous beam searching setup design.

In this study, the downlink communication wavelength is 850 nm due to the god communication wavelength while the uplink communication wavelength is 660 nm due to the vision chip peak respond wavelength. The proposed communication bit rate is approximately 100 Mbps. In order to obtain Gbps level, all opto-electronic and signal processing module must be implemented in the very large scale integrated (VLSI) circuit.

Chapter 3

Experimental Results Using Primitive Design System

The designs of OMC system both of optics, electronics, and signal processing designs were discussed in chapter 2. As mentioned in previous chapter, the optical link communications, which are optical downlink and uplink communications, are focused on. Due to eye-safe standard and cost optimization, the 850 nm communication wavelength is employed for the optical downlink communication. However, the 660 nm communication wavelength is employed for the uplink communication, due to the specification of peak exciatation wavelength of vision chip. In addition, the performance of the autonomous beam searching and alignment of the mobile user terminal during operation under the service area and the operation under the handover region are experimentally tested. Moreover, the position detection of the hub node for the optical uplink communication is also experimentally perform.

In this chapter, the experimental setups are described, and then the experimental results are consequently discussed. Finally, the discussions and system performance will be given at the end of this chapter.

3.1 Downlink Communication Experiments

The hub node and the mobile user terminal designs were explained in chapter 2. In this section, the service area experimental result is firstly demonstrated. The downlink communication including the autonomous beam searching and alignment of the mobile user terminal and the handover process are experimentally discussed. In addition, the signal quality or eye diagram of the downlink communication is also presented.

For the experimental setup, the actual service area must be experimentally determined. The 1x8 in-line VCSEL array, which has 250 μm pitch (see Fig. 3.1), is implemented with a thin lens that has 4.5 mm focal length as the optical Tx array of hub node. The distance between the VCSEL surface and the thin lens surface is equal to 3.5 mm. Tested operating distance is set to be 1 m. The service area, which is the circular shape, has the average service area of

7.12 cm with the 1.57 cm average handover region as shown in Fig. 3.1. Consequently, the total service area length is equal to 46.5 cm.

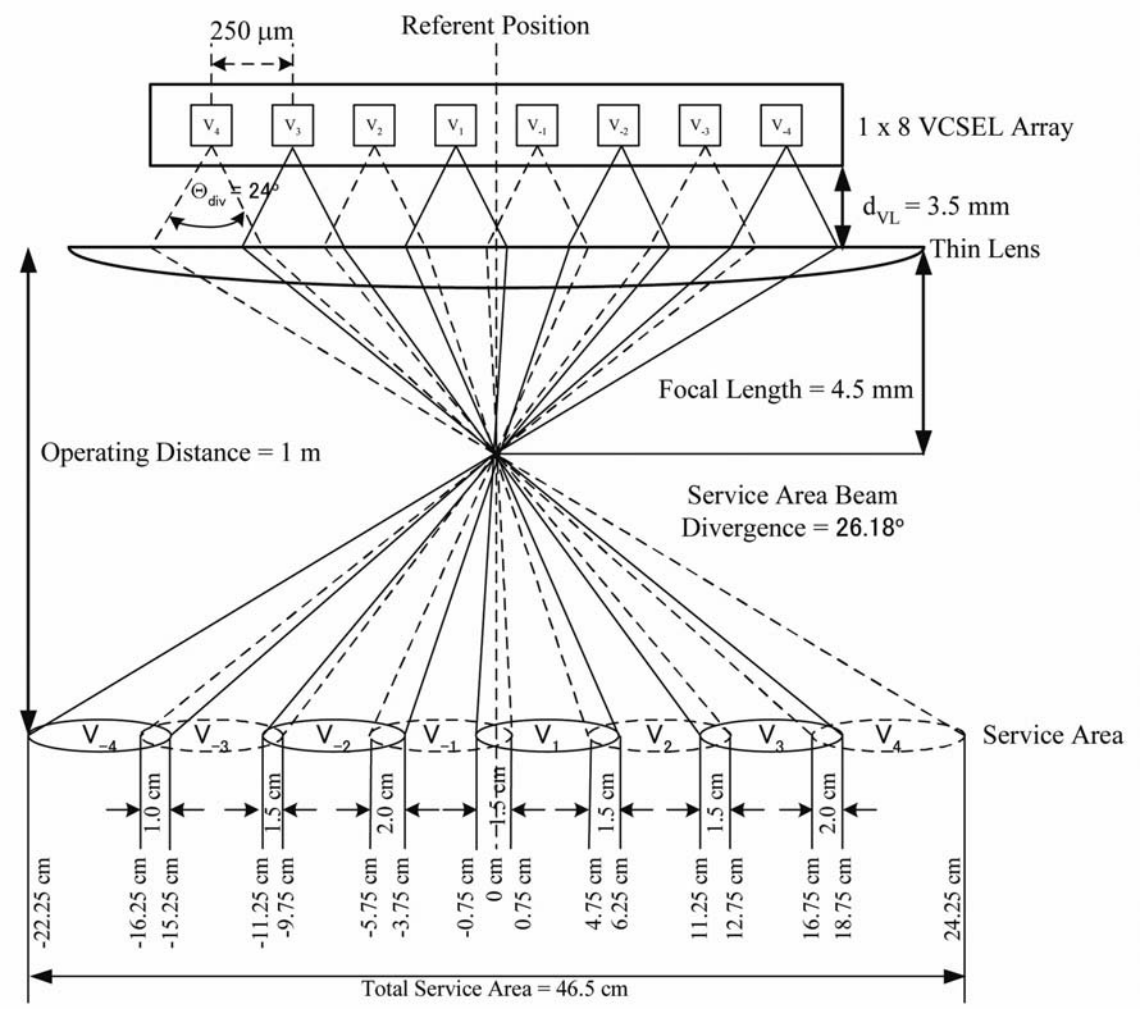

Fig. 3.1. Experimental setup and experimental result of service area verification at 1 m height.

Using eq. (2.5) to estimate the model in Fig. 3.1, the average diameter of the service area is equal to 32.91 cm with 38.44 cm handover region. Consequently, the total service area length is equal to 71.62 cm. To compare with the estimation with the experimental result, there are 4.62 and 24.48 times difference of the service area diameter and the handover region, respectively. The experimental results showed the much smaller of service area and overlapped region because the estimated model based on the end-to-end beam profile. The end-to-end beam profile is not applicable for the practical utilities, thus, the effective beam profile is only half power beam width.

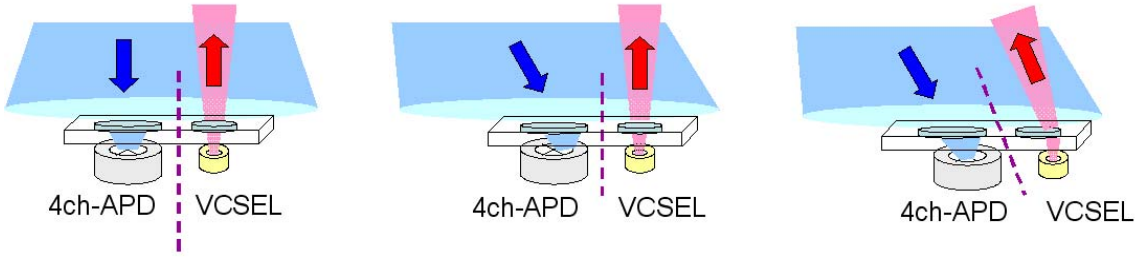

(a) (b) (c)

Fig. 3.2. Misalignment effect with/without movable lenses unit control of the mobile user terminal (a) 0º downlink beam, (b) downlink beam with stationary lenses unit, and (c) downlink beam with lenses revision.

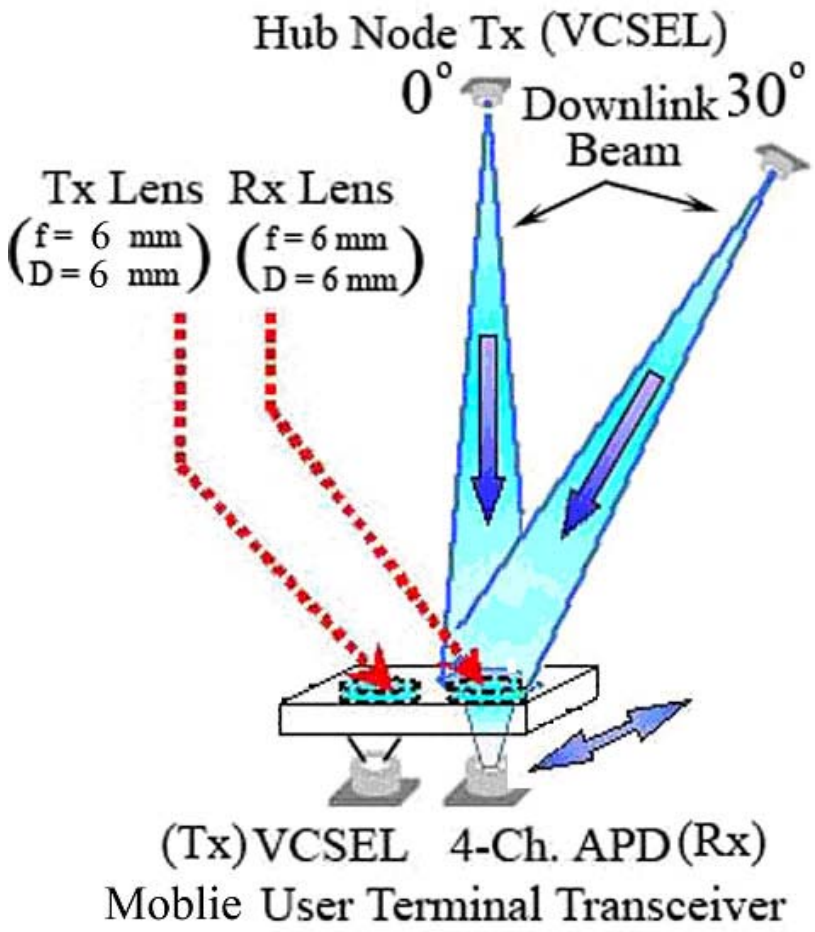

Fig. 3.3. Experimental setup of angle dependence of the mobile user terminal with movable lenses unit[72].

The service area and the handover region were experimentally determined. The mobile user terminal is experimentally discussed. The VCSEL and the 4-channel APD with the movable lenses unit were implemented as the optical Tx and Rx, respectively, as shown in Fig. 3.2. When the downlink beam is aligned at 0º the uplink beam automatically directly returned to the hub node as shown in Fig. 3.2(a). If the mobile user terminals move their position, the beam misalignment is occurred as shown in Fig. 3.2(a). In order to return the uplink beam to the hub node, the movable lenses unit that can balance the detected signal to the 4-channel APD is able to automatically return the uplink beam to the hub node as shown in Fig. 3.2 (c).

The 4-channel APD that was implemented in study has 1 mm detecting surface. Refer to Fig. 2.10, the beam position with various incident beam angles of the stationary lens unit of the mobile user terminal Rx. It implies that ±10º of FOV or the incident beam angle can detect the incident beam. Fig. 3.3 shows the experimental setup of angle dependence of the mobile user terminal with movable lenses unit. As mentioned in chapter 2, the lenses that were implemented in this study are identical lenses, which have 6 mm focal length with 6 mm lens diameter. With stationary lens unit, the experimental result of the detected downlink beam with various downlink beam angle is shown in Fig. 3.4. The experimental result was agreed with the estimated model in Fig. 2.10.

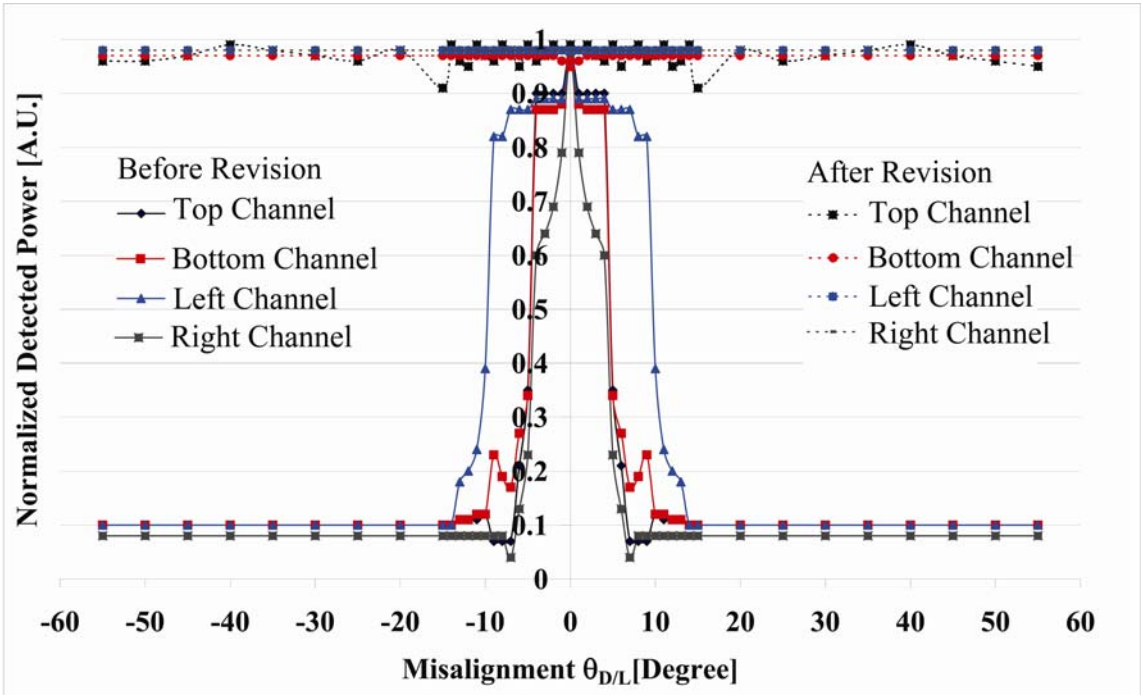

Fig. 3.4. Experimental result of angle dependence of the mobile user terminal Rx.

When the misalignment is occurred within 1 mm detected area of the 4-channel APD surface, the autonomous beam alignment can well perform the lens revision and make the balance of the detected optical signal. In addition, applying the autonomous beam alignment, the FOV increased to be ±60º (see Fig. 3.4), which is wide enough for the operation under the service area of the hub node or handover operation.

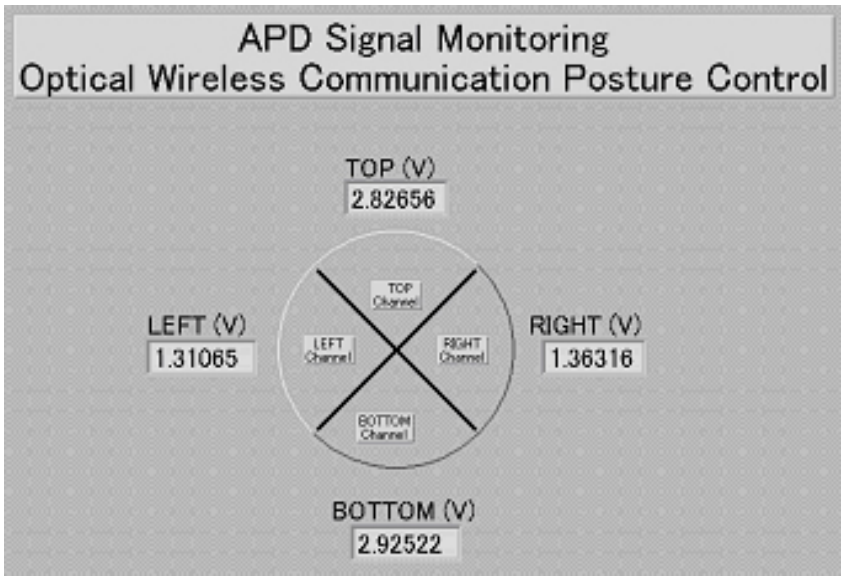

(a)

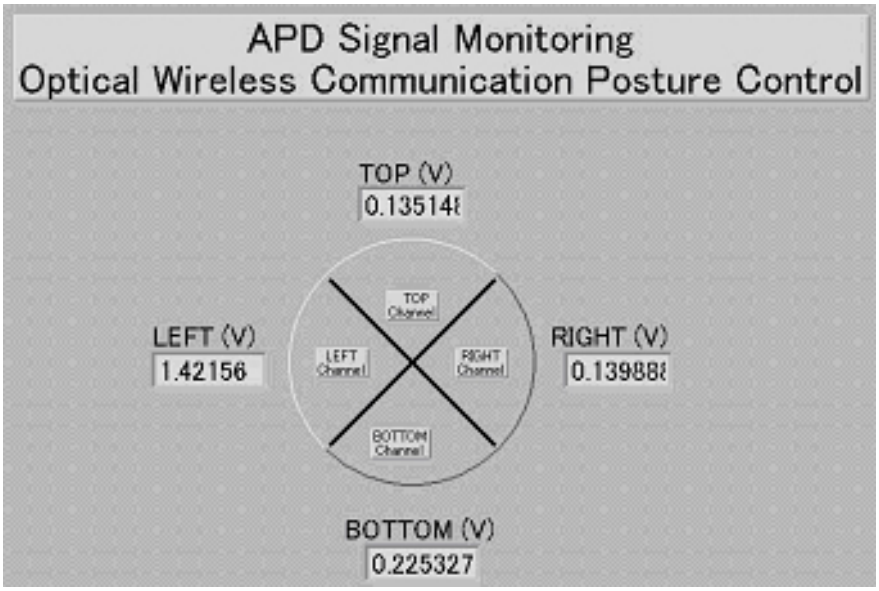

(b)

Fig. 3.5. APD signal monitoring of 4-channel APD (a) at balance condition and (b) misalignment beam detection condition.

Laboratory virtual instrumentations engineering workbench (LabVIEW) was programmed to monitor the detected beam as shown in Fig. 3.5. The detail programming is explained in Appendix D. Fig. 3.5(a) shows the balance condition of the 4-channel APD. It seems to be unbalanced in x-axis and y-axis. However, the control condition of the autonomous beam alignment is x-axis independent and y-axis independent. So, the autonomous beam alignment requires only equal signal in only x-axis or y-axis. However, the absolute equal signal is practically impossible, so only 5% fluctuation is small enough for the beam alignment control. Fig. 3.5(b) shows the misalignment detection of the 4-channel APD; only left channel can detect the incident downlink beam. After the autonomous beam alignment was operated, the balanced condition of the downlink beam detection was realized as shown in Fig. 3.5(a). Fig. 3.6 shows the actual transceiver of the mobile user terminal with movable lenses unit.

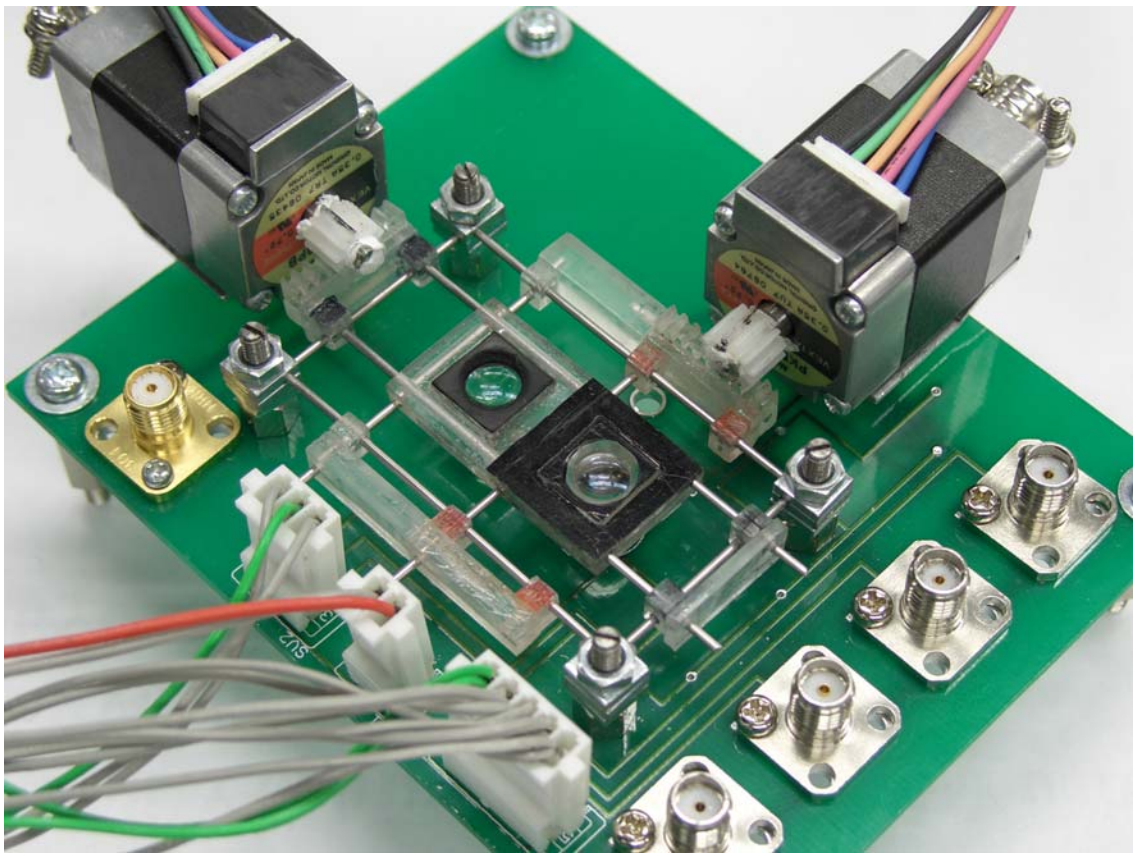

Fig. 3.6. The actual transceiver of the mobile user terminal with the movable lens unit.

For the handover region, the overlapped area of two nearby service areas is required as shown in Fig. 3.7. When the mobile user terminal moves only inside a single service area, only a few degrees is required to revise the posture of the movable lenses unit, due to non-uniform

distribution of optical field. However, if the mobile user terminal moves from cell 1 to cell 2, the misalignment detection is occurred; only one channel can detect the downlink beam (see Fig. 3.7). At the edge of cell 1, the mobile user terminal sends a command to request for the handover process. Thus, the hub node switches on the nearby cell (the request cell), after that the mobile user terminal revises the posture of the movable lenses unit to obtain the balance condition of the 4-channel APD. Apply this procedure; the link communication break has never occurred. The mobile user terminal with the autonomous beam alignment is able to make the flexible optical link communication without optical link break down.

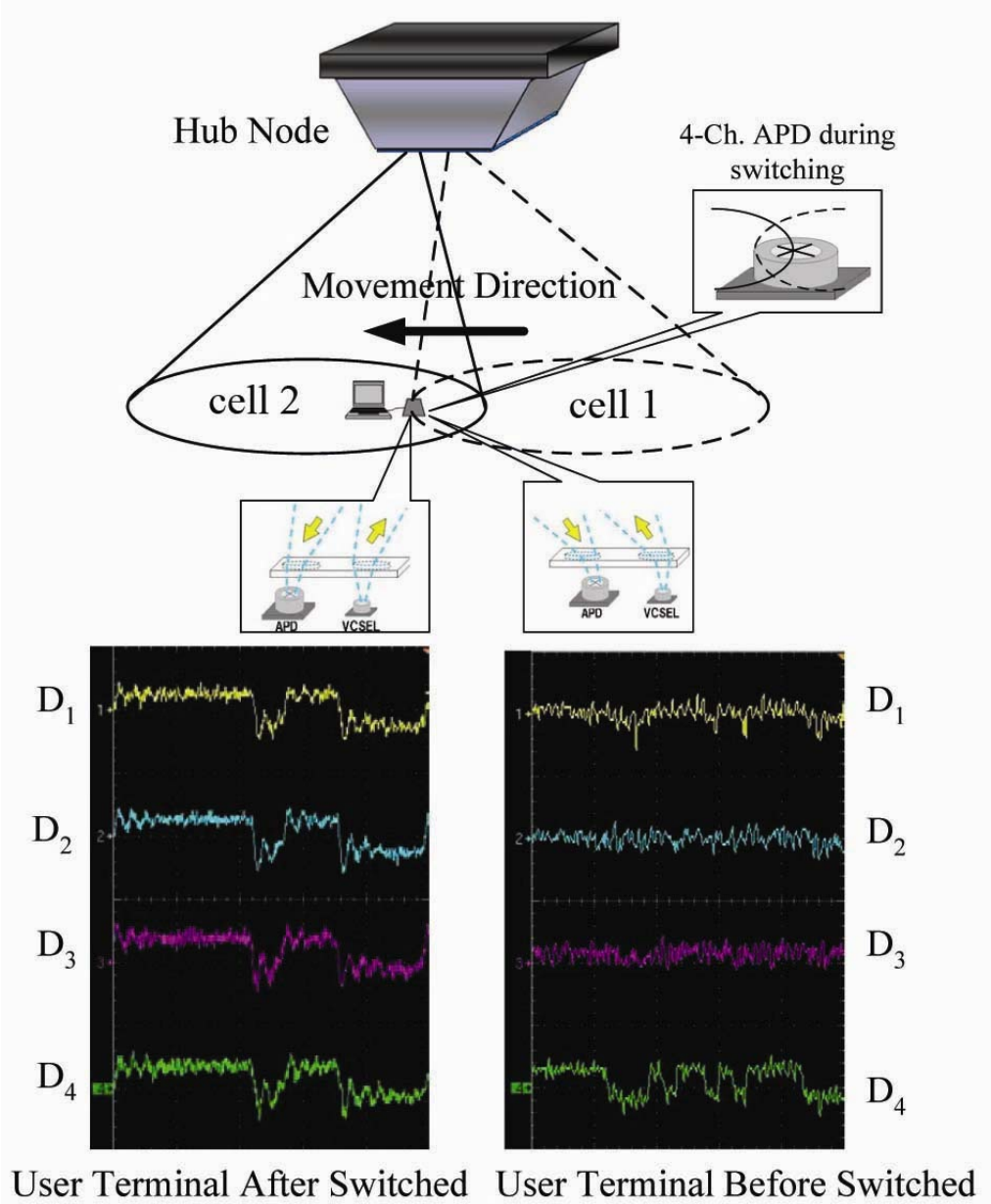

Fig. 3.7. Handover process of the mobile user terminal[72].

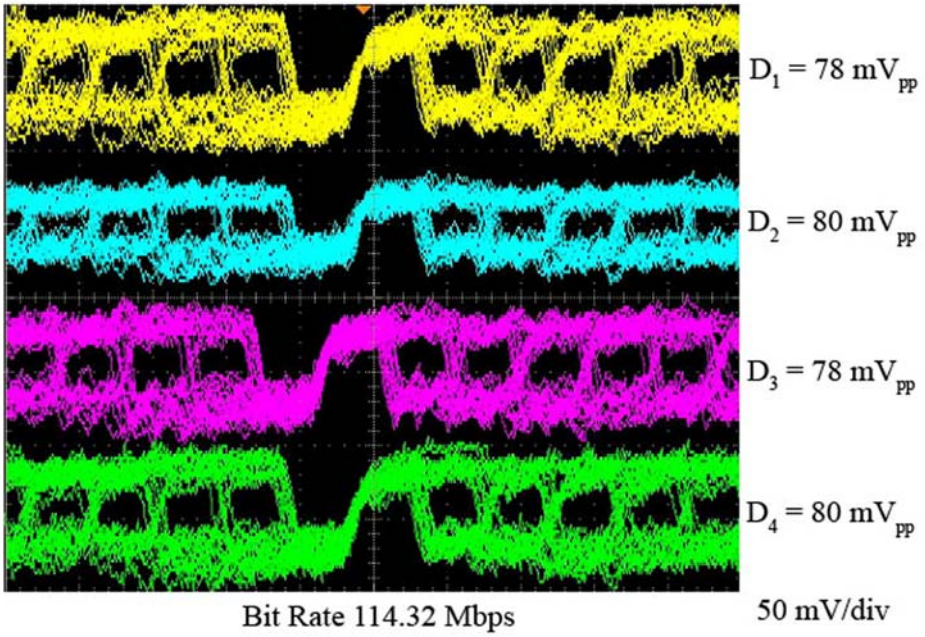

Fig. 3.8. The detected downlink beam at balance condition of the mobile user terminal 4-channel APD[72].

Fig. 3.8 shows the signal performance of the detected downlink beam at balance condition of the mobile user terminal 4-channel APD. As mentioned in chapter 2, these signals must be amplified, filtered, and summed and then sent to the signal and control splitter to decode the communication signal and control command for the high speed communication and the OMC mechanism control, respectively.

In case of low optical signal or out of service area, the autonomous beam alignment cannot work properly because the low voltage signal causes malfunction of the mobile user terminal processing control. Thus, the autonomous beam searching must be implemented to overcome low optical signal and out of service area. If the mobile user terminal processing controller senses the low optical signal, the mobile user terminal processing controller sets the starting point for the autonomous beam searching. Consequently, the processing controller searches the downlink beam by moving the movable lenses unit according to the spiral shape. After the detected downlink beam is over the threshold, the autonomous beam alignment will be operated instead of the autonomous beam searching. On the other hand, if the movable lenses unit searches for the whole area of the movable lenses unit, the processing controller will show the out of service indication.

3.2 Uplink Communication Experiments

The service area estimation and the downlink beam communication including the autonomous beam searching and alignment were experimentally discussed in previous section. In this section, the uplink communication including the returned uplink beam from the mobile user terminal after the autonomous beam alignment is operated and the position detection of vision chip are experimentally discussed.

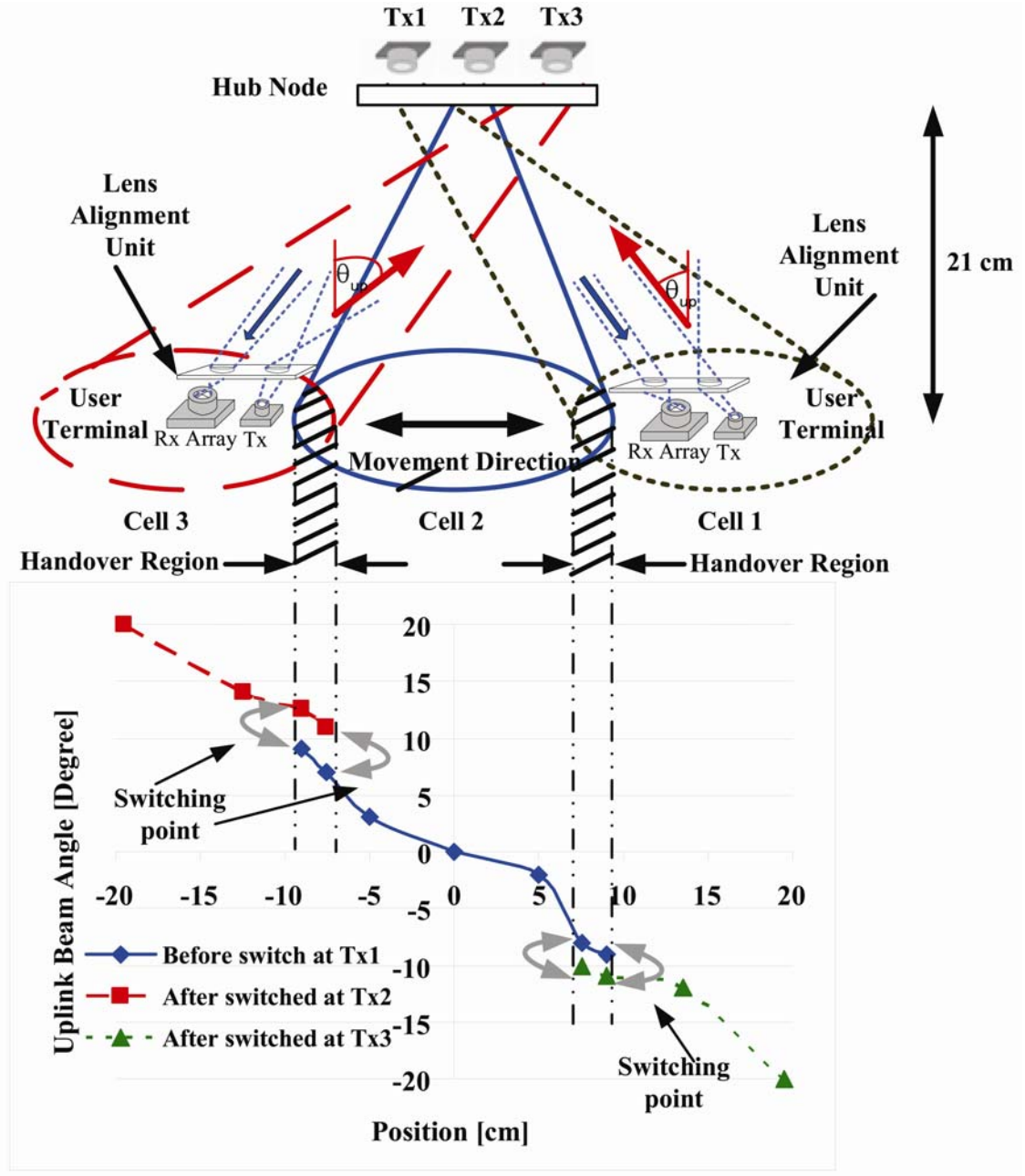

Fig. 3.9. Experimental setup and result of uplink beam communication at the operating distance of 21 cm[71].

This section is the consequent result of the downlink beam communication with the autonomous beam alignment. Refer to Fig. 3.2, the uplink beam is automatically returned to the hub node. However, the return angle of uplink beam must be experimentally investigated. Fig. 3.9 shows the experimental setup and result of uplink beam communication at the operating distance of 21 cm. In this experiment, the 3 VCSEL with different downlink beam angles were tested. The service area is 20 cm with 3.5 cm handover region. The mobile user terminal moves from cell 1 to cell 2 and cell 2 to cell 3. The total moving distance is 40 cm. At 21 cm operating distance, the ratio of the uplink beam angle with the moving distance is approximately equal to 1. In addition, the uplink beam angle during the handover process of cell 1 and cell 2 is suddenly shifted by a few degrees. Moreover, the uplink beam angle during the handover process of cell 2 and cell 3 is also suddenly shift by a few degrees. The downlink and uplink beam angles experimentally shows in Fig. 3.10. The ratio of downlink beam angle with the uplink beam angle is approximately equal to 1. Whereas, the average uplink beam angle change during handover process is equal to 3.2 degree. It implies that the change of the downlink beam angle with respect to the uplink beam angle in any operating height is equal to 1. In addition, during the handover process the average uplink beam angle is suddenly change by a few degrees in any operating height.

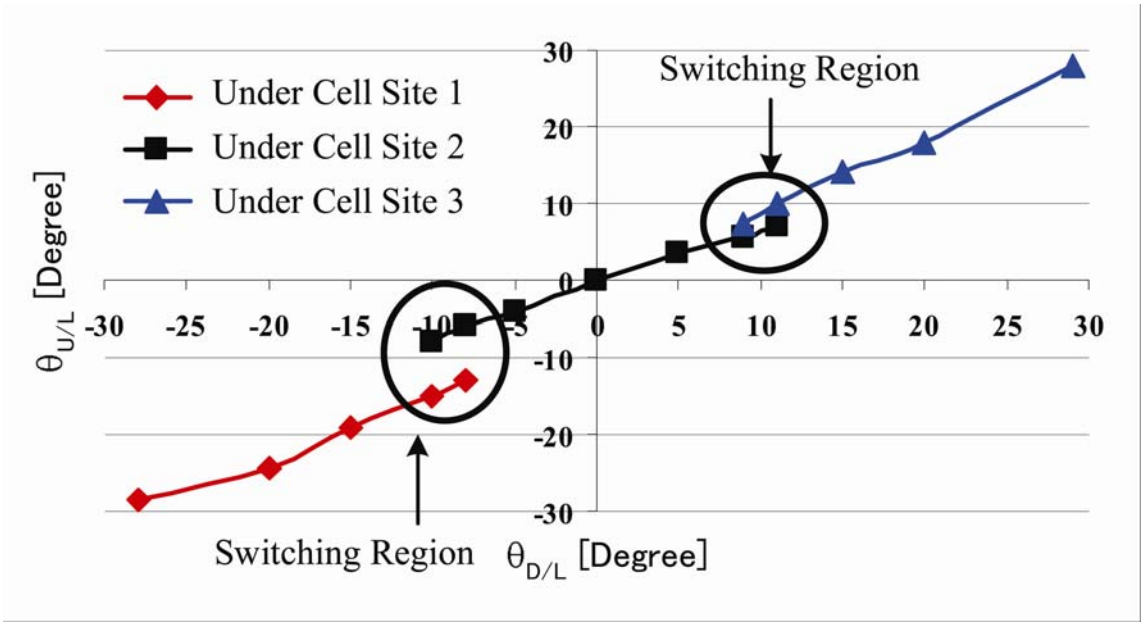

Fig. 3.10. The experimental result of uplink and downlink beam angle.

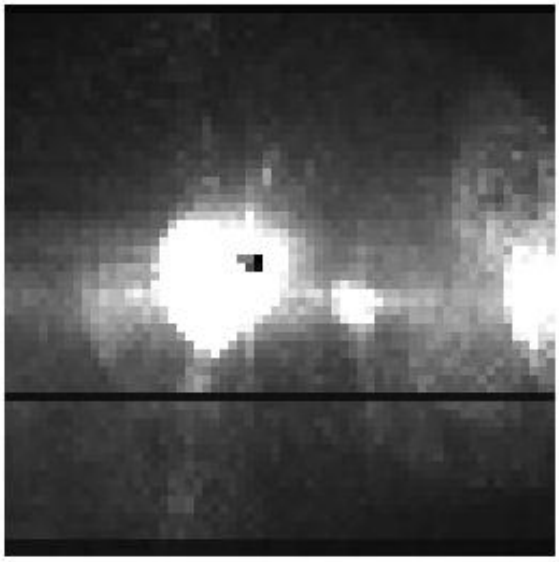

(a)

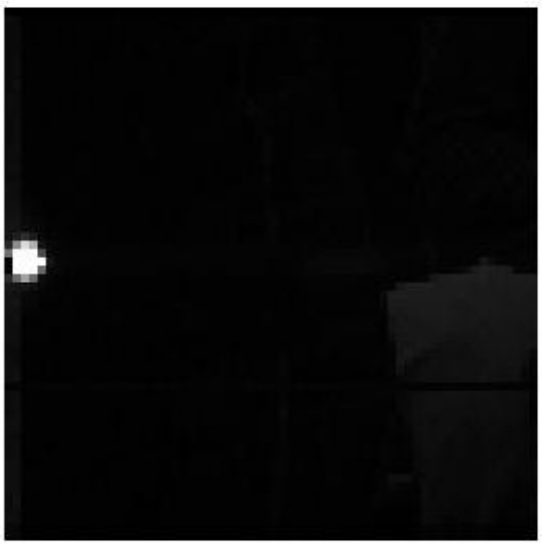

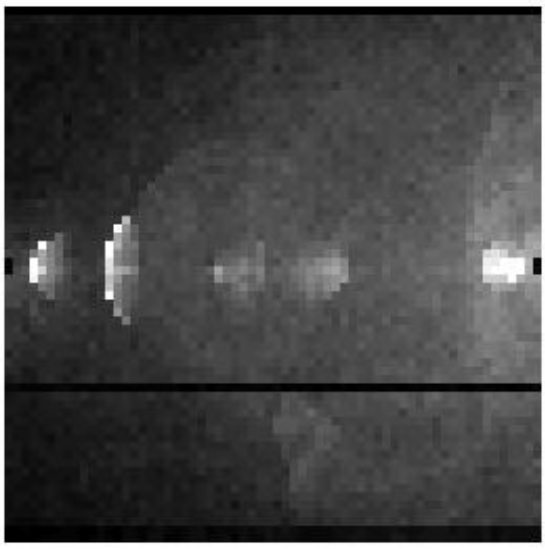

(b) (c)

Fig. 3.11. The position detection of vision chip (a) 0º uplink beam angle, (b) -19º uplink beam angle, and (c) 19º uplink beam angle.

The vision chip with lens set has the approximately ±19º beam divergence. Fig. 3.11 shows the position detection of vision chip with 0º, -19º, and 19º uplink beam angle. Because of the employed vision chip is the set from NAIST, the detected beam is not well focused. Thus, the beam at the vision chip surface is very large which covers approximately 9x9 pixels. In

addition, this vision chip sensitivity is very low. It required incident power approximately 1 mW or more of focusing beam to operate with the communication data. Up to present, we cannot modify the vision chip by ourselves. So, the experimental result of the vision chip is only the position detection of the mobile user terminal at various uplink beam angle.

3.3 Discussions

The downlink communication that was implemented in this study is 850 nm, due to eye-safe and effective cost. The uplink communication that was implemented in study is 660 nm, due to the peak respond wavelength of vision chip. Applying the autonomous beam searching and alignment mobile user terminals with the OMC hub node and electronic switching matrix, the multi user p-to-p accessibility can well perform without any link break down. Consequently, it utilized the flexibility for the mobile user terminals.

The primitive design in this study is 1 m operating distance with the 4.5 mm focal length thin lens and the 3.5 mm distance between VCSEL surface and thin lens surface resulting of the 32.91 and 38.44 cm service area diameter and handover region, respectively. From the experiment, the full beam width cannot be estimated the service area; only the half power beam width is an effective beam divergence that is estimated the service area. The average effective service area diameter and handover region from the experiment were 7.12 and 1.57 cm, respectively. There are 4.62 and 24.48 times differences between estimated and experimental results. Thus, the effective total service area diameter at 4 m operating distance is 1.86 m with 28.48 cm service area and 6.28 cm handover region. To adjust the service area size and the handover region, the focal length of lens that is employed to defocus the VCSEL beam, the distance between VCSEL surface and lens surface, and the operating distance must be carefully calculated. With the same operating distance, the changes of focal length of lens and distance between VCSEL surface and lens surface are inversely proportional to the service area size and the handover region. As can be seen from the estimated model and experimental result, the longer VCSEL pitch is required to obtain the proper handover region. In this study, the 1x8 in-line VCSEL with 250 μm was employed, so the solution to obtain the proper handover region is not to operate all VCSEL cell but operate one cell and non-operate 1 or 2 nearby cells because service area diameter was spread out at the longer operating distance. At the 4 m operating distance, the proper VCSEL pitch with the 4.5 mm focal length

thin lens and 3.5 mm distance between VCSEL surface and thin lens surface is more than 1 mm pitch.

On the other hand, the vision chip was employed as the hub node optical Rx array. Due to this vision chip was implemented by fixed specification from NAIST, the modification is quite difficult for us. The functions of the vision chip that were verified are the position detection of the mobile user terminals and uplink signal. The position detection of the mobile user terminals can well perform. The FOV of this vision chip is ±19º. The effective detected service area is 2.76 m that is approximately 50% larger coverage area of the 1x8 in-line VCSEL array. However, the signal quality of this vision chip is not good enough because it requires the focused beam spot of 1 mW incident power to operate for the data communication. In order to obtain the better optical signal quality, the design of vision chip lens must be revised to obtain the focus beam diameter of less than 100 μm, which is the vision chip pixel size. In addition, the operating bit rate of this vision chip is as low as 10 Mbps.

At the mobile user terminals, when the mobile user terminals move their position with stationary lens unit, the misalignment of downlink beam is occurred. With our design, the misalignment effect with stationary lens can detect the downlink beam approximately ±10º, which was fit to the calculation results. When the misalignment is occurred, the autonomous beam alignment must be applied to optimized downlink beam communication resulting of the flexible mobile user terminals. The autonomous beam alignment can increase FOV up to ±60º. This was limited by the can case of the 4-channel APD. However, the FOV of ±60º is wide enough for the mobile user terminal operation. In addition, the FOV of our design can be wider but it was limited due to the 4-channel APD case. In case of low optical downlink beam power or out of service area, the autonomous beam searching must be applied. The low detected signal causes malfunction of processing controller due to the quantization noise of processing controller internal A/D. When the autonomous beam searching is under operation and the detected downlink beam power is over the threshold power, the autonomous beam searching would be stopped and return to the autonomous beam alignment operation. By apply the autonomous beam searching and alignment, the link communication will not break down.

Table 3.1 System performance evaluation.

Function	Expected Performance	Primitive Design Performance
Service area size/Divergence	≈ 80 cm diameter/ > 30º at 4 m	7.12 cm diameter/ 26.18º at 1 m
Downlink bit rate	> 1 Gbps	114.32 Mbps
Uplink bit rate	> 1 Gbps	Undetermined
Hub node sensitivity	< 0.1 μW	> 1 mW
Mobile user terminal sensitivity	< 0.1 μW	≈ 10 μW
P-to-p multi user accessibility	Require	Done
Handover process	Require	Done
Autonomous beam alignment	Require	Done
Autonomous beam searching	Require	Done

Table 3.1 shows the system performance evaluation of the expected design performance and primitive design performance. From the system design, an approximately 80 cm service area diameter with 30º service area beam divergence is expected but from the experiment, 7.12 cm service area diameter with 26.18º beam service area beam divergence was obtained. The expected downlink bit rate is greater than 1 Gbps but 114.32 Mbps can be obtained from the experiment with good eye diagram. The expected uplink bit rate is also greater than 1 Gbps but it cannot be determined from the experiment due to very low sensitivity of vision chip. The expected mobile user terminal sensitivity is less than 0.1 μW but approximately 10 μW sensitivity can be obtained. For the p-to-p multi user accessibility, handover process, and autonomous beam alignment and searching are expected and well performed both of system design and primitive design.

The concept of OMC system was verified but the bit rate and signal quality both of downlink and uplink communication are not good. To improve the bit rate and signal quality, all opto-electronics and signal processing modules must be implemented into VLSI that can operate with the Gbps level. The potential of communication bit rate was expected to be faster than 1 Gbps. However, the higher bit rate and lower BER can cause increase of optical size due to photon limitation.

Chapter 4

Conclusions and Future Extended Study

The indoor ubiquitous optical free space communication using OMC system concept design was discussed in the chapter 2. The downlink and uplink experiments were also shown in Chapter 3. In this chapter, the conclusions, the key features of this study will be given.

4.1 Summary of Results

The key features of the indoor ubiquitous optical free space communication using OMC system are high bit rate communication, high security, low power consumption, light weight, compact size, point-to-point multi user accessibility, and high flexibility. Using photonics as the medium, the potential of high bit rate communication is possible but depending on the detected optical power and the desired BER. Consequently, high security, low power consumption, light weight, and compact size are the consecutive results of using photonics as the medium. However, the compactness of optical size is directly proportional to the bit rate and BER. For point-to point multi user accessibility, the optical Tx/Rx array with lenses and the electronic switch matrixes are capable. Moreover, using the lens with the optical Tx or Rx is able to determine the location of the mobile user terminal. This function is the great valuable feature of OMC system. However, in order to control the switching of the electronic switch matrixes, the control command consisting of the MAC address, current cell position of hub node, request for the handover, *etc.* must be inserted into a single frame communication with the communication data. The communication data acts as the carrier frequency of the control command. The combiner of signal and control command requires the PPL acts as frequency synthesizer at 100 MHz for logic “0” and 100.1 MHz for logic one. Reverse process of the PLL is able to act as frequency recovery to read the communication data and control command. The autonomous beam searching and alignment can make the flexibility to the mobile user terminals. Even the mobile user terminals change their position in the service area of any OMC hub node; the communication signal (optical power) can be optimized, due to the autonomous beam alignment. In addition, when the communication signal is weak, the autonomous beam searching is required to justify the optimum communication signal location.

In this study, the uplink and downlink communication were experimentally realized. The 850 nm downlink oscillation wavelength was employed because it is one of the communication wavelengths. However, the 660 nm uplink oscillation wavelength was employed due to the limitation of vision chip specification. The downlink communication bit rate was tested at approximately 114 Mbps that was limited by the TIA design using op-amp while the uplink communication bit rate was tested at approximately 6.33 Mbps that was limited by the vision chip specification. The feature of point-to-point multi user accessibility, which is able to determine the location of the user terminal, is the great result of the OMC system that can extend for the future studies. The features of autonomous beam searching and alignment of the mobile user terminals can optimize the link communication performance that makes the system more flexible.

Due to the advance technology in opto-mechno-electronics, the OMC system has the good future to increase the communication speed, to optimize size, and improve other performance. In order to obtain all design specifications, the opto-electronics and signal processing scheme must be implemented in VLSI. Gbps level communication bit rate and a few cm^3 of the optical transceiver of the mobile user terminals are possible.

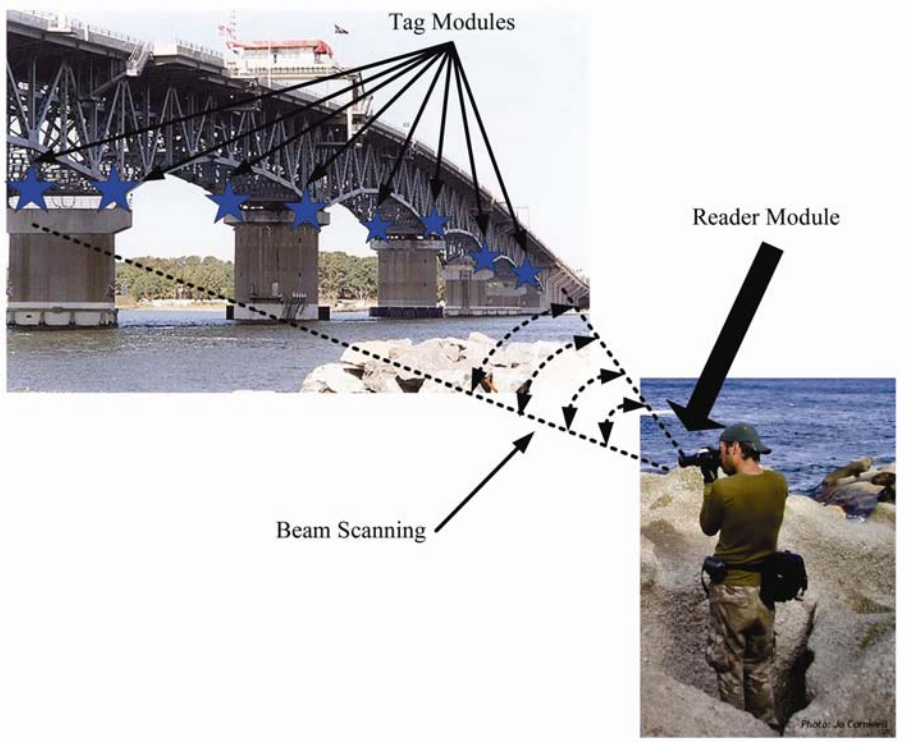

Fig. 4.1. An application of the proposed optical IC tag.

4.2 Future Extended Study

Vision chip is not only applicable for the indoor ubiquitous optical free space communications but it is also applicable for optical IC tag. The optical IC tag is designed and implemented using the similar concept of radio frequency identification (RFID) but medium is photonics. The useful of optical IC tag is long operating distance wireless communication (potential of 100 meter or more) without RF interference to other electronic appliances. The optical IC tag project concept had been proposed for future extended study.

One of the applications of the proposed optical IC tag is monitoring infrastructure as shown in Fig.4.1. The infrastructure, *e.g.* bridge *etc.*, always requires maintenance. At present, the sensors, *e.g.* strain gauge, *etc.*, are attached to the main structure and link with many long cables to the monitoring station. Moreover, it dissipates a lot of power. To overcome the cable problem and power consumption, the optical IC tag is proposed. The optical IC tag consists of reader module and tag modules. Fig.4.2 shows the overall optical IC tag proposed design.

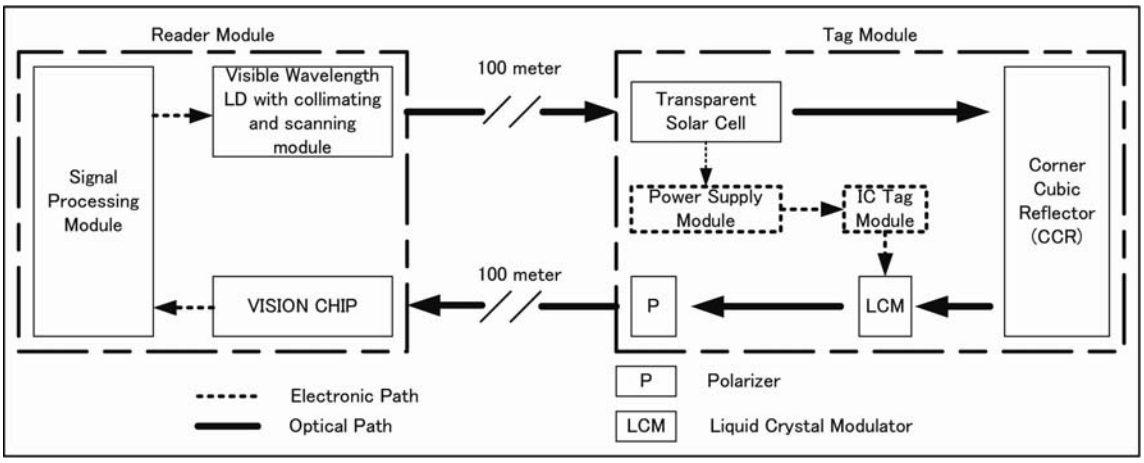

Fig. 4.2. Overall optical IC tag system proposal design.

A 633 nm red LD with collimating and beam scanning modules was designed as a transmitter of reader module launching optical power tag module. A 100-meter operating distance was designed. Light from reader module was launched to tag module pass thru transparent solar cell producing a small power supply for IC tag module and liquid crystal modulator (LCM), corner cubic reflector (CCR) reflecting light into the same path that launched in, LCM

modulating the signal from IC tag module (by rotating polarization axis by 90º), and polarizer to block the 90º rotated polarization axis light from LCM. After that, the modulated optical signal is transmitted back to reader module and is detected by vision chip to convert optical signal to electronic signal and process by signal processing module. Apply the same concept of position scanning as the hub node of the indoor ubiquitous optical free space communication, the data reader and position recognition can be realized. Up to present, the polarization dependent of CCR was tested. There is no polarization dependence in any incident angle of CCR. Signal modulation using LCM was tested and well operated at wavelength 633 nm.

In summary, optical IC tag is a very low power consumption long distance communication device due to transparent solar cell based power supply and photonic as medium. The operating distance was designed approximately 100 meter or more. Due to the switching operation of LCM is not so fast, signal data rate was expected to reach only kbps level.

Acknowledgements

The author wishes to express his gratitude to his advisor, Prof. Dr. Koji Nonaka, who has helped and encouraged him throughout this study. His special thank is offered to Dr. Nonaka not only taking care of him in study but also in everything else.

The author is grateful to Prof. Dr. Katasushi Iwashita, Prof. Dr. Masahiro Kimura, Prof. Dr. Masayoshi Tachibana, and Prof. Dr. Masanori Hamamura, committee members, who have given several fruitful comments and suggestions in many topics of this study and on improvements of his study. Furthermore, the author would like to sincerely thank to Assoc. Prof. Dr. Keiichiro Kagawa from NAIST who has prepared for the vision chip and given several valuable comments and suggestions on his study.

The author extends his sincere thanks to Asst. Prof. Dr.Prinya Tantaswadi and Asst. Prof. Dr. Chalie Charoenlarpnopparut, the author master course's advisor and thesis committee, respectively, for their fruitful suggestions and comments for improvements.

The author would like to thank Dr. Taweesak Samanchuen and Mr. Sarun Ratananan for technical discussions and assistances on the electronic ideas. Without their brilliant guidances and assistances, the author could not come up with this dissertation. Mr. Toshihiro Kato, Mr. Yoichi Hamada, Mr. Tsuyoshi Itagaki, and students in Nonaka Laboratory are thanked for supporting and assisting the author to complete his study. Without their brilliant assistance, the author may not success with this dissertation.

The author would like to thanks for the devotions from many teachers in the past. Thanks are also offered for the author's family, father, mother, and sisters for sharing and discussing all his problems. Everything they have done gives him an inspiration and strength to pass through tough time.

Finally, the author thanks his friends for helping, sharing the new ideas to solve his problems through this study. He also would like to thank and acknowledge every supports and he would like to dedicate this work to all people mentioned.

References

[1] W. J. Severin, J. W. Tankard, Communication Theories: Origins, Methods, and Uses in the Mass Media, New York: Hastings House, pp. 2 – 8, 1979.

[2] D. J. Marie, From Tele-Communicare to Telecommunications, 2004.

[3] Telecommunication, tele- and communication, New Oxford American Dictionary 2nd Edition, 2005.

[4] S. Haykin, Communication Systems, 4th Edition, John Wiley & Sons, pp. 1 – 3, 2001.

[5] A. Ambardar, Analog and Digital Signal Processing, 2nd Edition, Cengage-Engineering, pp. 1 – 2, 1999.

[6] E. M. Lenert, "A Communication Theory Perspective on Telecommunications Policy," Journal of Communications, Vol. 48, No. 4, pp. 3 – 23, 1998.

[7] L. H. Röller and W. Leonard, "Telecommunications Infrastructure and Economic Development: A Simultaneous Approach," American Economic Review, Vol. 91, No. 4, pp. 909 – 923, 2001.

[8] A. Riaz. "The role of telecommunications in economic growth: proposal for an alternative framework of analysis," Media, Culture & Society, Vol. 19, No. 4, pp. 557 – 583, 1997.

[9] T. William, Native American Smoke Signals, 2005.

[10] Talking Drums, Instrument Encyclopedia, Cultural Heritage for Community Outreach, 1996.

[11] J. B. Calvert, The Electromagnetic Telegraph, 2004.

[12] G. Elisha, Oberlin College Archives, Electronic Oberlin Group, 2006.

[13] http://chem.ch.huji.ac.il/~eugeniik/history/meucci.html.

[14] History of AT&T, AT&T, 2006.

[15] L. Vujovic, "Tesla Biography," Tesla Memorial Society of New York, 1998.

[16] L. I. Anderson, Nikola Tesla — Guided Weapons & Computer Technology, Tesla Presents Series, 2007.

[17] The Pioneers, MZTV Museum of Television, 2006.

[18] N. Postman, "Electrical Engineering,Time 100 Special Issue," Time Magazine, Vol. 153, No. 12, pp. 92 – 94, 1999.

[19] K. Hafner, Where Wizards Stay Up Late: The Origins Of The Internet. Simon & Schuster, 1998.

[20] Data transmission system, Olof Solderblom, PN 4293948, 1974.

[21] R. Flickenger, Wireless Hackers 100 Industrial-Strength Tops & Tools, O'Reilly Media, pp. 1 – 19, 2003.

[22] B. Sklar, Digital Communications: Fundamentals and Applications, Prentice Hall International Editions, pp. 1 – 11, 1998.

[23] G. D. Gibson, The Communications Handbook, Second Edition (Electrical Engineering Handbook), New York, pp. 31-1 – 31-20, 2002.

[24] ATIS Committee, T1A1 Performance and Signal Processing. ANS T1.523-2001, Telecom Glossary, 2000 (http://www.atis.org/tg2k/).

[25] A. Thomas, A story of wireless telegraphy, New York, 1994.

[26] A. G. Bell, "On the Production and Reproduction of Sound by Light," American Journal of Sciences, Third Series, Vol. 20, No. 118, pp. 305 – 324, 1880.

[27] A. G. Bell, "Selenium and the Photophone," Vol. 22, Nature, pp. 237, 1880.

[28] C. D. Christopher, I. S. Igor, and D. M. Stuart, "Flexible Opitcal Wireless Links and Networks," IEEE Communications Magazine, pp. 51 – 57, 2003.

[29] D. Kedar and S. Arnon, "Urban Optical Wireless Communication Networks: The Main Challenges and Possible Solutions," IEEE Optical Communications, pp. 52 – 57, 2004.

[30] D. Trinkwon, "Technology of Fixed Wireless Access," Telecommunications Policy, Vol. 21, No. 5, pp. 437 – 450, 1997.

[31] H. Takano and s. Shimamoto, "A Proposal of Optical Wireless Communications with RF Subcarrier," IEEE Topical Conference on Wireless Communication Technology, pp. 327 – 328, 2003.

[32] N. Araki and H. Yashima, "A Channel Model of Optical Wireless Communications during Rainfall," International Symposium on Wireless Communication Systems, pp. 205 – 209, 2005.

[33] J. Wang, D. Huang, and Y. Xiuhua, "Adaptive Detection Technique for Optical Wireless Communication Over Strong Turbulence Channels," International Journal for Light and Electron Optics, pp. 1 – 6, 2006.

[34] W. Pan, L. Liu, D. Zhao, and H. Lang, "Wireless Optical Communication-based Spatial Pattern," International Journal for Light and Electron Optics, pp. 13 – 18, 2007.

[35] K. S. Chen, C. P. Yu, C. Yu, and N. F. Huang, "Provisioning Multicast QoS for WDM-Based Optical Wireless Networks," Computer Communications, Vol. 27, No. 10, pp. 1025 – 1035, 2004.

[36] A. C. Boucouvalas, “Symmetry of IrDA Optical Links,” IEE Colloquium on Optical Free Space Communication Link, pp. 6/1 – 6/8, 1996.

[37] V. M. Melian, R. P. Jimenez, and M. J. Betancor, “2 Mb/s DPSK Modem for Infrared Wireless LAN and Data Communications,” Conference on Emerging Technologies and Applications in Communications, pp. 158 – 161, 1996.

[38] M. Yoshikawa, A. Murakami, J. Sakurai, H. Nakayama, and T. Nakamura, “High Power VCSEL Devices for Free Space Optical Communications,” Electronic Components and Technology Conference, Vol. 2, pp. 1353 – 1358, 2005.

[39] T. Komine and M. Nakagawa, “Integrated System of White LED Visible-Light Communications and Power-Line Communication,” IEEE Transactions on Consumer Electronics, Vol. 49, No. 1, pp. 71 – 79, 2003.

[40] T. Komine and M. Nakagawa, “Fundamental Analysis for Visible-Light Communication System using LED Lights,” IEEE Transactions on Consumer Electronics, Vol. 50, No. 1, pp. 100 – 107, 2004.

[41] T. Komine and M. Nakagawa, “A Study of Shadowing on Indoor Visible-Light Wireless Communication Utilizing Plural White LED Lightings,” International Symposium on Wireless Communication Systems, pp. 36 – 40, 2004.

[42] A. Oram, “RONJA: At 10 Mbps, The Next Stage in Wireless Mesh Networking?,” O’Reilly Network, 2007.

[43] J. M. H. Emirghani, “Timing Synchronisation and Jitter-Induced Performance Penalty in Optical Wireless Systems,” IEE Colloquium on Optical Free Space Communication Links, pp. 2/1 – 2/6, 1996.

[44] S. R. Forrest, “Photoconductor Receiver Sensitivity,” IEEE Electron Device Letters, Vol. EDL-5, No. 12, pp. 536 – 539, 1984.

[45] P. Rako, “Photodiode Amplifiers: Changing Light to Electricity,” National Semiconductor Technical Paper, pp. 1 – 19.

[46] M. F. L. Abdullah, R. Green, and M. Leeson, “Optical Wireless Communication Front-Ends,” High Frequency Postgraduate Student Colloquium, pp. 3 – 8, 2004.

[47] J. Conradi, “A Simplified Non-Gaussian Approach To Digital Optical Receiver Design with Avalanche Photodiodes: Experimental,” Journal of Lightwave Technology, Vol. 9, No. 8, pp. 1027 – 1030, 1991.

[48] N. Kobayashi, R. Furukawa, Y. Ozeki, T. Ushikubo, and M. Akiyama, “A Low Noise and Broad-Band Optical Receiver for 10 Gb/s Communication Systems,” Gallium Arsenide Integrated Circuit (GaAs IC) Symposium, pp. 287 – 290, 1992.

[49] T. V. Muoi, “Receiver Design for High-Speed Optical-Fiber Systems,” Journal of Lightwave Technology, Vol. LT-2, No. 3, pp. 243 – 267, 1984.

[50] J. J. Gustincic, “A Quasi-Optical Receiver Design,” MTT-S International Microwave Symposium Digest, Vol. 77, No. 1, pp. 99 – 101, 1977.

[51] K. Ogawa, “Considerations for Optical Receiver Design,” IEEE Journal on Selected Areas In Communications, Vol. SAC-1, No. 3, pp. 524 – 532, 1983.

[52] F. Yuan and B. Sun, “A Comparative Study of Low-Voltage CMOS Current-Mode Circuits for Optical Communications,” The Midwest Symposium Circuits and Systems 2002, Vol. 1, pp. 315 – 319, 2002.

[53] Z. Ghassemlooy and A. C. Boucouvalas, “Optical Wireless Communications: System and Networks,” International Journal of Communications System, Vol. 13, pp. 517 – 518, 2000.

[54] A. C. Boucouvalas, “Optical Wireless Communications,” IEE Proceeding on Optoelectronics, Vol. 150, No. 5, pp. 425 – 26, 2003.

[55] A. C. Boucouvalas, “IEC 825-1 Eye Safety Classification of Some Consumer electronic Products,” IEE Colloquium on Optical Free Space Communication Links, pp. 13/1 – 13/6, 1996.

[56] R. R. Iniguez and R. J. Green, “Indoor Optical Wireless Communications,” IEE Colloquium on Optical Wireless Communications, pp. 14/1 – 14/7, 1999.

[57] R. Szweda, “Lasers for Free-Space Optical Communications,” Review The Advanced Semiconductor Magazine,” Vol. 14, No. 9, pp. 46 – 49, 2001.

[58] A. Oladipuno, “Free Space Optical Connectivity,” Norfolk State University Optical Wireless Final Report, pp. 1 – 5, 2003.

[59] S. G. Hild and P. Robinson, “Mobilizing Applications,” IEEE Personal Communications, Vol. 4, No.5, pp. 26 – 34, 1997.

[60] The Institute for System Research, Optical Wireless System.

[61] S. Arnon, “Optimization of Urban Optical Wireless Communications Systems,” IEEE Transactions on Wireless Communications, Vol. 2, No. 4, pp. 626 – 629, 2003.

[62] P. Nicholls, S. D. Greaves, and R. T. Unwin, “Optical Wireless Telepoint,” IEE Colloquium on Optical Free Space Communication Links, pp. 4/1 – 4/6, 1996.

[63] D. Kedar and S. Arnon, “Backscattering-Induced Crosstalk in WDM Optical Wireless Communication,” Journal of Lightwave Technology, Vol. 23, No. 6, pp. 2023 – 2020, 2005.

[64] D.C. O'Brien, et. al., "High-speed integrated transceivers for optical wireless," IEEE Comm. Magazine, pp. 5 – 62, 2003.

[65] D.C. O'Brien, et. al., "Integrated transceivers for optical wireless communications," IEEE J. Selected Topics in Quantum Electron., Vol. 11, No. 1, pp. 173 – 183, 2005.

[66] D.C. O'Brien, et. al., "Experimental Characterization of Integrated Optical Wireless Components," IEEE Photonics Technology Letters, Vol. 18, No. 8, pp. 977 – 979, 2006.

[67] K. Nonaka, et. al., "High speed Optical Wireless Access with a Smart Beam Control Mechanism," APOC03, Wuhan, China, 2003.

[68] K. Nonaka, et. al., "High speed Optical Wireless Access with VCSEL-Array Beam Micro-Cell System," ECOC 2004, Stockholm, 2004.

[69] K. Nonaka, Y. Shima, A. Posri, and M. Tachibana, "Highspeed optical micro-cell wireless system for moving user access terminal with VCSELs and receivers array," LEOS Summer Topical Meetings, 2005, San-Diego, pp. 37 – 38, 2005.

[70] C. Tangtrongbenchasil, Y. Hamada, T. Kato, T. Watanabe, and K. Nonaka, "Indoor, Compact, and Smart Control High Speed Optical Wireless Communications," ITC-CSCC 2006, Chiangmai, Thailand, Vol. 2, pp. 5 – 8, 2006.

[71] C. Tangtrongbenchasil, T. Kato, and K. Nonaka, "Autonomous Downlink and Uplink Beam Alignment and Searching Techniques for Smart Link Multi-User Accessibility Optical Wireless Micro-Cell System," MOC 2007, Takamatsu, Japan, Oct. 2007.

[72] C. Tangtrongbenchasil, Y. Hamada, T. Kato, and K. Nonaka, "Optical Wireless Communications and Autonomous Beam Control Moving User Terminal," IEICE Transactions on Communications, Vol. E90-B, No. 11, pp. 3224 – 3231, 2007.

[73] R. Maestre, DualPath Architecture Blends Optical Wireless and RF into High Bandwidth, High Availability Outdoor Point-to-Point Solutions, www.rfdesign.com.

[74] G. Baister, P. Gatenby, B. Laurent, and J. Lewis, "Applications for Optical Free Space Links in Inter-Satellite and Intra-Satellite Communications," IEE Colloquium on Optical Free Space Communication Links, pp. 9/1 – 9/6, 1996.

[75] B. Huiszoon, G. D. Khoe, and A. M. J. Koonen, "End-to-End Optical Transparency in The Personal Network Concept," Proceeding NEFERTITI MPWI, 2005.

[76] S. E. Lyshevski and M. A. Lyshevski, "Microoptoelectromechanical Systems and Frequency Control," IEEE International Frequency Control Symposium and PDA Exhibition, pp. 837 – 844, 2003.

[77] S. B. Alexander, "Optical Communication Receiver Design," SPIE Optical Engineering, Vol. 46, No. 2, pp. 129 – 135, 1997.

[78] P. H. Siegel, “Terahertz Technology,” IEEE Transactions on Microwave Theory and Techniques, Vol. 50, No. 3, pp. 910 – 928, 2002.

[79] K. L. Sterchkx, J. M. H. Elmirghani, and R. A. Cryan, “Sensitivity Assessment of A Three-Segment Pyramidal Fly-Eye Detector in A Semidisperse Optical Wireless Communication link,” Proceeding IEE Optoelectronics, Vol. 47, No. 4, pp. 286 – 294, 2000.

[80] A. G. Al-Ghamdi and J. M. H. Elmirghani, “Performance Evaluation of a triangular Pyramidal Fly-Eye Diversity Detector for Optical Wireless Communications,” IEEE Communications Magazine, pp. 80 – 86, 2003.

[81] G. Pang, “Information Technology Based on Visible LEDs for Optical Wireless Communications,” TENCON 2004, Vol. B, pp. 395 – 398, 2004.

[82] X. Zhu, V. S. Hsu, and J. M. Kahn, “Optical Modeling of MEMS Corner Cube Retroreflectors with Misalignment and Nonflatness, ” IEEE Journal on Selected Topics in Quantum Electronics, Vol. 8, No. 1, pp. 26 – 32, 2002.

[83] T. Mikaelian, M. Weel, and A. Kumarakrishnan, “A High-Speed Retro-Reflector for Free-Space Communications Based on Electro-Optic Phase Modulation,” Proceeding of IEEE Aerospace Conference, Vol. 3, pp. 3-1487 – 3-1492, 2002.

[84] L. Zhou, J. M. Kahn, and K. S. J. Pister, “Corner-Cube Retrofeflectors Based on Structure-Assisted Assembly for Free-Space Optical Communication,” Journal of Microelectromechanical Systems, Vol. 12, No. 3, pp. 233 – 242, 2003.

[85] S. Teramoto and T. Ohtsuki, “Optical Wireless Sensor Network System Using Corner Cube Retroreflectors (CCRs),” Global Telecommunications Conference, Vol. 2, No. 29, pp. 1035 – 1039, 2004.

[86] R. Ramirez-Iniguez and R.J. Green, “Indoor optical wireless communications,” Optical Wireless Communications (Ref. No. 1999/128), IEE Colloquium on, pp. 14/1 – 14/7, 1999.

[87] Nabeel A. Riza, “Reconfiguration Optical Wireless,” Lasers and Electro-Optics Society 1999 12th Annual Meeting. LEOS '99, Vol. 1, pp. 70 – 71, 1999.

[88] D. Wisely and I. Neild, “A 100 Mbit/s Tracked Optical Wireless Telepoint,” Personal, Indoor and Mobile Radio Communications, Vol. 3, pp. 964 – 968, 1997.

[89] K. Nishida, “A Proposal of Multi Beam Transmitter for Non-Directed Diffuse Indoor Optical Wireless Communication System,” Personal, Indoor and Mobile Radio Communications, Vol. 1, pp. 242 – 246, 1996.

[90] R. J. Dickenson and Z. Ghassemlooy, “A feature Extraction and Pattern Recognition Receiver Employing Wavelet Analysis and Artificial Intelligence for Signal Detection in Diffuse Optical Wireless Communications,” IEEE Wireless Communications, pp. 64 – 72, 2003.

[91] P. Ampornrat, et. al., “Design of Transmitting and Receiving Section of Optical Wireless Access Using PLL,” IQEC/CLEO-PR, 2005.

[92] G. Keiser, Optical Fiber Communications, McGraw-Hill, 3rd ed., pp. 243 – 320, 2000.

[93] F. Parand, G. E. Faulkner, D. C. O’Brien, and D. J. Edwards, “A Cellular Optical Wireless System Demonstrator,” IEE Colloquium on Optical Wireless communications , pp. 12/1 – 12/6, 1999.

[94] D. Bushuev and S. Arnon, “|Enhance Detector array Receiver for Optical Wireless Communication Network,” The 22nd Convention of Electrical and Electronics Engineers in Israel, No. 1, pp. 178 – 180, 2002.

[95] A. Polishuk and S. Arnon, “Optical Wireless Communication Network with Adaptive Transmitter Array,” The 22nd Convention of Electrical and Electronics Engineers in Israel, No. 1, pp. 293 – 295, 2002.

[96] A. G. Kirk, D. V. Plant, M. H. Chateauneuf, and F. Lacroix, “Design Rules for Highly Parallel Free-Space Optical Interconnects,” IEEE Journal of Selected Topics in Quantum Electronics, Vol. 9 No. 2, pp. 531 – 547, 2003.

[97] S. Jivkova, B.A. Hristov, and M. Kavehrad, “Power-Efficient Multispot-Diffuse Multiple-Input-Multiple-Output Approach to Broad-Band Optical Wireless Communications,” IEEE Transactions on Vehicular Technology, Vol. 53, No. 3, pp. 882 – 889, 2004.

[98] M. Yoshikawa, A. Murakami, J. Sakurai, H. Nakayama, and T. Nakamura, “High Power VCSEL Devices for Free Space Optical Communications,” Proceeding 55th Electronic Components and Technology Conference, Vol. 2, pp. 1353 – 1358, 2005.

[99] P. P. Smyth and D. J. Hunkin, “A High Performance 2.4 Gbit/s PIN GaAs IC Optical Receiver,” ECOC, Brighton, UK, Vol. 1 pp. 408 – 411, 1988.

[100] B. Leskovar, “Optical Receiver for Wide Band Data Transmission Systems,” IEEE Transactions on Nuclear Science, Vol. 36, No. 1, pp. 787 – 793, 1989.

[101] J. L. Gimlet, “Ultrawide Bandwidth Optical Receivers,” Journal of Lightwave Technology, Vol. 7, No. 10, pp. 1432 – 1437, 1989.

[102] N. Takachio, K. Iwashita, S. Hata, and K. Katsura, “A 10 Gb/s Optical Heterodyne Detection Experiment Using a 23 GHz Bandwidth Balanced Receiver,” IEEE MTT-S Digest, pp. 149 -151, 1990.

[103] M. Makiuchi, H. Hamaguchi, O. Wada, and T. Mikawa, “Monolithic GaInAs Quad-p-i-n Photodiodes for Polarization-Diversity Optical Receivers,” IEEE Photonics Technology Letters, Vol. 3, No. 6, pp. 535 – 536, 1991.

[104] M. S. Park and R. A. Minasian, “Ultra-Low-Noise and Wideband-Tuned Optical Receiver Synthesis and Design,” Journal of Lightwave Technology, Vol. 12, No. 2, pp. 254 – 259, 1994.

[105] D. A. V. Blerkom, C. Fan, M. Blume, and S. C. Esener, “Optimization of Smart Pixel Receivers,” IEEE/LEOS Summer Topical Meetings, pp. 68 – 69, 1996.

[106] T. Y. Yun, M. S. Park, J. H. Han, I. Watanabe, and K. Makita, “10-Gigabit-per-Second High-Sensitivity and Wide-Dynamic-Range APD-HEMT Optical Receiver,” IEEE photonics Technology Letters, Vol. 8, No. 9, pp. 1232 – 1234, 1996.

[107] J. Rue, M. Itzler, N. Agrawal, S. Bay, and W. Sherry, “High Performance 10 Gb/s PIN and APD Optical Receivers,” Electronic Components and Technology Conference, pp. 207 – 215, 1999.

[108] P. Gui, F. E. Kiamilev, X. Q. Wang, X. L. Wang, M. J. MaFadden, M. W. Haney, and C. Kuznia, “A 2-Gb/s 0.5 μm CMOS Parallel Optical Transceiver with Fast Power-On Capability,” Journal of Lightwave Technology, Vol. 22, No. 9, pp. 2135 – 2148, 2004.

[109] F. C. Lin and D. M. Holburn, “A 0.35 μm Low-Noise Adaptive pad Driver for High-Speed Optical Wireless Receivers,” IEEE Africon, pp. 563 – 566, 2004

[110] D. M. Kuchta, Y. H. Kwark, C. Schuster, C. Baks, C. Haymes, J. Schaub, P. Pepeliugoski, L. Shan, R. John, D. Kucharski, D. Roger, M. Ritter, J. Jewell, L. A. Graham, K. Schrodinger, A. Schild, and H. M. Rein, “120-Gbs VCSEL-Based Parallel-Optical Interconnect and Custom120 Gb/s Testing Station,” Journal of Lightwave Technology, Vol. 22, No. 9, pp. 2200 – 2212, 2004.

[111] W. Z. chen, Y. L. Cheng, and D. S. Lin, “A 1.8-V 10-Gb/s Fully Integrated CMOS Optical Receiver Analog Front-End,” IEEE Journal of Solid-State Circuits, Vol. 40, No. 6, pp. 1388 – 1396, 2005.

[112] C. T. Chan, and O. T. C. Chen, “A 10 Gb/s CMOS Optical Receiver using Modified Regulated Cascade Scheme,” Midwest Symposium on Circuits and Systems, Vol. 1, pp. 171 -174, 2005.

[113] Y. Akatsu, Y. Miyagawa, Y. Miyamoto, Y. Kobayashi, and Y. Akahori, “A 10 Gb/s High Sensitivity, Monolithically Integrated p-i-n-HEMT Optical Receiver,” IEEE Photonics Technology Letter, Vol. 5, No. 2, pp 163 – 165, 1993.

[114] J. M. Jacob, Applications and Design with Analog Integrated Circuits, Prentice Hall, New Jersey, USA, pp. 143 – 179, 1982.

[115] A. Gerrard and J. M. Burch, Introduction to Matrix Methods in Optics, Dover Publications, pp.24 – 75, 1994.

Appendix A

Publications and Award

A.1 Publications

A.1.1 International Journals

1. **C. Tangtrongbenchasil**, Y. Hamada, T. Kato, and K. Nonaka, "Optical Wireless Communications and Autonomous Beam Control Moving User Terminal," IEICE Transactions on Communications, Vol. E90-B, No. 11, pp. 3224 – 3231, 2007.

2. **C. Tangtrongbenchasil**, K. Ohara, T. Itagaki, P. Vesarach, and K. Nonaka, "219-nm Ultra Violet Generation Using Blue Laser Diode and External Cavity," JJAP, Vol. 45, No. 8A, pp. 6315 – 6316, 2006.

3. **C. Tangtrongbenchasil** and K. Nonaka, "Tunable 220 nm UV-C Generation Basing on Second Harmonic Generation Using Tunable Blue Laser Diode System," JJAP, Vol. 47, No. 4A. (To be published at Apr 15, 2008)

4. **C. Tangtrongbenchasil** and K. Nonaka, "A Comparison of Different Coherent Deep Ultraviolet Generations Using Second Harmonic Generation with Blue Laser Diode Excitation," JNOPM, Vol. 17, No. 1. (To be published at Mar 1, 2008)

A.1.2 International Conferences

1. **C. Tangtrongbenchasil** and K. Nonaka, "Widely Tunable Ultraviolet C Generation Using Wavelength Selective External High-Q Cavity and Blue Laser Diode System," *ICPN 2007*, Dec. 2007, Pattaya, Thailand.

2. **C. Tangtrongbenchasil**, T. Kato, and K. Nonaka, "Autonomous Downlink and Uplink Beam Alignment and Searching Techniques for Smart Link Multi-User Accessibility Optical Wireless Micro-Cell System," *MOC 2007*, Oct. 2007, Takamatsu, Japan.

3. **C. Tangtrongbenchasil**, K. Nonaka, and K. Ohara, "220-nm Ultra Violet Generation Using an External Cavity Laser Diode with Transmission Grating," *MOC 2006*, Sep. 2006, Seoul, Korea, Vol. 2, pp. 5 – 8.

4. **C. Tangtrongbenchasil**, Y. Hamada, T. Kato, T. Watanabe, and K. Nonaka, "Indoor, Compact, and Smart Control High Speed Optical Wireless Communications," *ITC-CSCC 2006*, Jul. 2006, Chiangmai, Thailand, Vol. 2, pp. 5 – 8.

A.1.3 Japanese Conferences

1. T. Kato, Y. Hamada, H. Nishimura, T. Itagaki, O. Yokota, K. Nonaka, and **C. Tangtrongbenchasil**, "Beam Control of Optical Micro Cell Wireless System Using VCSEL and 4-channel APD," *IEICE Conference 2007*, Mar. 2007, Tokyo, Japan.

2. Y. Tanaka, **C. Tangtrongbenchasil**, K. Hirose, S. Yamada, T. Hayashi, D. Takahashi, and K. Nonaka, "Synchronies RGB Lasers Beam Construction for Full-Color Hologram Movie," *IEICE Conference 2007*, Mar. 2007, Tokyo, Japan.

A.2 Award

Second Place SPIE Best Student Paper Award

Fig. A.1 Certificate of Second Place SPIE Best Student Paper Award.

Appendix B

Ray Transfer Matrix Introduction

Ray transfer matrix, which is also known as ABCD matrix analysis, is an elegant method that used in the design of some optical systems, particularly lasers. Ray transfer matrix describes the optical system; tracing of a light path through the system can be performed by multiplying these matrices with a vector representing the light ray. Ray transfer technique uses the paraxial approximation of ray optics, i.e., all rays are assumed to be at a small angle (θ in radian) and a small distance (*x*) relative to the optical axis of the system.

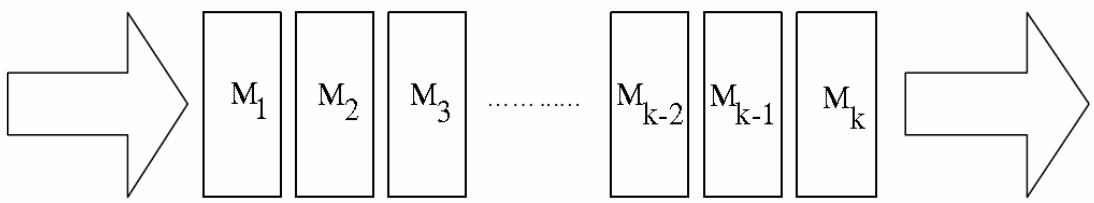

Fig. B.1 Elementary building blocks.

This is an example of ABCD matrices. Let an optical system has a configuration as shown in Figure B.1. It is composed of element M_1, M_2, M_3, …, M_k (k = 1, 2, 3, …). Elements' equation (M) which arranges in reverse order of elements which light enters first is given by[115]

$$M = M_k \cdot M_{k-1} \cdot M_{k-2} \cdot \ldots \cdot M_3 \cdot M_2 \cdot M_1 \qquad \text{(B.1)}$$

There are several ray transfer matrices to represent the optical elements. Only the matrices of propagation in free space or in a medium of constant refractive index and thin lens are shown in Table B.1.

Table B.1 Examples of ray transfer matrices[115].

Element	Matrix	Note
Propagation in free space or in a medium of constant refractive index	$\begin{pmatrix} 1 & d \\ 0 & 1 \end{pmatrix}$	d is propagation distance.
Thin lens	$\begin{pmatrix} 1 & 0 \\ -\frac{1}{f} & 1 \end{pmatrix}$	f is focal length of lens where $f > 0$ for convex/positive (converging) lens. Valid if and only if the focal length is much greater than the thickness of the lens.
Ray light vector	$\begin{pmatrix} x \\ \theta \end{pmatrix}$	x is ray position and θ is ray angle.

Appendix C

Bias Current Compensation Technique

The ideal op-amps draw no current from the source driving it as shown in Fig. C.1. Both of inverting and non-inverting inputs look and respond identically. However, practical op-amps do not work as mentioned. Current is taken from the source into the op-amp inputs. There are slight differences in the way two inputs respond to current and voltage. The practical op-amps shift its operation with temperature. These non-ideal DC characteristics and compensation techniques will be described in this section.

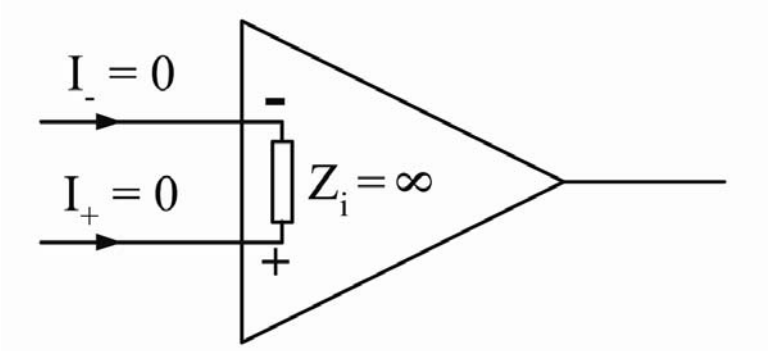

Fig. C.1 The ideal op-amp.

The op-amp input is a differential amplifier. It is made from bipolar junction transistor (BJT) or field effect transistor (FET). Using the active elements (BJT or FET), bias current is required and this takes current. Usually, the practical op-amps has very small bias current e.g. op-amp 741 bias current is 500 nA or less at room temperature. Fig. C.2(a) shows basic inverting amplifier without compensation using op-amp. When input (e_i) is set to zero volts, the output (e_o) should be zero volts too. However, the inverting and non-inverting terminals of op-amp draw bias current from external circuit. Current I_{B+} comes directly from ground and produces no voltage, while current I_{B-} comes through the feedback impedance (Z_F). Therefore, I_{B-} produces voltage across Z_F. Since

the inverting terminal of op-amp act as virtual ground, the output voltage of zero input can be approximated as

$$e_o = I_{B-} Z_F \tag{C.1}$$

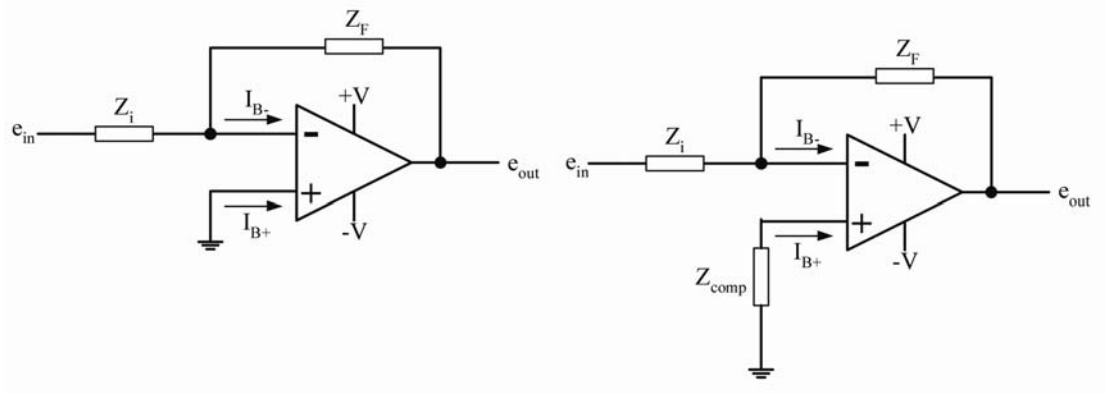

(a) (b)

Fig. C.2 Practical Op-amps (a) without compensation and (b) with compensation.

This effect can be compensated as shown in Fig. C.2(b). Compensated impedance has been added between ground and the non-inverting terminal of op-amp. Current I_{B+} flowing through the compensated impedance produces voltage at the non-inverting terminal of op-amp. Apply the Kirchhoff's voltage law (KVL) around the input-feedback-output loop

$$-V_{Z_{comp}} + V_{R_F} - e_o = 0 \tag{C.2}$$

So, the proper compensated impedance is chosen, $V_{Z_{comp}}$ cancels V_{R_F} and the output is compensated to be zero. The derivation of the compensated impedance is shown as

$$V_{Z_{comp}} = I_{B+} Z_{comp} \tag{C.3}$$

or

$$I_{B+} = \frac{V_{Z_{comp}}}{Z_{comp}} \tag{C.4}$$

$$I_{Z_i} = \frac{V_{Z_{comp}}}{Z_i} \tag{C.5}$$

$$I_{Z_F} = \frac{V_{Z_F}}{Z_F} \tag{C.6}$$

For compensation $V_{Z_{comp}} = V_{R_F}$, and then the current I_{B-} is the summation of I_{Z_i} and I_{Z_F},

$$\begin{aligned} I_{B-} &= \frac{V_{Z_{comp}}}{Z_F} + \frac{V_{Z_{comp}}}{Z_i} \\ &= V_{Z_{comp}} \left(\frac{Z_i + Z_F}{Z_i \cdot Z_F} \right) \end{aligned} \tag{C.7}$$

Assume $I_{B+} = I_{B-}$ then

$$Z_{comp} = \frac{Z_i + Z_F}{Z_i \cdot Z_F} \tag{C.8}$$

To compensate the bias currents, the compensated impedance should be equal to the parallel of the input impedance and the feedback impedance.

Appendix D

LabVIEW Programming

LabVIEW or laboratory virtual instrumentation engineering workbench is a software tool for multi input and output measurement, monitoring and control. In order to process external signal, LabVIEW requires data acquisition (DAQ), which is the analog/digital input/output module, to interface. LabVIEW consists of two main windows which are front panel (see Fig. D.1) and block diagram (see Fig. D.2). Front panel is for operating features (measurement, monitoring, and control) that link with the block diagram. The main operation or control algorithm is programmed in block diagram.

For autonomous beam searching and control, the quasi-DC signal from the 4-channel APD is employed as the monitoring and control signal. Fig. D.1 shows the front panel that monitors the quasi-DC signal from the 4-channel APD which are top, bottom, left, and right channel.

In order to monitor the quasi-DC signal from the 4-channel APD, the block diagram must be programmed. Fig. D.2 shows the block diagram programming for the quasi-DC signal from the 4-channel APD monitoring. In the block diagram, the DAQ assistant, which is an interface module that deals with input and output signal management, are required. Then, the low pass filters are required to suppress the high frequency noise. Filter parameters setup is shown in Fig. D.3. The 3^{rd} order digital Bessel low pass filters were implemented with the cutoff frequency of 10 Hz, due to monitoring only the quasi-DC signal.

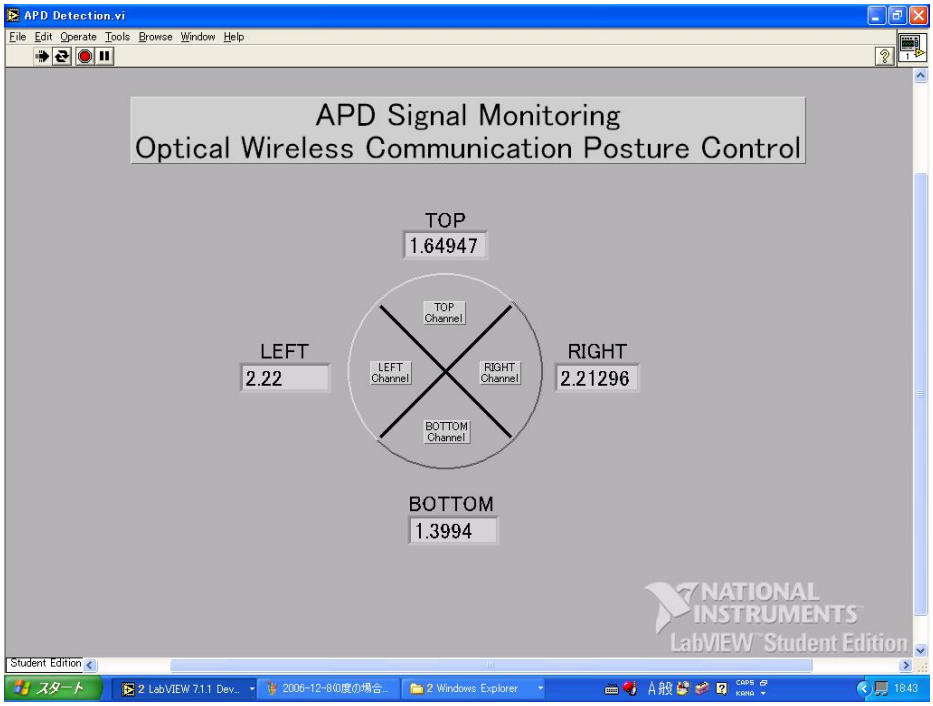

Fig. D.1 LabVIEW front panel for autonomous beam searching and alignment monitoring.

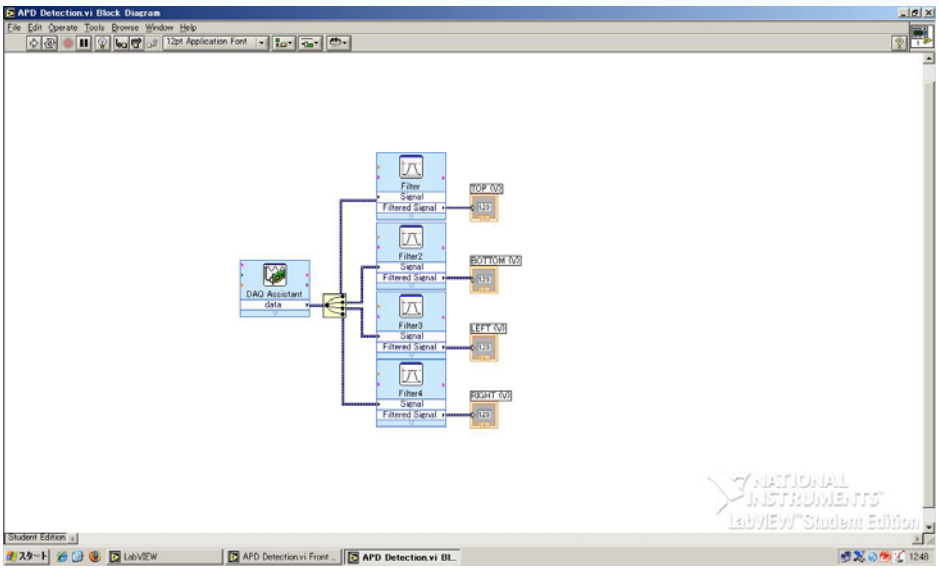

Fig. D.2 LabVIEW block diagram for autonomous beam searching and alignment monitoring.

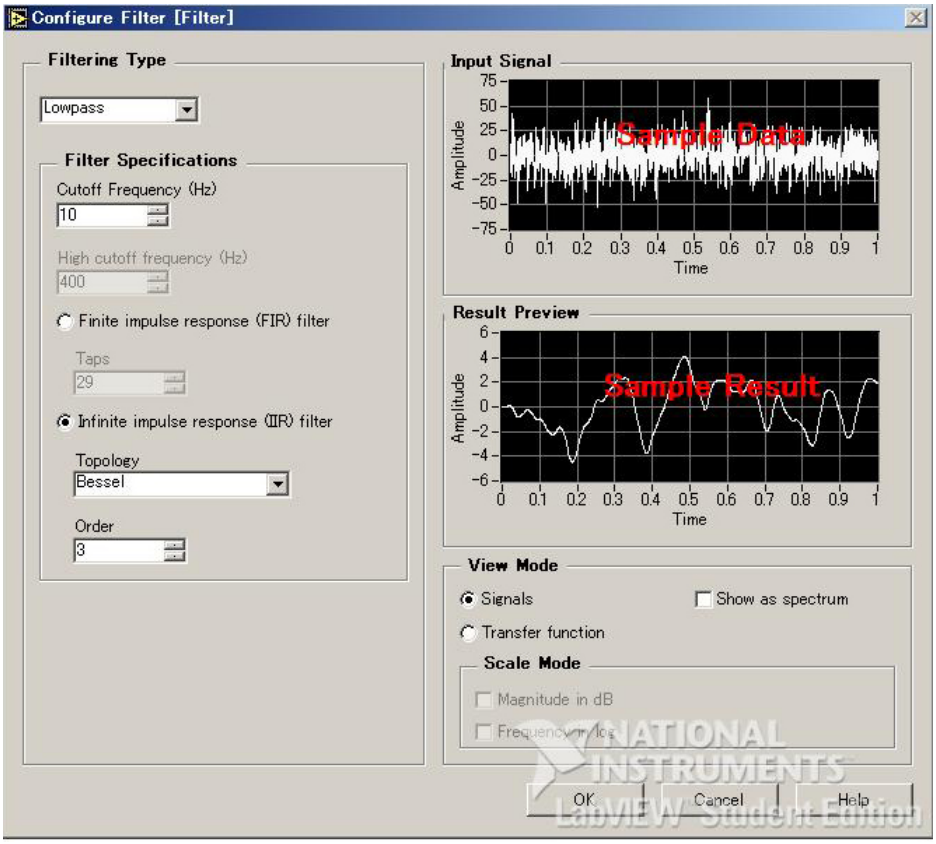

Fig. D.3 LabVIEW filter parameter setting for autonomous beam searching and alignment monitoring.